NORWEGIAN UNIVERSITY OF SCIENCE AND TECHNOLOGY

Ice induced resistance of ship hulls

A comparison of resistance estimated from measurements and analytical formulations

Torstein Skår

14.06.2011

Academic advisor: Bernt J. Leira

Abstract

Due to global warming and hydrocarbon exploration in the Arctic areas, there is an increasing maritime activity in ice infested waters. Today one can with good accuracy predict if a vessel will be able to survive an encounter with ice of a given thickness, but the knowledge is not good enough to predict the increased fuel cost for ice navigation.

This thesis has investigated the validity of two analytical formulations for ice resistance in Arctic areas. The formulations are based on full-scale ice trials in the Finnish-Swedish waters, which have lower salinity and warmer climate than the Arctic areas. This is done by comparing the resistance estimated from onboard measurements of vessel speed, ice thickness and engine power with the estimates from the analytical formulations. The ratio between the two is investigated using statistical tools.

While most of the data have too much variation for any conclusions to be made, some time sequences without large variation in the resistance has been identified. Analysis from these sequences indicate that the formulation presented by Riska et al. (1997) appears to be able to describe the speed dependency of ice resistance in the Arctic, but is inaccurate when describing the ice thickness dependence. The formulation presented by Lindqvist (1989) is found to be inaccurate when describing both ice thickness and speed dependency.

It is unclear whether the source of inaccuracy comes from incorrect ice property values or if the formulations have been used outside their area of application (both are based on ice trials in the Baltic Sea).

Preface

This master thesis marks the end of my study in Marine Constructions at Institute of Marine Technology at the Norwegian University of Science and Technology. The scope of work has been written by me and my teaching supervisor, Bernt J Leira, in cooperation.

The topic has been challenging, interesting and rewarding. I have learned much, not only about ice resistance, but also about statistics, Matlab plots and MS Word formatting. It has been challenging to present the large data material in a clear way, without requiring the reader to have profound knowledge of the topics discussed. It has sometimes been challenging to work with a topic that has not been subject to extensively research before, but this has also been rewarding. The feeling of finding a correlation in the data long after one has stopped to believe that such correlation actually exists is surprisingly satisfying.

During the work with this thesis, I have received invaluable guidance from my supervisor, who has steered me in the right direction while letting me find the actual solutions myself. I have also received assistance from PhD student Abdillah Suyuthi on topics regarding data interpretation. At last I would like to thank Larry Page and Sergey Brin, without their work on research tools the research work would have been much more time-consuming.

If the reader has further questions, the author can be contacted by e-mail:
torsteinskar@gmail.com

…….

Torstein Skår
Trondheim, 14.06.2011

Table of contents

Figures

Tables

Nomenclature

All symbols, abbreviations and technical terms are defined when they are used the first time. If they are used more than once, they are also defined in this list.

1.1 Technical terms and abbreviations

Brine	Liquid with high salt content
First- year ice	Ice that has not yet been exposed to melting (summer). Ice thickness *h* between 30 and 200 cm.
Lindqvist ratio	Ratio between resistance estimated from onboard measurements and resistance estimated from Lindqvist's formulation
Multi- year ice	Ice that has survived at least two melting seasons
Old ice	Ice that has survived at least one melting season
Riska ratio	Ratio between resistance estimated from onboard measurements and resistance estimated from Riska's formulation
RMSE	Root mean square error
SSR	Sum of squares due to error

1.2 Symbols

B	Breadth
E	Young's modulus
E	Energy (in chapter 5)
F	Average resistance force
g	Acceleration of gravity
h_i	Ice thickness [m]
L	Length
L_{bow}	Length of bow section
L_{par}	Length of parallel sides
M	Mass of vessel
P	Probability of obtaining the given data set (or one more extreme) under the assumption of a selected probability distribution
$P_{Delivered}$	Power delivered to azimuth thruster
R^2	Coefficient of determination
R_B	Breaking by bending resistance

R_c	Crushing resistance
r_i	Residual of data point i (difference between true and predicted value)
R_{ice}	Total ice resistance
$R_{open\ water}$	Open water resistance
R_S	Submergence resistance
S_i	Salinity of ice [ppt]
T	Draught
T_i	Average ice temperature [°C]
V	Velocity
W	Work
y_i	Data value of point i
$\hat{y}_i$	Predicted data value of point i
$\overline{y}$	Mean data value

1.3 Greek letters

ν_T	Total porosity
ν_a	Relative air content
ν_b	Relative brine content
ρ_{ice}	Density of ice
$\rho_{salt\ water}$	Density of salt water
σ_b	Flexural/ bending strength [MPa]
χ^2	Chi square test
α	Waterline entrance angle

μ	Friction coefficient
μ	Mean value (chapter 6 and 8)
ν	Poisson's ratio
σ	Standard deviation (chapter 6 and 8)
ψ	Angle between hull normal and vertical plane
ϕ	Stem angle

1 Introduction

The global warming and the melting of the Arctic ice cap creates the opportunity for a new possible shipping route between Europe and Asia, using the North-East passage instead of the Suez channel. This would reduce the travel time significantly and thereby the transportation costs. The Arctic area is also highly interesting for exploration of hydrocarbons and other natural resources.

The main challenge for shipping activities in these waters is the presence of sea ice, which is a complex material and induces high contact pressures during ship impact. Several analytical formulations describing this interaction exist, but the research and knowledge in this area is still limited compared to other aspects of shipping.

In this thesis, the accuracy of two such analytical formulations will be investigated, and compared to estimated resistance based on onboard measurements of a selected ship in Arctic waters. The overall long term goal for this research is to improve the resistance formulations, in order to be able to predict increased fuel consumption due to ice induced resistance.

1.1 Related research

The theoretical basis for this thesis is the works done by Lindqvist (1989) [1] and Riska (1997) [2]. The *ice resistance models* they proposed has been widely used since then, and are considered to be fairly accurate, at least in the area they were developed for (Finnish- Swedish waters).

Most of the more recent ice resistance research has been attempting to estimate the ice resistance based on *Finite Element Methods,* for instance Valanto (2001) [3] and Su et al. (2010) [4]. These works have been able to estimate the resistance quite well, but the procedure is much more time consuming compared to the analytical models proposed by Riska and Lindqvist.

2 Description of sea ice characteristics

The following chapter is to a great extent based on information from [5] and [6]. The focus will be on ice characteristics relevant for the thesis. In cases where [5] directly refers to other publications, the original reference is cited to increase readability. For information about other sea ice properties, see [5].

2.1 Different sea ice types and physical appearance

This section will attempt to define different sea ice types, and to clarify the differences between them. The purpose is to give the reader an introduction to the topic, and illustrate some of the complexity.

2.1.1 Sea ice types

Sea ice is normally classified in different groups depending on age and how far away from land the ice is located. Figure 2-1 describes ice classification based on distance from land, while Table 2-1 lists ice type classifications based on age. When using the distance classification, it is usually distinguished between *Fast ice zone* and *Pack ice zone.* The fast ice zone is the area where the sea ice is firmly connected to the seafloor, while the pack ice zone is the area where the ice is more or less drifting free.

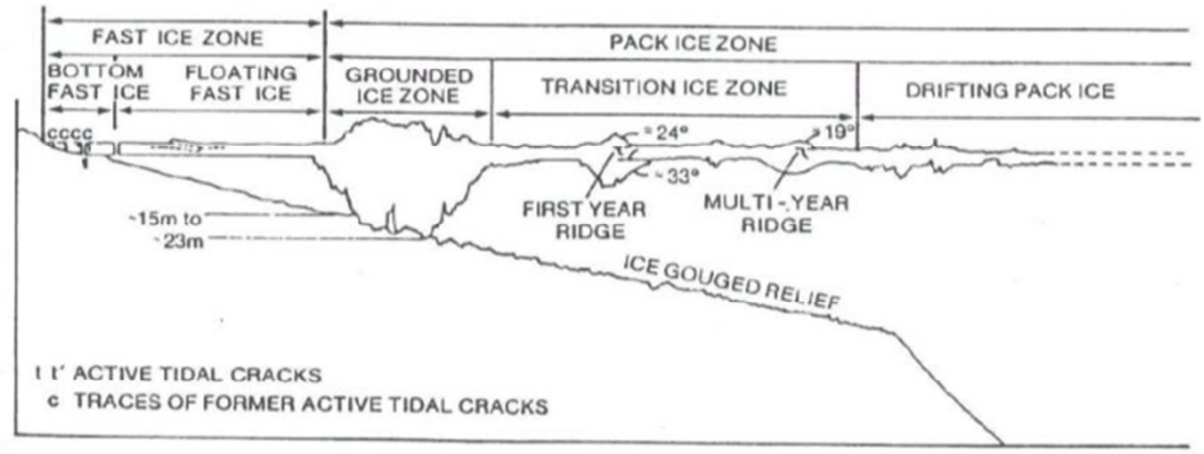

Figure 2-1 Sea ice zones [7]

When categorizing based on age, it is mainly divided between ice that has survived a melting season and ice that has not yet been subjected to melting. The rationale behind categorizing based on this is the importance of both mechanical wear and tear, and salinity in the ice. Both these parameters are highly dependent on the ice age.

Table 2-1: Sea Ice types categorized based on age[6]

Sea ice Type	**Description**
New ice	General term for newly formed ice
Young ice	Ice in transition between new ice and first- year ice. Ice thickness *h* between 10 to 30 cm
First- year ice	Ice that has not yet been exposed to melting (summer). Ice thickness *h* between 30 and 200 cm.
Old ice	Ice that has survived at least one melting season
Multi- year ice	Ice that has survived at least two melting seasons

2.1.2 Sea ice features

Sea ice is constantly changing, being subjected to both mechanical wear and freezing or melting. This means that it is necessary to distinguish between several different types of sea ice features, and the most important are listed in Table 2-2

Table 2-2 Sea ice features [6]

Sea ice feature	Description
Frazil ice	Consolidations of ice crystals in water
Nilas	Frazil ice frozen at the surface under calm conditions, will bend if subjected to waves
Grease ice	Accumulations of frazil ice prevented from freezing together by wave influence
Pancake ice	Relatively small pieces of newly formed ice, normally with circular shape and upturned edges (due to wave action). Diameter between 30 cm and 3 m
Ice floe	Flat piece of ice, less than 20 m across and 1 m thickness
Level ice	Continuous undeformed sea ice
Deformed ice	General term for ice that is no longer "level"
Rafted ice	Ice where relatively large ice floes have been pushed on top of each other
Brash ice	Highly fragmented ice. Normal in ship lanes made by ice breakers
Ridge	A "wall" of broken ice forced up by pressure
Hummocked ice	Ice deformed by pressure, where pieces are arbitrarily piled

2.2 Physical and mechanical properties

The physical and mechanical properties of ice are greatly influenced by environmental parameters. The microstructure is influenced by both the temperature and waves. In order to account for some of the differences in prevailing environmental conditions, it is common to distinguish between *First year ice* and *Multiyear ice.* The rationale behind this division is the significant difference in microstructure between the two general ice types, caused by melting and mechanical consolidation. As the focus for the thesis is first-year ice, this section will also mainly focus on first-year ice.

2.2.1 Ice thickness

Ice thickness is one of the most important ice parameter when determining the ice load. The thickness is determined by the average air temperature, the freezing time, wind speed, ocean heat flux, snow type and thickness, and surface radiation balance. The two first factors are governing, giving larger thickness in artic areas compared to more temperate areas.

The maximum expected thickness from thermal growth can be calculated by *The Stefan equation*

$$h_i = \sqrt{\frac{2\kappa_i}{\rho_{ice} L_f}\left[T_b - T_a\right] t_{freeze}} \tag{2.1}$$

where h_i is ice thickness, κ_i is the thermal conductivity, ρ_{ice} is the density, L_f is latent heat from fusion, T_b and T_a is temperature at bottom and top of ice sheet, and t_{freeze} is total freezing time.

This equation is only applicable for first-year ice, and will always overpredict the ice thickness, since it does not consider snow cover insulation, wind and ocean heat flux. To account for this, the equation is normally applied together with an α factor (less than 1.0) to adjust the result.

For old ice there has not been proposed any simple analytical formulas, since ice thickness for old ice is a function of both thermal growth and decay, and mechanical consolidation.

2.2.2 Ice salinity and density

The ice density influences submersion resistance, which is an important part of the total resistance. The density for first-year ice is influenced by both temperature and salinity. Salinity is again a function of ice thickness and age. For first-year ice, the following relationship between ice thickness and salinity has been proposed [8]:

$$S_i\,[ppt] = 4.606 + \frac{91,603}{h_i\,[cm]} \tag{2.2}$$

where S_i is the average salinity of the ice sheet.

The temperature dependency of density has been determined in lab tests, and is described in Figure 2-2. The figure shows that density for ice with high salinity is much more temperature dependent than density for low salinity ice. This is due to brine inclusions in the ice, which is sensitive to temperature changes [6].

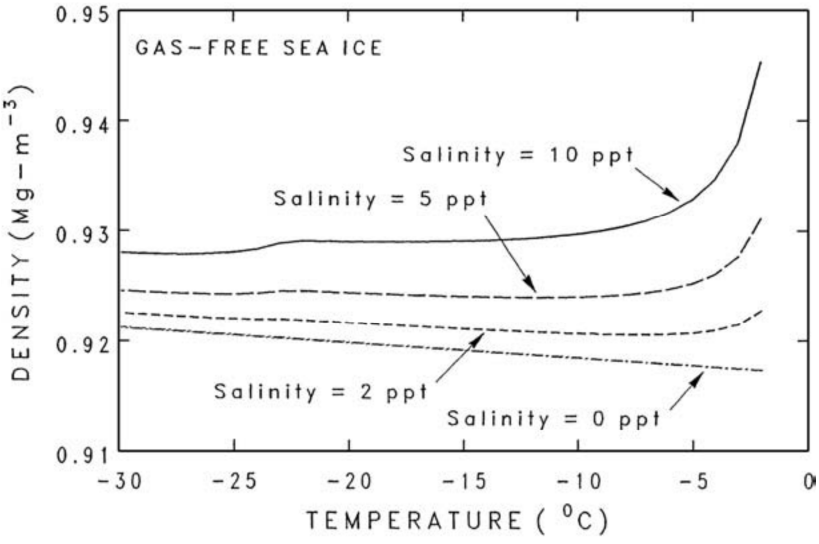

Figure 2-2: Density as a function of temperature for different salinities.
The gas free density is an upper limit of density, as gas inclusions will decrease the density. [9]

2.2.3 Porosity

The porosity is a measure of the level of "pollution" in the ice (volume fraction of substance different from solid H_2O), and is normally measured in parts per thousand or ‰. The porosity for sea ice is mainly caused by two main components, brine (liquid with high salt content) and gas (air). The relative brine content in first- year ice is dependent on ice temperature and salinity, as described by eq. (2.3) [10]. This formula is valid for ice temperatures in the range -0,5°C to -22,9°C.

$$\nu_T = \nu_b + \nu_a = S_i \left[\frac{49{,}185}{|T_i|} + 0{,}532 \right] + \nu_a \tag{2.3}$$

where T_i is the average temperature of the ice, in degrees Celcius, ν_T, are total porosity, ν_a and ν_b are relative air and brine content, respectively.

The relative air content ν_a is important if brine drainage has occurred (associated with ice melting), and the relative air content may be significant for old ice, especially above the sea level[5]. Due to difficulties in obtaining accurate formulations for relative air content in first year ice, this contribution to porosity is neglected in this thesis, and the relative brine content is taken as an approximation of the total porosity.

2.2.4 Flexural strength

The flexural strength is a measure of how a material resists bending before failure, and therefore highly relevant for this thesis. Several studies have been attempting to determine the flexural strength as a function of the brine volume. The rationale behind this is the assumption that increasing porosity means decreasing strength, since less solid ice has to be broken. Brine volume is used instead of total porosity, since the relative air content is difficult to measure during field tests. The following relationship between brine volume and flexural strength has been suggested by [4] for first-year ice

$$\sigma_b = 1{,}76 \exp\left(-5{,}88 \cdot \sqrt{\nu_b} \right) \tag{2.4}$$

where σ_b is the flexural strength of ice (in MPa), and ν_b is the brine volume fraction. As the strength is a function of brine volume, which again is a function of salinity, one will find stronger ice in fresh or brackish water than in sea water. This will influence the ice induced resistance. The influence of ice strength on resistance is discussed in section 4.4.2.

This relationship is illustrated in Figure 2-3. It is important to note that the flexural strength equation is not valid for decaying ice. This is due to the change in structure that is caused by melting brine creating *brine channels* (vertical channels in the ice, where brine has "leaked" out of the ice).

Combining the dependency for brine volume (eq (2.3)) with the formulation for flexural strength (eq (2.4)), the following relationship is obtained

$$\sigma_b = 1{,}76 \exp\left(-5{,}88 \cdot \sqrt{S_i \left[\frac{49.185}{|T_i|} + 0.532 \right]} \right) \tag{2.5}$$

If the average ice salinity as function of ice floe thickness (eq. (2.2)) is introduced, it is possible to obtain an equation for flexural strength as a function of average ice temperature and ice floe thickness, as shown in eq.(2.6)

$$\sigma_b = 1,76 \exp\left(-\frac{147}{2500} \sqrt{10\left(\frac{9837}{200|T_i|} + 0,532 \right)\left(\frac{91,603}{H_i[cm]} + 4,606 \right)} \right) \tag{2.6}$$

This has been plotted for applicable values, and the result is shown in Figure 2-4

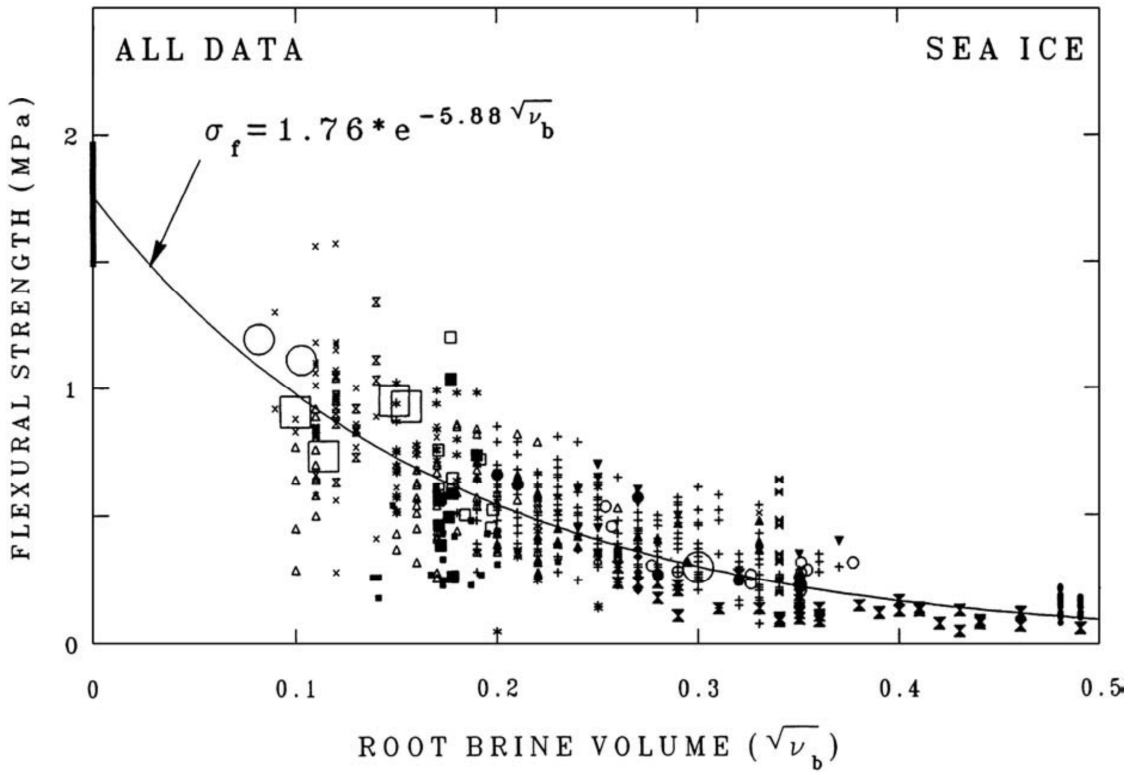

Figure 2-3: Flexural strength
Plotted against the square root of brine volume for first year ice [4]

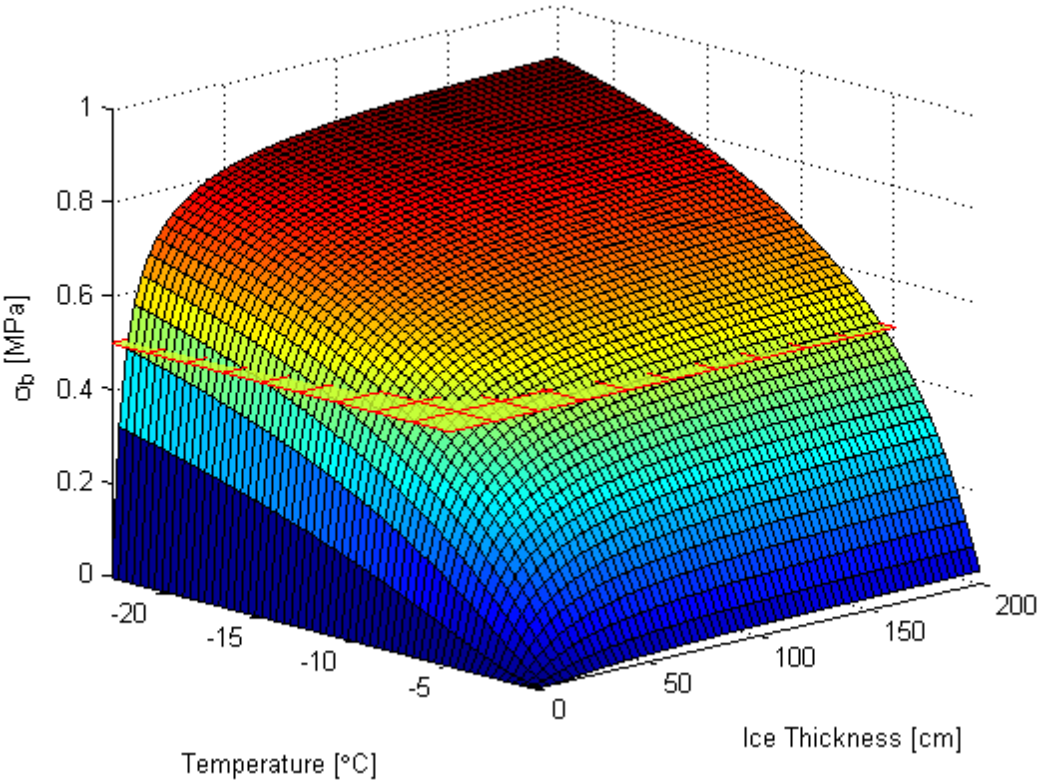

Figure 2-4: Flexural strength as a function of ice thickness and average ice temperature.
The value used for calculation is indicated by the horizontal plane. Only valid for first-year ice before melting process begins

It is seen from the figure that the strength as function of ice thickness converges rather fast, meaning that the strength mainly is dependent on the temperature in the ice (which is unknown for the data set used in this thesis). It is important to note that eq. (2.6) and Figure 2-4 is based on curve fitting of field measurement data, and should therefore not be taken as an exact value, but it may provide an indication of expected values.

2.2.5 Compression strength

This parameter is not used in the ice resistance formulations, but it illustrates an important characteristic of ice, the influence of loading rate. As seen in Figure 2-5, the strain rate (displacement velocity over sample length) influences the failure strength significantly, and the compressive strength varies from 500 [kPa] to approximately 8 [MPa]. This may influence the resistance, if the ship velocity is sufficiently low.

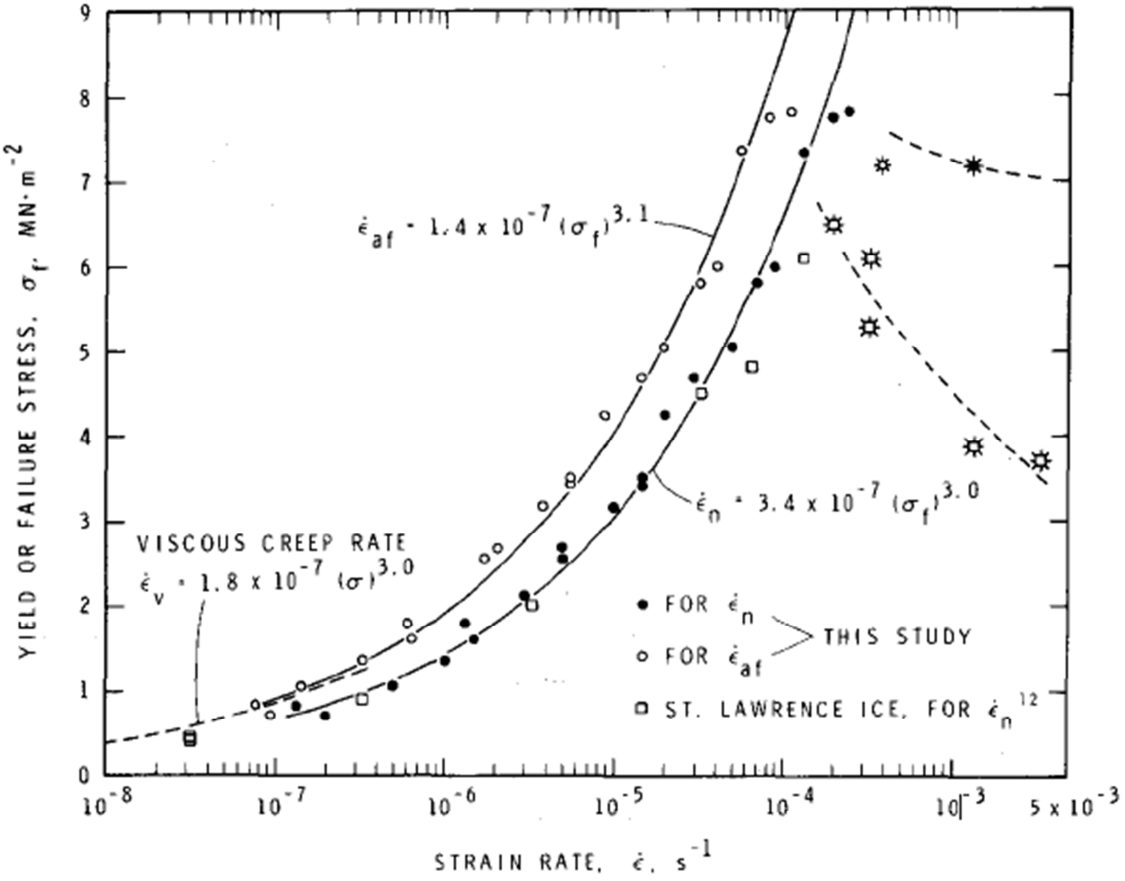

Figure 2-5 Dependence of yield or failure stress on strain rate
Nominal strain rate, $\dot{\epsilon}_n$, and average strain rate to peak stress, $\dot{\epsilon}_{af}$, for columnar-grained ice of average grain size, 4-5 mm, at -10°C Premature failures are marked with asterisks [11]

2.3 Chapter summary

It is seen that the properties of sea ice is highly dependent on a number of variables, most of which are hard to determine without leaving the vessel. For the purpose of this thesis, the values chosen by Riska et al. have been used for calculation purposes. These values are given by eq.(2.7)

$$\sigma_b = 500[kPa] \qquad \mu = 0.15[-]$$
$$E = 2000[MPa] \quad \rho_{\text{salt water}} = 1025\left[\frac{kg}{m^3}\right] \tag{2.7}$$
$$\nu = 0.3[-] \qquad \rho_{\text{ice}} = 900\left[\frac{kg}{m^3}\right]$$

This is done both to be able to compare the resistance estimated by Riska et al. and Lindqvist, and because it is difficult to determine these values correctly. The sensitivity of estimated resistance to change in these parameters is discussed in section 4.4.

3 KV Svalbard

The contents in this chapter are to a great extent based on information in [12] and [13].

The full scale data used in this thesis is gathered from the Norwegian coast guard vessel *KV Svalbard*, which was instrumented for scientific use during a voyage around the Svalbard area in late March 2007. The data has previously been used to investigate ice loads as part of the research project *Ice Load and Monitoring*.

3.1 Relevant hull parameters

The ship hull dimensions and geometry are important for ice resistance [14]. The relevant parameters for KV Svalbard are given in Table 3-1, with both symbols and units.

Table 3-1: Hull shape and dimensions for KV Svalbard[13]

Variable name	symbol	value	unit
Breadth	B	19,1	[m]
Draught	T	6,5	[m]
Length of water line	L	89	[m]
Length of parallel sides	L_par	36,32	[m]
Length of bow section	L_bow	27,24	[m]
Stem angle	phi - ϕ	34	[deg]
Waterline entrance angle	alfa - α	35	[deg]

The main dimensions are publicly available, and hence known with low uncertainty. The shape parameters (lengths of different sections and angles) are found by measuring of for instance Figure 3-1, and have some uncertainty, as the drawings available are not very detailed. The relative influence of these parameters is discussed in detail in section 4.4**.**

3.2 Monitoring system

The system installed on KV Svalbard is a prototype of a planned Ice Load Monitoring system, which is planned to include the following components:

1. Fiber optic strain sensors at selected frames
2. Electromagnetic ice thickness sensor
3. Software to analyze and display results on bridge
4. Meteorological and satellite data displayed on electronic chart
5. Continuously update of displays

The prototype did only include the three first components, which will be described shortly. For detailed descriptions, see references [12] and [13].

3.2.1 Ice thickness sensor

The ice thickness is measured using a combination of sonic and electromagnetic (EM) sensors. The configuration is shown in Figure 3-1 (a) and (b).

An EM sensor measures the distance from the sensor to the seawater, using the conductivity properties of water compared to ice and snow. This is done by inducing a magnetic field in the water, and calculating the distance based on the strength of the field. It is important to note that this measurement method gives an average distance to the water over an area of about 12 [m^2],

and underestimates the thickness of ridge keels. The latter is due to the fact that ridge keels consist of a mixture of ice and water.

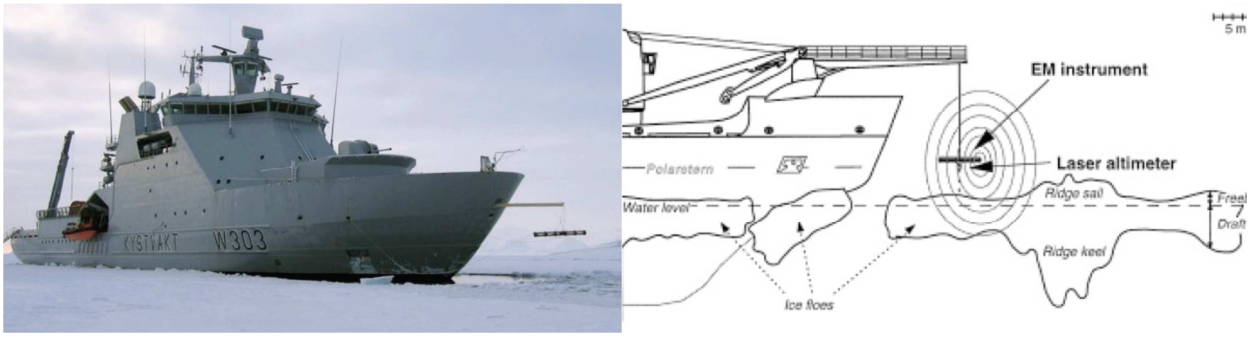

(a) Ice thickness sensor mounted in bow (b) Schematic illustration of ice thickness sensor

Figure 3-1: Ice thickness sensor [15]

The distance from the sensor to the ice is measured by a sonic distance- measurement device, which measures the distance to any surface. The distance is measured instantaneously, without the same averaging effects as the EM device has. Snow cover will influence the measurements greatly, since the instrument is unable to disguise between snow and ice.

The accuracy of the sensor is dependent on the ice conditions and the calibration accuracy. In undisturbed level ice the accuracy is believed to be rather good, but the accuracy drops if disturbances are introduced. In the area in front of a ship in motion, there will to some extent be ice cracks due to the breaking process. Since the distance to the sea is measured over a rather large area, and the distance to the top of the ice is measured at a point, there may be large variations in measured ice thickness compared to real ice thickness.

3.2.2 Strain sensors

Forces on the hull is estimated based on a total of 66 fiber-optic strain sensors mounted on eight frames in the bow section and one midshipsframe. The measurements are taken from the support structure to avoid measurement errors due to vibration, and to include forces from a larger area without increasing the number of sensors. Figure 3-2 shows the location of these sensors.

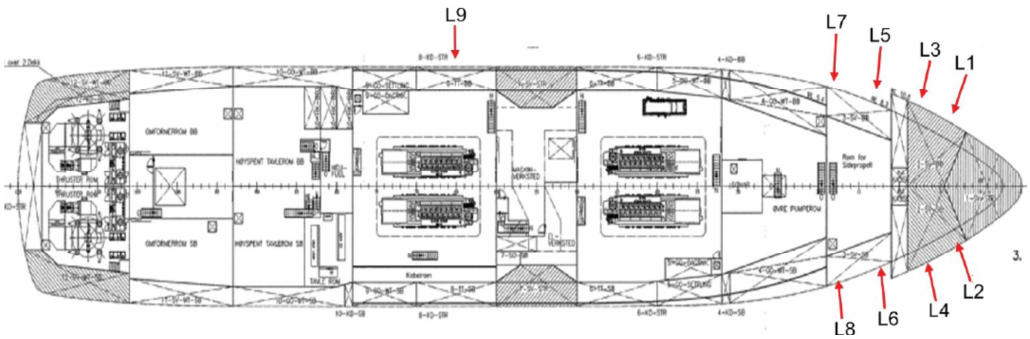

Figure 3-2: Strain sensor locations [13]

The results from these sensors have not been used in this thesis.

3.2.3 Ship equipment sensors

In addition to data from the strain sensors, data from sensors on the equipment on board is collected. This includes thruster power and navigation data, which is of particular interest in this thesis. The thruster data includes power consumption in each of the two thrusters, which may be used to estimate the vessel resistance. The navigation data includes both speed and heading, which may be used to find time sequences with stable conditions. The accuracy of these sensors is considered to be good.

3.2.4 Bridge display

All relevant data, including statistical variables, is displayed on the bridge, in real-time. This enables the crew to monitor hull utilization during the voyage, and reduce vessel speed if necessary.

3.3 Section summary

The monitoring system gives accurate data for navigation and machinery parameters. The ice thickness parameter accuracy is dependent on the amount of cracks and other disturbances, and whether or not snow cover is present. This introduces an unknown uncertainty in the resistance calculation, which may influence the results. The hull shape parameters could be more accurate, but are considered to be sufficiently accurate for the purpose of this thesis.

4 Models for calculating ice induced resistance for ship hulls

This chapter will present two analytical methods for calculating ice- induced resistance on hulls, presented by Lindqvist (1989) and Riska et al (1997). Both formulas are developed by researchers with connection to either Finland or Sweden, and they are based on tests done in the waters between Finland and Sweden. They both use the same geometrical definitions of the ship hull angles, which are given in Figure 4-1.

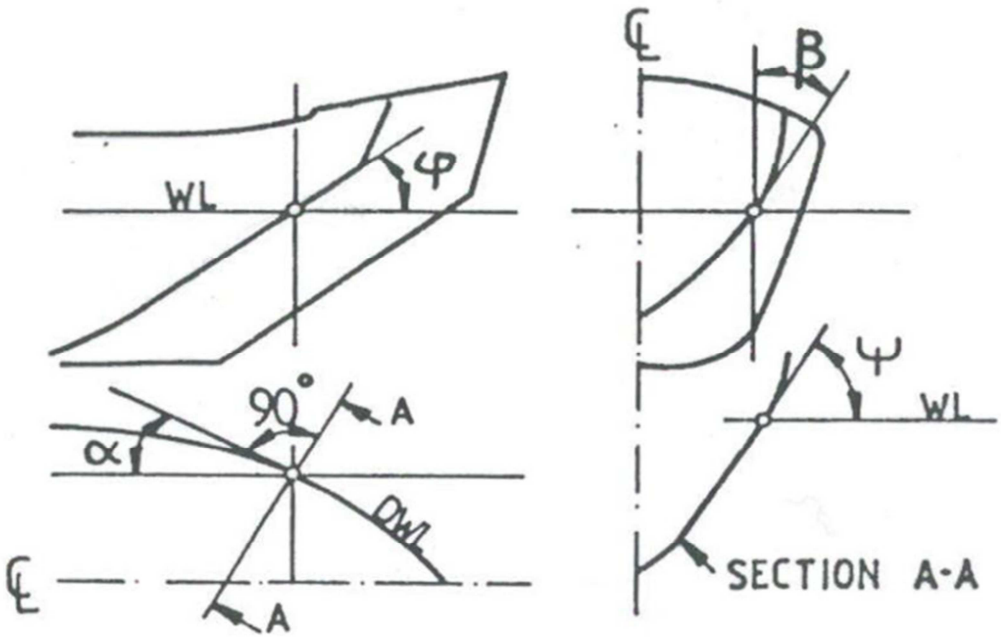

Figure 4-1: Ship geometry angle definition [14]

The stem angle φ is the angle between the waterline and the bow, taken parallel to the ship longitudinal direction. The waterline entrance angle α is the angle between the longitudinal axis of the ship and the waterline. For most relevant hull types, these angles are not constant over the ship breadth. Both models recommend that the angles used for calculation should be the average value. This average value has not been possible to determine, and approximate values are used in this thesis.

Figure 4-2 shows a schematic summary of the main resistance components from ice. Both formulations account for these components, but there are some differences. The main difference is related to how they model the physics behind the resistance.

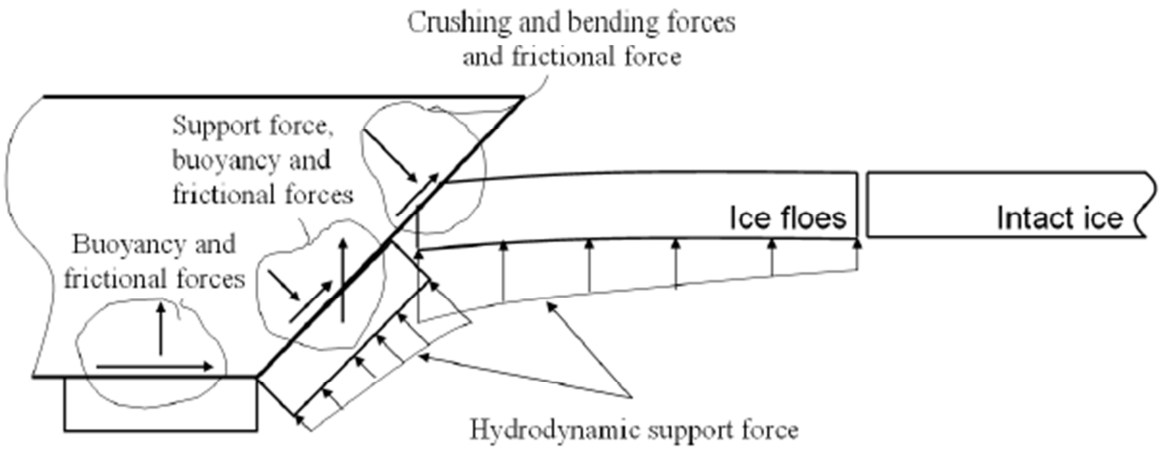

Figure 4-2: Different ice resistance components. From [14]

4.1 Validity in the Arctic area

The ice in the Finnish/Swedish area has some important differences from the arctic sea ice. The first major difference is that the ice in the Bay of Bothnia is only seasonal, meaning that there is no multi-year ice. This should not influence the result in this particular thesis, since the ice encountered are believed to be first year ice only [15].

Another important difference is the salinity of the water. The Bay of Bothnia has brackish water (both [16] and [17] indicates salinity in the order of 5‰), while the Arctic water has a salinity of approximately 35‰. It is believed that a change in water salinity also will influence the salinity of the ice. This may give the Arctic ice a relatively low strength compared to the Bay of Bothnia. The connection between average ice salinity and flexural strength are discussed in section 2.2, while the consequences of a change in flexural strength are discussed in section 4.4.2.

4.2 Lindqvist [1]

The model was presented in 1989, and presents a rather simple way of estimating the resistance due to ice. In this model, the resistance is divided into crushing, bending- induced breaking and submergence. The model gives resistance as a function of main dimensions, hull form, ice thickness, ice strength and friction.

4.2.1 Crushing

Crushing is the main force component at the stem, where the contact area between the hull and the ice is not large enough to give bending failure before crushing occurs.

The crushing force is difficult to calculate, and is estimated in this model. Using engineering judgment, the vertical force acting on the ice is assumed to be

$$F_V = \frac{1}{2}\sigma_b h_i^2 \tag{4.1}$$

σ_b = Ice strength in bending

h_i = Ice thickness

Using geometrical considerations while analyzing the crushing process, one may derive the following expression for the crushing resistance:

$$R_c = F_V \frac{\tan\phi + \mu\cos\phi/\cos\psi}{1-\mu\sin\phi/\cos\psi} \tag{4.2}$$

R_c = Crushing resistance

μ = friction coefficient

ϕ = stem angle

α = waterline entrance angle

$$\psi = \arctan\left(\frac{\tan\phi}{\sin\alpha}\right)$$

4.2.2 Breaking by bending

The bending failure of ice will be induced when a sufficiently large contact area between the ice floe and the ship hull is present. When the hull comes into contact with a corner of the floe, ice is crushed until shearing failure occurs. The shearing failure takes place close to the contact point, and this process continues until the force transmitted is large enough to cause bending failure. The process is illustrated in Figure 4-3. The formulation for bending resistance is given in eq.(4.3).

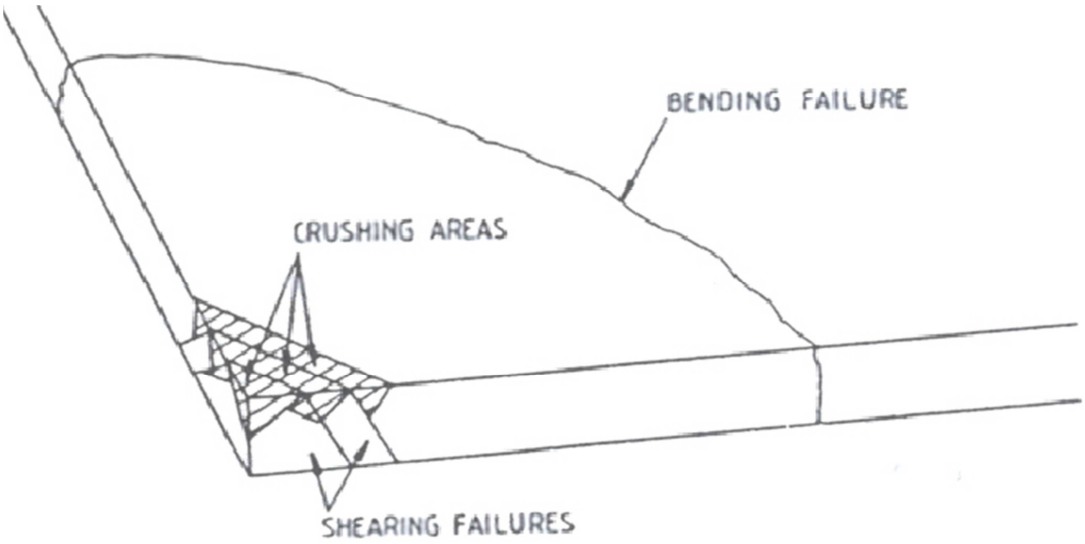

Figure 4-3: Bending failure process.
Shearing failure will occur until the contact area is large enough to transform critical bending strength without exceeding shear capacity. From [1]

$$R_b = \frac{27}{64}\sigma_b B \frac{h_{ice}^{1.5}}{\sqrt{\frac{E}{12\left(1-\nu^2\right)g\rho_w}}} \frac{\tan\psi + \mu\cos\phi}{\cos\psi\sin\alpha}\left(1+\frac{1}{\cos\psi}\right) \tag{4.3}$$

where B is breadth, E is Young's modulus and ν is the Poisson ratio. ρ_w is the density of sea water. For detailed calculations, see [1].

4.2.3 Resistance due to submersion

This resistance component comes from normal force and friction between the ship hull and the ice below the hull. For the friction part, it is assumed that 70% of the submerged hull is covered by ice. The normal force part is calculated through potential energy. The submergence resistance is given by

$$R_s = (\rho_w - \rho_{ice})\, g h_{tot} B \left(T \frac{(B+T)}{B+2T} + k \right) \tag{4.4}$$

$$k = \mu \left(0,7L - \frac{T}{\tan\phi} - \frac{B}{4\tan\alpha} + T\cos\phi\cos\psi \sqrt{\frac{1}{\sin\phi^2} + \frac{1}{\tan\alpha^2}} \right)$$

where h_{tot} is the total ice and snow thickness, and ρ_{ice} is the density of ice.

4.2.4 Speed dependency

The Lindqvist model assumes that all three resistance components increase linearly with speed, and uses empirical constants to account for this. The velocity term is made dimensionless by dividing it with the square root of acceleration of gravity times a length relevant for the resistance term in question (length for submersion resistance and ice thickness for breaking and crushing resistance). The formula for total resistance is given in eq.(4.5)

$$R_{ice} = (R_c + R_b)\left(1 + 1.4\frac{v}{\sqrt{g h_{ice}}} \right) + R_s \left(1 + 9.4\frac{v}{\sqrt{gL}} \right) \tag{4.5}$$

4.2.5 Speed and ice thickness dependency of the resistance estimate

In Figure 4-4, Lindqvist resistance is plotted against speed and ice thickness, respectively. It is seen that the resistance increases linearly with speed, and with the ice thickness raised to the power of 1.5.

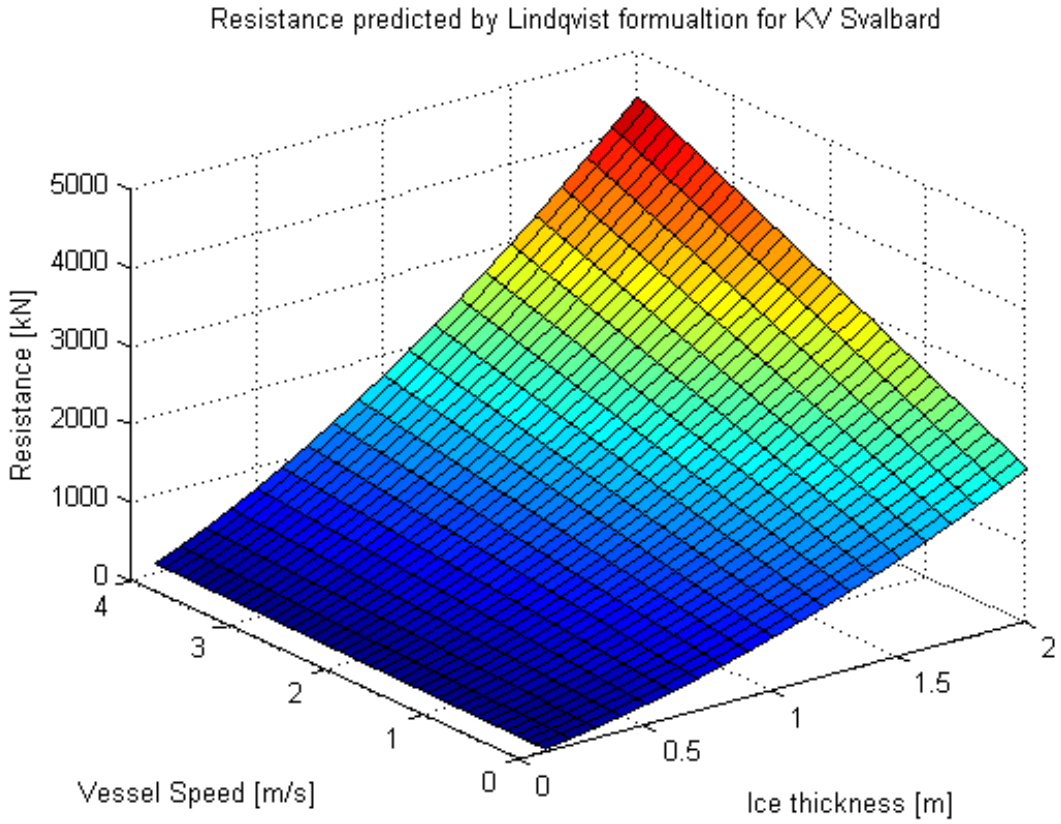

Figure 4-4: Lindqvist resistance as function of ice thickness and speed

It is noted from Figure 4-4 that the resistance is zero for zero ice thickness, also with non-zero speed, which is not realistic. The speed dependency is described as "*To simple and requires refinement*" by Lindqvist ([1], page 730), and it is evident that the model does not properly describes the resistance as ice thickness approaches zero.

4.3 Riska et al. [2]

This more recent paper (from 1997) focuses mainly on resistance in ice channels, which is not relevant for this thesis, but has a rather small chapter regarding navigation in level ice, which is highly relevant.

The fundamental concept in this model is decoupling of open water resistance and ice resistance, where the open water resistance is assumed to be known, as seen in eq.(4.6). The validity of this assumption is outside the scope of this thesis.

The formulation is based on a set of empirical coefficients, derived from full- scale tests of a number of ships in ice conditions in the Baltic Sea. The main resistance formula is given in eq. (4.7), while constants are found in eq. (4.8) and Table 4-1.

$$R_{tot} = R_{ice} + R_{openwater} \tag{4.6}$$

$$R_{ice} = C_1 + V \cdot C_2 \tag{4.7}$$

$$C_1 = f_1 \frac{1}{2\frac{T}{B}+1} BL_{par}h_i + (1+0.021\phi)\left(f_2 Bh_i^2 + f_3 L_{bow}h_i^2 + f_4 BL_{bow}h_i \right)$$
$$C_2 = (1+0.063\phi)\left(g_1 h_i^{1.5} + g_2 Bh_i \right) + g_3 h_i \left(1+1.2\frac{T}{B} \right)\frac{B^2}{\sqrt{L}} \quad (4.8)$$

where V, B, T and L are vessel speed, breadth, draught and length, h_i is ice thickness, ϕ is the stem angle in degrees and L_{bow} and L_{par} are the length of bow and parallel sides section, respectively. The formulation assumes a linear relationship between vessel speed and ice thickness, similar to Lindqvist. An important difference is however that Riska does not normalize the velocity, which may influence the result to some degree.

Table 4-1: Constants in Riska formulation for Ice resistance in level ice

Constants		
name	value	unit
f1	0,23	[kN/m^3]
f2	4,58	[kN/m^3]
f3	1,47	[kN/m^3]
f4	0,29	[kN/m^3]
g1	18,9	[kN/(m/s*m^1,5)]
g2	0,67	[kN/(m/s*m^2)]
g3	1,55	[kN/(m/s*m^2,5)]

Due to the extensive use of empirical constants, much of the physical meaning of the formula is lost, but some parameter dependency has been investigated.

4.3.1 Speed and ice thickness dependency of the resistance estimate

As one would assume, these two parameters have high influence on the resistance. In Figure 4-5 these two parameters have been plotted against the resulting resistance for KV Svalbard. The figures show that the resistance is increasing linearly with speed, and cubic with ice thickness.

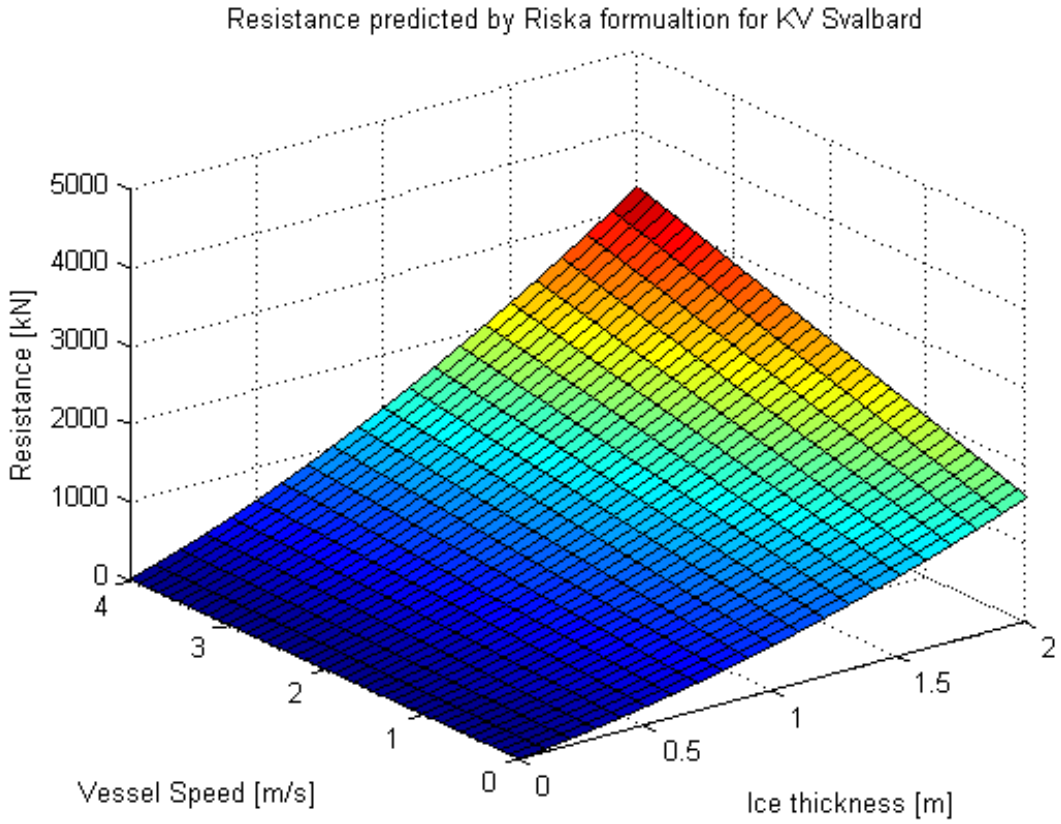

Figure 4-5: Riska ice resistance as function of speed and thickness

It is also worth noting that the Riska formulation gives significant less estimate of ice resistance for high ice thickness and vessel speed (maximum resistance estimated by Lindqvist is 4.4 MN, while Riska estimates 3.25 MN for the same vessel speed and ice thickness).

4.4 Parameter sensitivity analysis

In this section, the sensitivity of both Riska and Lindqvist formulation with regard to selected parameters is investigated. The parameters that have been analyzed are all to a varying degree difficult to determine, meaning that there may be an error in the parameter value that has been used for calculation. For discussions regarding the resistance dependency of basic ship dimensions, see [1, 2]. When only one of the resistance formulations includes the parameter, this is commented upon.

The sensitivity is described as the ratio between calculated estimate and a reference estimate for KV Svalbard with given speed and ice thickness. This is summarized in Table 4-2, and shown in greater detail throughout this section. Sensitivity plots for a wider range of combination of speed and ice thickness is shown in appendix B**.**

It should also be noted that some of these calculations are somewhat arbitrary, as one cannot change one ship parameter 50% independently of all other parameters. It will however illustrate the relative importance of the variables.

Table 4-2: Summary of parameter dependency in resistance formulations
The dependency is shown as a ratio between calculated resistance prediction with changed parameter, and resistance prediction with original value. This means that if bow angle ϕ is reduced to 50%, Lindqvist resistance estimate is reduced to 78%, and Riska resistance estimate is reduced to 83% (for the low resistance scenario)

		Low Resistance		Medium Resistance		High Resistance	
		h = 0,5 [m] v = 0,5 [m/s]		h = 1,5 [m] v = 2,5 [m/s]		h = 2,5 [m] v = 4,5 [m/s]	
Parameter	change factor	Lindqvist	Riska et al	Lindqvist	Riska et al	Lindqvist	Riska et al
Bow angle ϕ	0,5	0,78	0,83	0,67	0,81	0,64	0,8
	1,5	1,47	1,17	1,69	1,19	1,76	1,2
Ice flexuaral strength σ	0,5	0,79	-	0,68	-	0,65	-
	1,5	1,21	-	1,32	-	1,35	-
Waterline entrance angle α	0,5	1,34	-	1,41	-	1,41	-
	1,5	0,94	-	0,92	-	0,92	-
Friction coefficient μ	0,5	0,76	-	0,79	-	0,8	-
	1,5	1,24	-	1,22	-	1,22	-
Length of bow section L_{bow}	0,5	-	0,73	-	0,85	-	0,89
	1,5	-	1,27	-	1,15	-	1,11
Length of parallell sides section L_{par}	0,5	-	0,91	-	0,96	-	0,97
	1,5	-	1,09	-	1,04	-	1,03

4.4.1 Bow angle φ

As shown in Figure 4-6, both Riska and Lindqvist formulation are sensitive to change in bow angle ϕ. A 20% increase in the bow angle ϕ gives a 20% increase in Lindqvist resistance, and 8% increase in Riska resistance for moderate speed and ice thickness. The trend is the same for all load cases, but the magnitude varies. For high speed and large ice thickness, the sensitivity of resistance for change in ϕ is larger, and for low speed and ice thickness, smaller. Sensitivity plots for additional load cases are shown in appendix C.1.

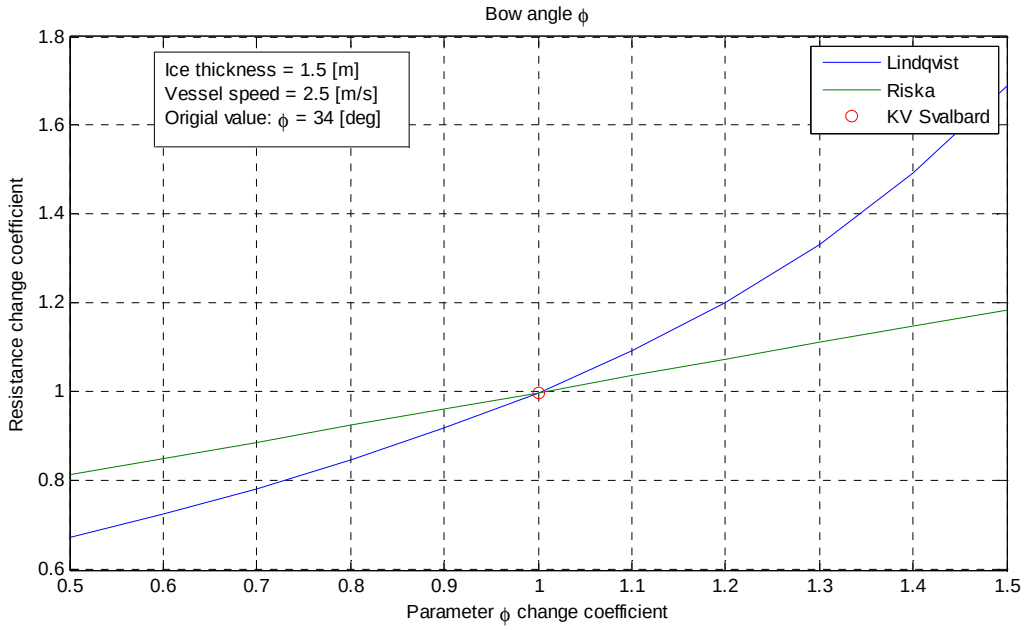

Figure 4-6: Sensitivity of resistance estimate for change in bow angle ϕ

4.4.2 Ice bending strength σ

Riska has chosen to include all mechanical properties of ice in a set of equation constants, meaning that the influence from bending strength σ is unclear. It is however natural to assume that the influence of ice strength will be in the same order of magnitude for both models, making ice bending strength an important parameter. In Figure 4-7, the sensitivity of the Lindqvist formulation to a change in σ is shown. It is seen that a 15% change in bending strength gives a 10% change in resistance. Sensitivity plots for other load cases are shown in C.3

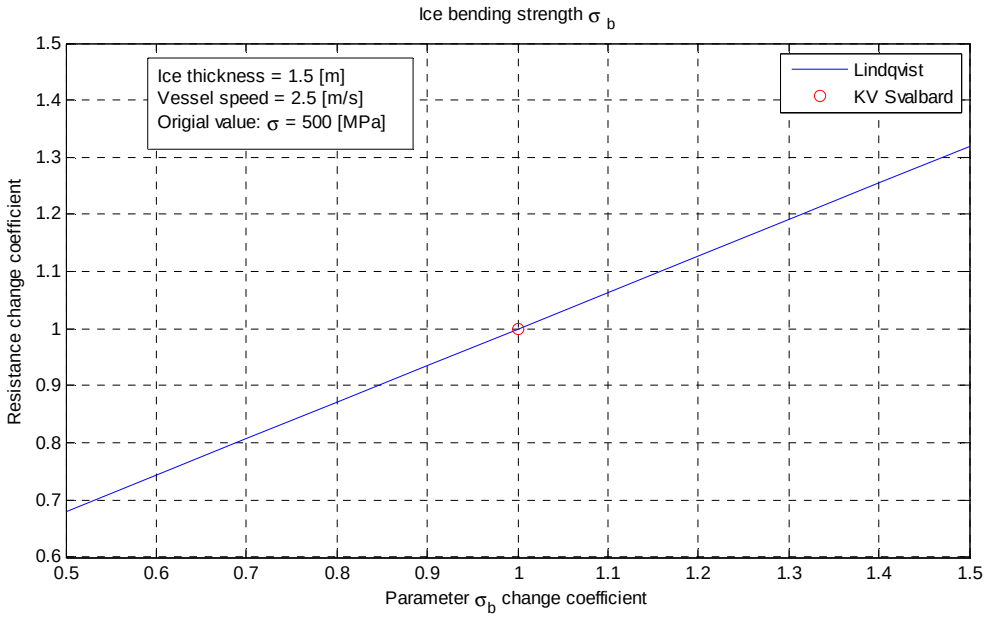

Figure 4-7: Sensitivity of resistance estimate for change in bending strength sigma

4.4.3 Waterline entrance angle α

The waterline entrance angle α is a part of the Lindqvist formulation, but not the Riska formulation. Riska arguments for neglecting this parameter since its importance is disputed ([2], p 36).

The Lindqvist resistance prediction is sensitive to a change in α, as shown in Figure 4-8. It is noted that a reduction in waterline angle will increase the resistance. The physical explanation for this is that a reduction in waterline angle α will give an increased angle between surface normal and vertical (ψ) for constant bow angle ϕ, and thereby influence resistance. This follows from the definition of ψ in Figure 4-1. Additional sensitivity plots are shown in appendix C.2

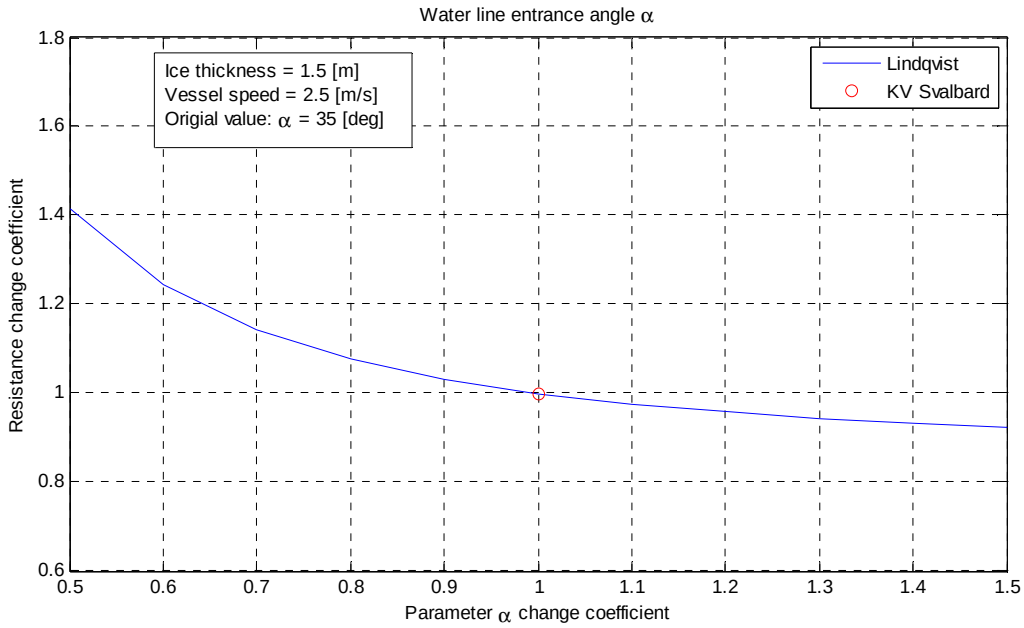

Figure 4-8: Sensitivity of resistance estimate for change in water line entrance angle

4.4.4 Ice friction coefficient μ

As with bending strength, this parameter is included in the equation constants for the Riska formulation. Figure 4-9 shows how the Lindqvist formulation is influenced by change in friction between ship hull and ice. The influence is almost constant for varying speed, and is somewhat dependent on ice thickness. Other relevant sensitivity plots are shown in appendix C.4.

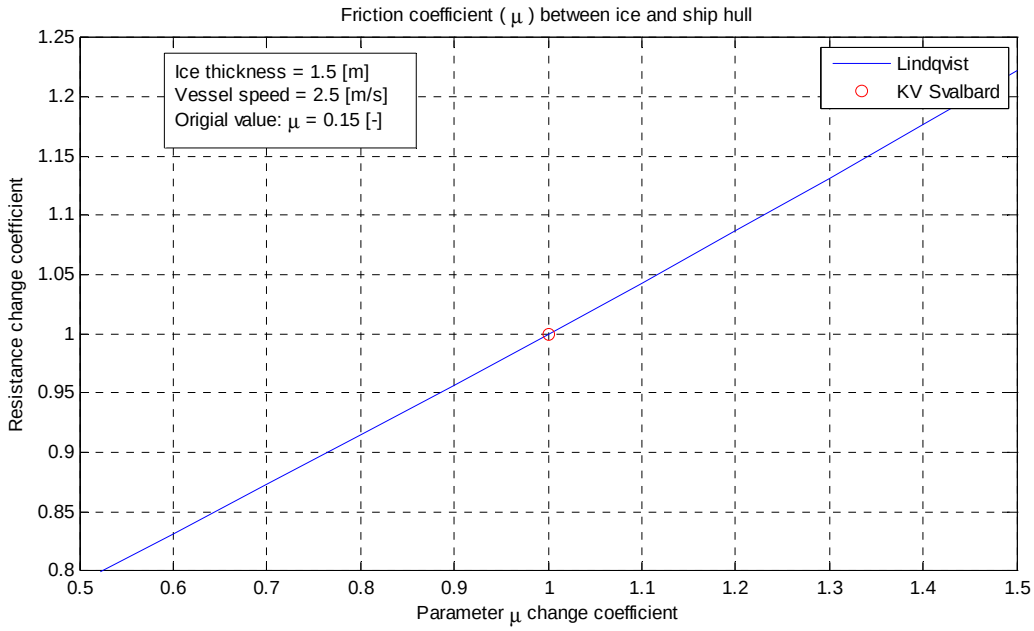

Figure 4-9: Sensitivity of resistance estimate for change in friction coefficient

4.4.5 Bow section length

The bow section length is one of the length parameters in the Riska formulation. It is seen from Figure 4-10 that a reduction in bow length will reduce the resistance. It is important to note,

however, that this is only valid if all other parameters are kept constant, which is unlikely (bow length cannot be changed significantly without changing main particulars, vessel displacement or hull angles). The change in sensitivity is small for changing ice thickness, but varies with changing speed (largest sensitivity for small speeds). Additional sensitivity plots are shown in appendix C.5

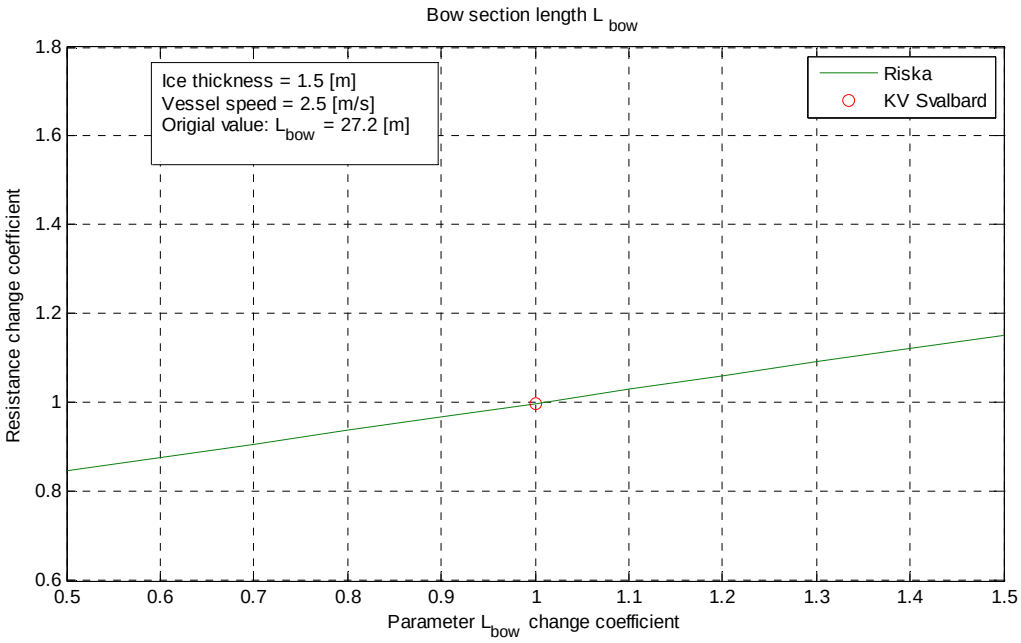

Figure 4-10: Sensitivity of resistance estimate for change in bow section length

4.4.6 Length of hull section with parallel sides

The other length parameter apart from the total length in the Riska formulation is length of hull with parallel sides. Figure 4-11 show that the sensitivity of the resistance prediction for change in this parameter is low, 10% change of parameter gives a 1% change in resistance. The sensitivity is dependent on both speed and ice thickness, with relatively high sensitivity for low speed and ice thickness (low resistance) and relatively low sensitivity at high speed and ice thickness. But the parameter has overall a small influence of the resistance (a 10% change in the parameter will give between 2% and 0.5% change in resistance). Additional sensitivity plots are shown in appendix C.6

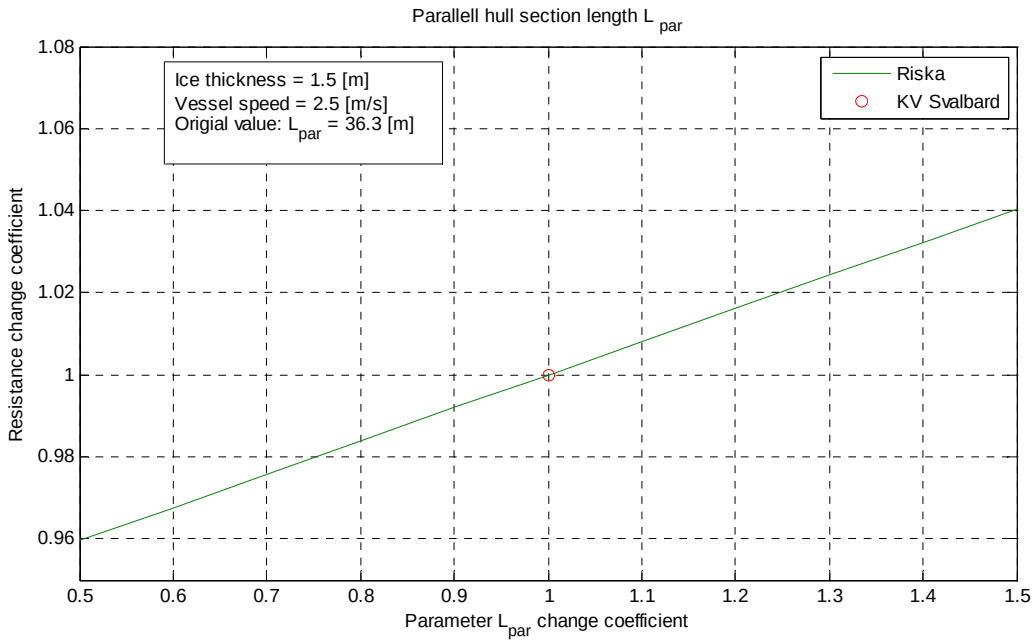

Figure 4-11: Sensitivity of resistance estimate for change in length of section with parallel sides

4.4.7 Sensitivity conclusions

The bending strength of ice is found to have a large influence on the predicted resistance by the Lindqvist formulation. The influence in the Riska resistance formulation is unclear since it is included in the constants, but it may be assumed to be in the same order of magnitude. When this is seen in relation to the difficulties in obtaining accurate values for ice bending strength, it is clear that one of the important uncertainties in the models are the ice bending strength.

Some of the geometrical parameters does also influence the predicted ice resistance significantly, in particular the bow shape angles. These have been difficult to obtain, since detailed drawings of the ship is not publicly available.

5 Estimation of ship resistance from measurements

In order to evaluate the analytical formulations, the resistance for KV Svalbard has to be estimated from measurements. In this section the necessary formulas for this purpose will be derived.

5.1.1 Conservation of energy

In order to estimate the total resistance on the ship, the principle of conservation of energy is applied. If the ship and the surrounding ice are considered to be a closed system, the only change in energy should be caused by work done either by the system or on the system. Mathematically, this can be formulated as

$$\Delta E_{sys} = W \tag{5.1}$$

where W is the work done on the system and ΔE_{sys} is the change in energy for the system. In Figure 5-1 this is schematically shown for a system with change in velocity from state 1 to state 2.

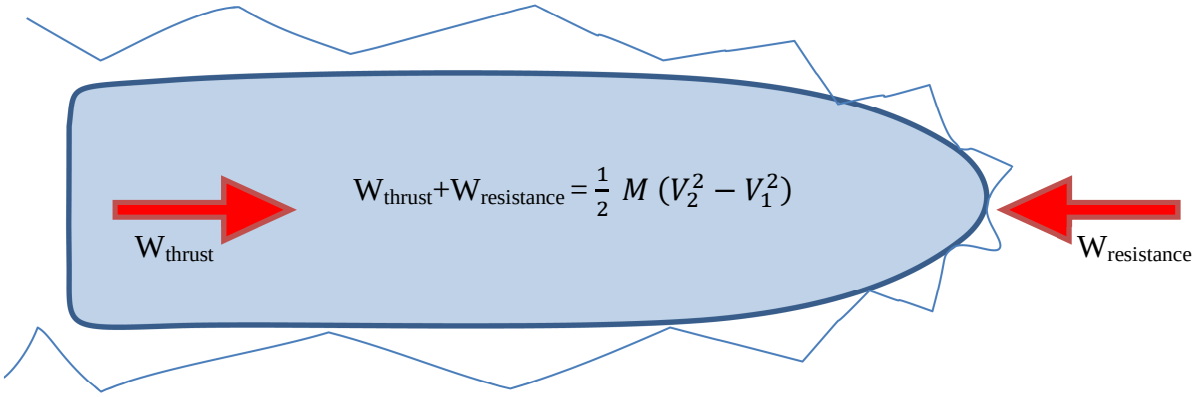

Figure 5-1: Conservation of energy from state 1 to state 2 in a system with acceleration

5.1.2 Change in kinetic energy

The change in kinetic energy of the ship during time step is found by integrating Newton's second law over one time period, as shown in eq. (5.2). This will describe the change in kinetic energy as a function of mass and velocity at the beginning and end of the time step.

$$\Delta E_{kinetic} = \int_1^2 Ma \cdot dt = \left[\frac{1}{2} M \cdot V^2\right]_1^2$$
$$\Delta E_{kinetic}^{k} = \frac{1}{2} M \left(V_2^{\,2} - V_1^2\right) \tag{5.2}$$

Here M is vessel mass, V is velocity and $E_{kinetic}$ is kinetic energy.

5.1.3 Work done by propulsion

The net propeller thrust is difficult to measure, since it requires advanced measurement instrumentation in the area surrounding the propeller, or model tests describing the efficiency of the propeller (known as *propeller curves*). Unfortunately, none of these are available. What can

be measured, however, is the energy delivered to the azimuth thrusters ($P_{delivered}$). This can then be used to give a first approximation to the thrust, as described in eq. (5.3). The use of delivered power as a measure of thrust is a large simplification, which is further discussed in section 5.2.

$$W_{Thrust} \approx \int_1^2 P_{delivered} \cdot dt \tag{5.3}$$

5.1.4 Work done by resistance

The resistance work is assumed to the only external force working on the system, which gives the following equation for resistance work

$$\begin{aligned} W_{res} &= W_{Thrust} - \Delta E_{kinetic} \\ W_{res} &\approx \int_1^2 P_{delivered} \cdot dt - \frac{1}{2} M \cdot \left(V_2^{\,2} - V_1^{\,2} \right) \end{aligned} \tag{5.4}$$

5.1.5 Resistance force

The average resistance force in one time step is found from the definition of work

$$W = \int_1^2 F ds \tag{5.5}$$

Using this and the result from eq. (5.4), the average force can be approximated as shown in eq. (5.6).

$$F = \frac{W_{res}}{\int_1^2 ds} = \frac{\int_1^2 P_{delivered} \cdot dt - \frac{1}{2} M \cdot \left(V_2^{\,2} - V_1^{\,2} \right)}{\int_1^2 ds} \tag{5.6}$$

F is the resistance force and ds are the distance covered during the timestep. This formula is implemented in Matlab using a build-in function for trapezoidal numerical integration, and the resistance force found is taken as the mean resistance in the given time period.

5.2 Simplification discussion

The assumption that the power delivered to the propeller is equal to the power output from the propeller is a large simplification. This simplification is made because it has not been possible to achieve enough information about the propulsion system of the vessel to make a good assumption of propeller efficiency. In order to improve this part of the resistance formulation, the propeller curves would have to be obtained from the Norwegian Coast Guard, something that has proven to be difficult. The simplification will result in an artificially high resistance, as the propeller efficiency is less than 1.

6 Data selection

The data set available is from a scientific voyage made by the Norwegian coast guard vessel *KV Svalbard* in 2007. During this voyage the vessel aided in many different scientific projects, the *Ice Load and Monitoring project (ILM*) being one of them. This means that a considerable portion of the collected data is unsuitable for the purpose of this thesis, as the vessel did not encounter stable conditions at all times. This section will describe the method used to identify time segments applicable for the purpose of this master thesis.

6.1 Selection criteria

In order to avoid biased data, an automated routine was developed for selection of data. Homogeneity in a statistical sense was chosen as a criterion for data selection. This is measured by the *coefficient of variation*, which is defined by eq.(6.1),

$$CV = \frac{\sigma}{|\mu|} \tag{6.1}$$

where σ and μ are the standard deviation and mean value.

This is considered to be a good measure of how much a selected< variable changes over the selected time span. The variables that are analyzed are *vessel speed* and *heading, ice thickness,* and *propeller engine power.* Table 6-1 describes the threshold values of coefficient of variation for the selected parameters. These values may be changed in the input file for the Matlab program.

Table 6-1: Maximum coefficient of variation for selected parameters

Parameter	Maximum coefficient of variation
Vessel speed	0.15
Ice thickness	0.6
Vessel heading	0.4
Propeller engine power	0.2

The high allowed coefficient of variation for the ice thickness is needed since the data has high variation of this variable. This is caused by the sensitivity and sampling frequency of the ice thickness sensor. The high sampling rate generates large amounts of data with a considerable scatter, and therefore relatively high standard deviation. As long as the speed and engine power is stable, the data is considered to be suitable for this thesis.

6.1.1 Removal of irrelevant data points

Some of the data points that were selected by the automated selection procedure had ice thickness values in the range of 7-8 meters. This is significantly larger than the expected maximum thickness of level first-year ice, which is approximately 2 meters [5]. This leads to the conclusion that these data points are either measurements errors, or encounters of multi-year ice ridges. In both cases the data are considered to be irrelevant for this thesis. The automated selection process removes all data points with ice thickness above 3 meters, which is believed to be a large enough margin to include all measurements with level ice.

6.2 Sampling time length

Resistance as a fuel consumption predictor is not an instantaneous value, but an average value over a certain time. The choice of sampling time length has significant influence on the quality of the results. A suggested time length is the time it takes the vessel to travel a few ship lengths, translating to approximately 60- 90 seconds [18]. When applying a time step length of 90 sec together with the coefficient of variation thresholds listed in Table 6-1, the Matlab program selects a total of 451 data points. Visual inspection of the selected data (see Figure 6-1) indicates that the data selected has rather low variation, and that the chosen thresholds are reasonable.

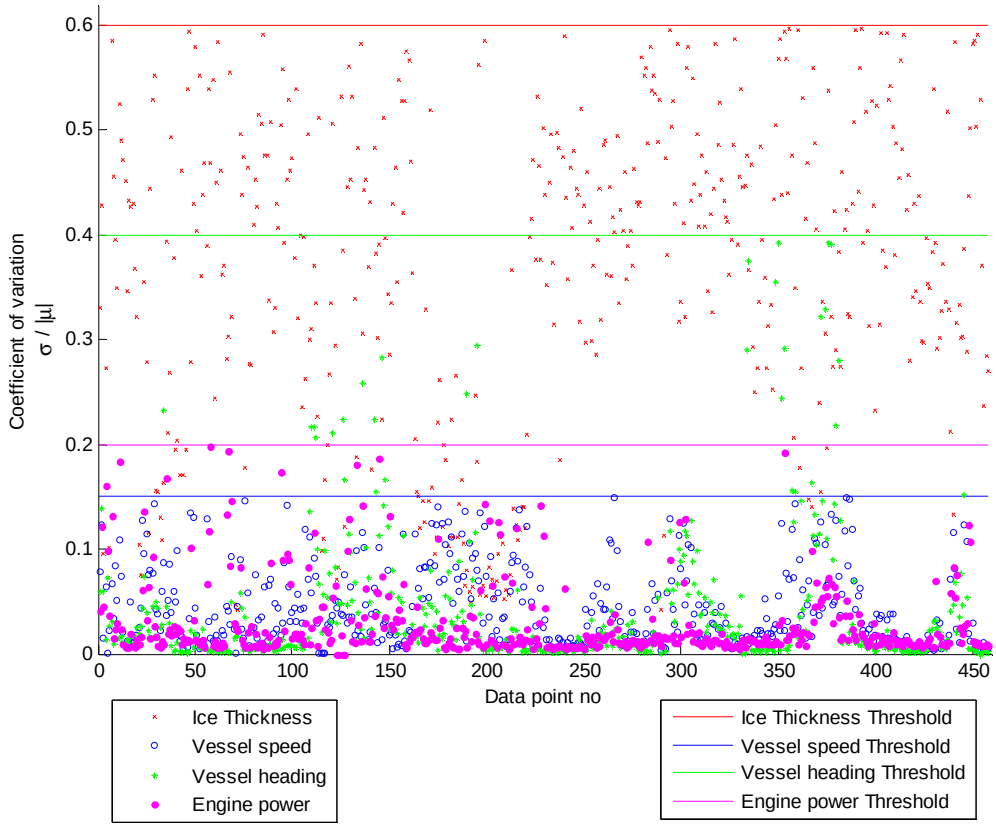

Figure 6-1 Coefficient of variation for selected parameters with threshold level for all data points

6.2.1 Splitting of time steps

In order to increase the number of observations, the selected data points are splitted in three, each with 30 sec duration. This increases the number of data points, while still ensuring that all data used have sufficiently low variation over a period of 90 seconds.

6.3 Data selection summary

A number of 30 second time sequences have been selected for this thesis. They are selected based on homogeneity in a statistical sense over time. The homogeneity is ensured by comparing the coefficient of variation for selected parameters with a predetermined threshold level. Some data points have been considered to be irrelevant for this thesis, and are therefore neglected.

7 Open water resistance

In order to be able to compare the calculated resistance with the analytical predictions, some assumptions have been made about the open water resistance. Riska et al [2] assumes that the ice resistance and open water resistance are independent, and can be calculated separately. This chapter will describe how the open water resistance is estimated for the vessel KV Svalbard.

In order to find the open water resistance, data points without ice where collected, and the resistance estimated. This was done using the same automated routines in MATLAB that were used to find the ice resistance. For the relative low vessel speeds in question (below 4 [m/s] or 8 [knots]), ship resistance is approximately proportional to the vessel speed squared [11]. Using this, a least square regression has been performed in order to predict open water resistance as a function of vessel speed.

In order to control the quality of the regression, a simple data cross validation procedure were adopted. 50% of the data points were selected for regression, while the remaining data points were used to test the regression.

The two data sets are plotted along with the obtained regression curve in Figure 7-1.

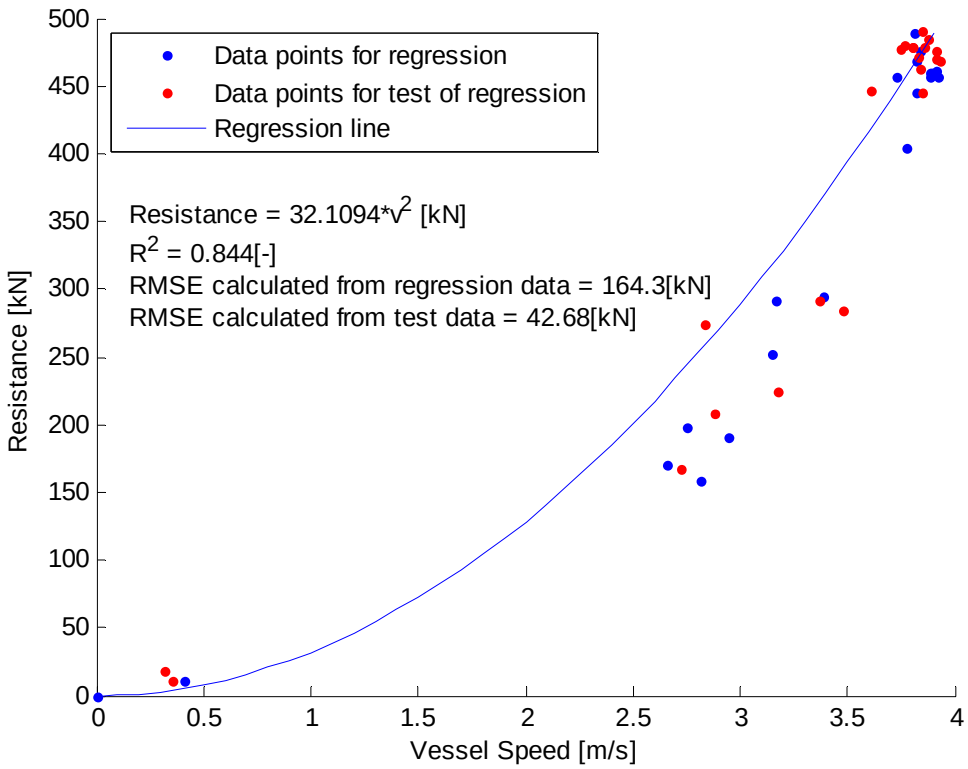

Figure 7-1: Open water resistance as a function of speed.
Blue data points are used to calculate the regression curve, while the red data points are used to test the quality of the regression

It is seen that the data points follow the regression curve quite very well, and the coefficient of determination (R^2) is reasonably high (0.84). This may be influenced by the large number of data points at the same velocity, and approximately the same resistance. It is seen that the data does

not describe the mid-level data points at a satisfactory accuracy. However, without additional data, this is believed to be the best model available.

7.1 Quality of regression

A simple way of controlling the quality of a regression is to test the regression against data points not used to calculate the regression itself. This is done by dividing the data in two sets, and performing the regression on one of the data sets. The resulting regression line is then compared with the other data set, and the *Root Mean Squared Error (RMSE)* found, using eq. (2.3). This is a measurement of the average deviation between a measured resistance and the predicted resistance for the same speed.

$$RMSE = \sqrt{E\left(\left(\hat{y} - y\right)^2\right)} = \sqrt{\frac{1}{n}\sum_{i=1}^{n}\left(\hat{y}_i - y_i\right)^2} \tag{7.1}$$

The resistance model has satisfactory accuracy, also when applied to data not used to create the model.

7.2 Error sources

The open water resistance model is based on the assumption of no loss of energy from azimuth engine to net thrust. This is a rather large simplification, which is discussed further in section 5.2, regarding ice resistance estimate. It also neglects other relevant predictor variables for vessel resistance, such as wind and waves. These are neglected since they were not logged during the voyage.

Another source of error is the fact that almost all data points have approximately the same velocity, which is assumed to be the operational speed. This makes it difficult to control the regression line in the domain below this speed, since few data points exist. This error source is believed to be of lesser importance compared to the thrust simplification.

8 Statistical analysis

After selecting measurement data as described in chapter 6, the relationship between the estimated resistance based on measurements and the estimated resistance from the formulations from Riska et al. and Lindqvist has been analyzed using various statistical tools.

For the data in this thesis, the purpose of the statistical analysis is to be able to predict the ratio between resistance estimated from measurements and resistance predicted by analytical formulations (made by Riska or Lindqvist), as shown in eq. (8.1).

$$ratio = \frac{R_{measurements}}{R_{Riska/Lindqvist}} \tag{8.1}$$

The ratio is denoted *Riska ratio* if the resistance estimated from measurements is compared with Riska resistance estimation and *Lindqvist ratio* if the estimated resistance from measurements is compared to Lindqvist resistance estimation. The vessel speed and ice thickness are chosen as predictor variables for this ratio.

The ratio will be described first as a regression surface in section 8.1, then by means of statistical distributions in sections 8.3 and 8.4. Sources of discrepancy are discussed in section 8.5, while a subsection of the data is analyzed in section 8.6.

8.1 Regression analysis

The goal of regression analysis is to describe the relationship between two or more variables, where a dependent variable is described as a function of one or more independent variables. As the data available include vessel speed and ice thickness, a reasonable approach is to fit a regression surface to both the Riska and Lindqvist ratio as function of thickness and speed. The simplification introduced by this approach is described in the end of this section.

8.1.1 Riska ratio

Using the *surface fitting tool* in Matlab (Curve fitting toolbox) a polynomial surface is fitted to the Riska ratio. After some experimenting, a second order surface was selected, based on a compromise between obtaining a high R^2 – value and avoiding overfitting of the model. The latter means artificially increasing the number of terms in order to improve the fit without considering the physical implications, and has been judged by visual inspection of fitted surface outside the data domain. Due to significant scatter in the data the robust fit method *bisquare* was chosen. This method is discussed in section 8.1.3.

The obtained surface is shown in Figure 8-1, while the residuals (distance from data points to calculated surface) are shown in Figure 8-2.

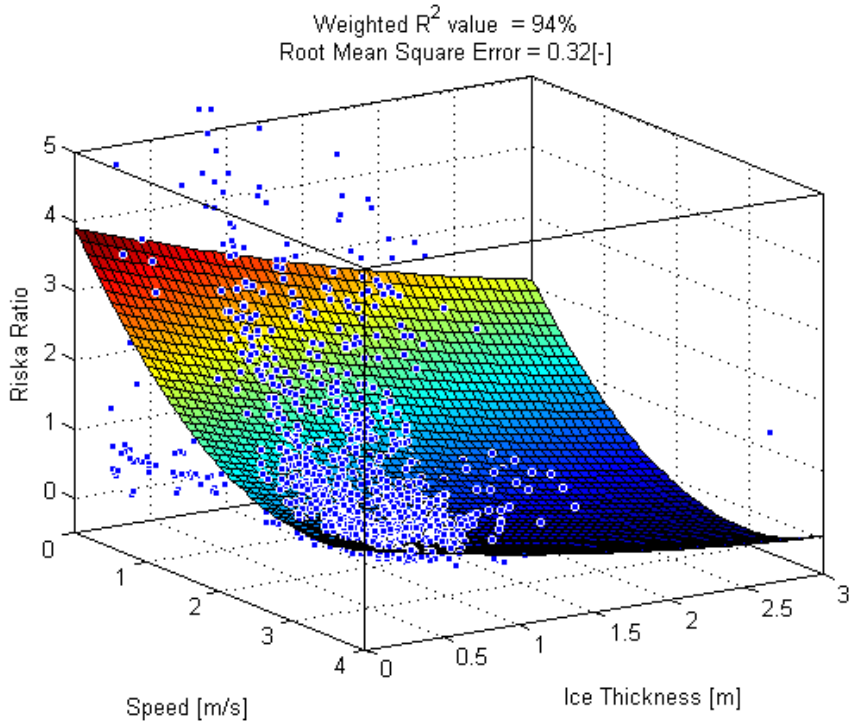

Figure 8-1 Riska ratio fitted to a second order surface using bisquare robust fitting

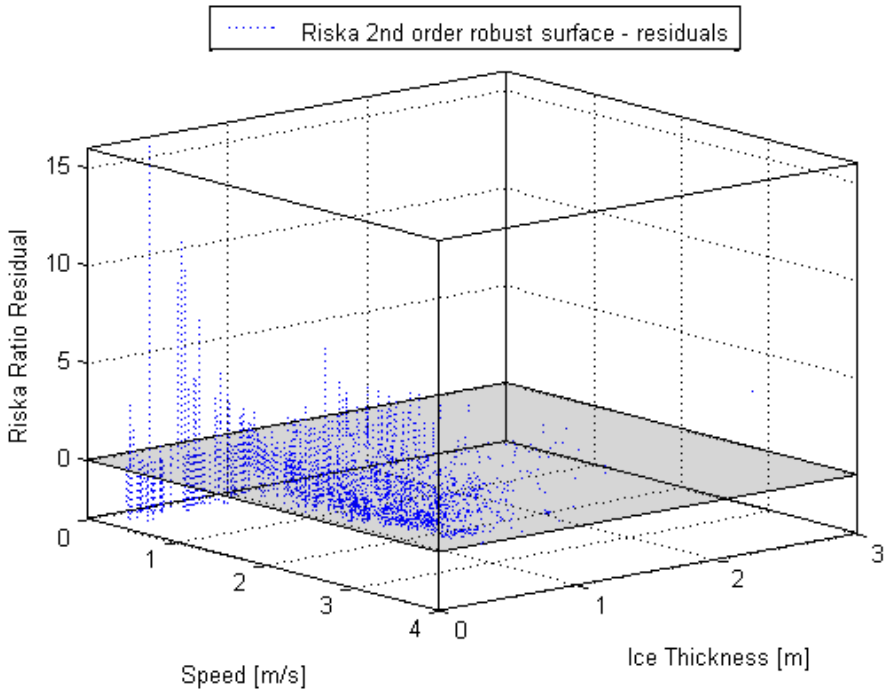

Figure 8-2 Residuals from fitting Riska ratio to second order surface (Figure 8-1).

The residuals in Figure 8-2 do not seem to be randomly distributed around zero, but appears to be larger for low speeds than for higher speeds. This indicates that there may be information the regression fit does not account for, which is further discussed in section 8.1.4.

Table 8-1 show various parameters used to describe the goodness of fit for a regression. It is worth noting that the R^2 value is rather high, indicating that a large part of the variance in the data is described by the model. This is not supported by visual inspection of the plot, and it is

found that the choice of robust least squares method increases the R^2 value. This is further discussed in section 8.1.3, including the calculation procedure for the goodness of fit parameters.

Table 8-1: Goodness of fit parameters for Riska surface fit:

Sum of squares due to error	156,1893
R^2	0,9347
Root mean square error	0,3398

Eq. (8.2) and Table 8-2 gives the equation for the fitted surface in Figure 8-1 including confidence bounds.

$$Surface_{RiskaRatio} = p_{00} + p_{10} \cdot V + p_{01} \cdot h + p_{20} \cdot V^2 + p_{11} \cdot hV + p_{02} \cdot h^2 \tag{8.2}$$

Table 8-2 Coefficient values for eq. (8.2) including 95% confidence bounds

Coefficient	Estimated value	Lower 95% confidence bound	Higher 95% confidence bound
p_{00}	4,240	4,080	4,399
p_{10}	-1,730	-1,852	-1,607
p_{01}	-1,815	-2,035	-1,595
p_{20}	0,282	0,255	0,309
p_{11}	-0,021	-0,090	0,048
p_{02}	0,557	0,487	0,628

8.1.2 Lindqvist ratio surface fit

The Lindqvist ratio is fitted to a surface using the same procedure as described in the previous section. The fitted surface is given in Figure 8-3, while the residuals are given in Figure 8-4.

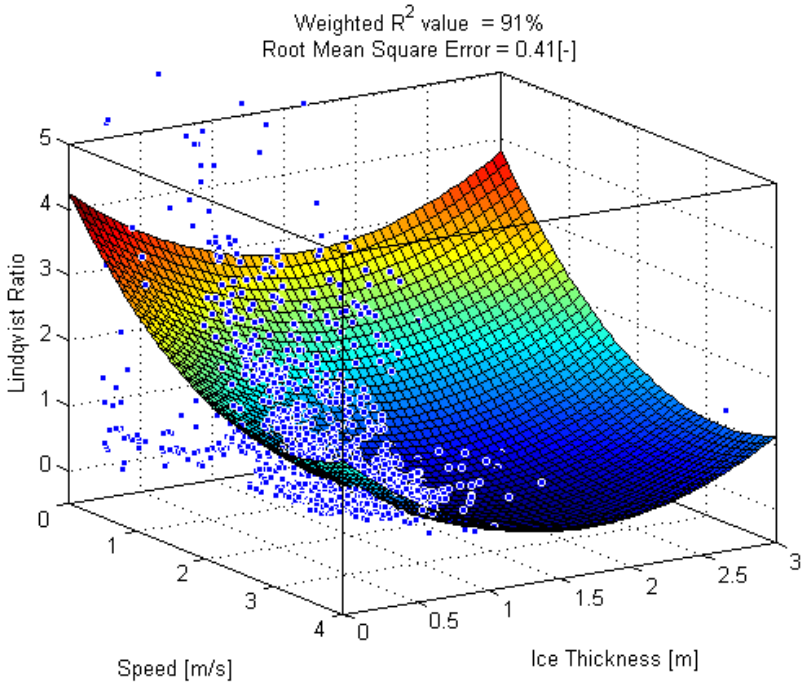

Figure 8-3 Lindqvist ratio fitted to a second order surface using bisquare robust fitting

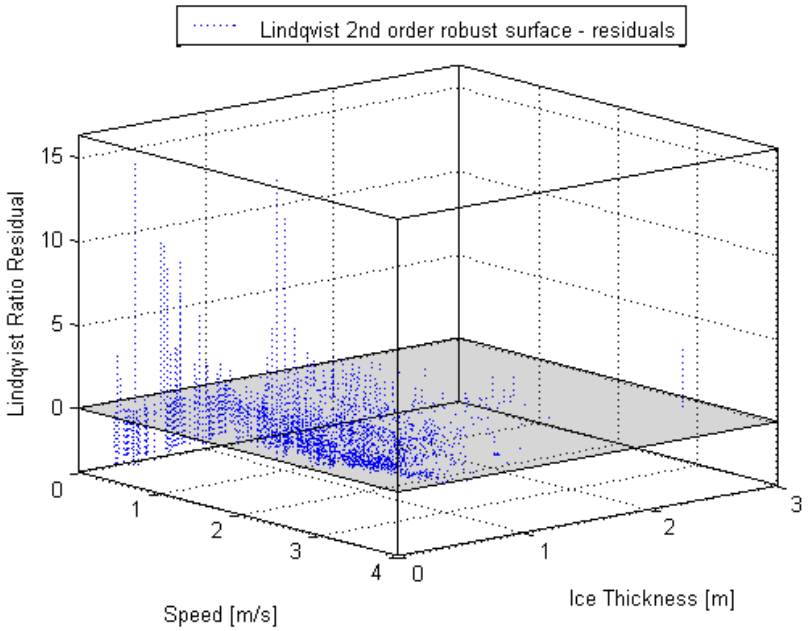

Figure 8-4 Residuals from fitting Lindqvist ratio to second order surface (Figure 8-3)

As with the fitting of the Riska ratio (section 8.1.1), the residuals do not appear to be randomly distributed, but appears to be decreasing as speed increases. This indicates that the regression model is not complete, and thus does not account for all relevant parameters. Unknown parameters which may influence the resistance is discussed in section 4.4.

The goodness of fit parameters is given in Table 8-3.

Table 8-3 Goodness of fit parameters for Lindqvist ratio fitted to surface

Sum of squares due to error	231,7159
R^2	0,9123
Root mean square error	0,4138

By comparing the goodness of fit parameters for both Riska and Lindqvist ratios (see Table 8-1 and Table 8-3), it is seen that the surface fitted to the Riska ratio has a better fit than the surface fitted to the Lindqvist ratio. The reasons for this difference are not clear, but a possible explanation may be the open water resistance part, which is not included in the Lindqvist formulation (resulting in a underprediction of resistance for thin ice). The differences between the two different formulations are discussed in detail in chapter 1. The surface polynomial is given by eq. (8.3) and Table 8-4.

$$Surface_{LindqvistRatio} = p_{00} + p_{10} \cdot V + p_{01} \cdot h + p_{20} \cdot V^2 + p_{11} \cdot hV + p_{02} \cdot h^2 \qquad (8.3)$$

Table 8-4: Coefficient values for eq. (8.3) including 95% confidence bounds

Coefficient	Estimated value	Lower 95% confidence bound	Higher 95% confidence bound
p_{00}	4,299	4,168	4,43
p_{10}	-2,011	-2,112	-1,911
p_{01}	-1,173	-1,354	-0,9925
p_{20}	0,3013	0,2793	0,3232
p_{11}	0,1211	0,0647	0,1775
p_{02}	0,1725	0,1146	0,2304

8.1.3 Bisquare robust fit [19]

The *Bisquare robust fit* is an iterative weighted least squares method, and is the default method for robust least squares in MATLAB. Robust methods are used when there is a large amount of outliers (measurement values with large deviance from the mean value). The method minimizes a weighted least square sum, where the weights are calculated based on the distance from the fitted surface to the data point. The fitting follows the following procedure:

1. Fit the model using *Ordinary Least squares method*, with optional user-defined weighting function. This minimizes the sum

$$SSR = \sum_{i=1}^{n} w_i \left(y_i - \hat{y}_i \right)^2 \tag{8.4}$$

   where w_i is the weight of point i, y_i is the data value and $\hat{y}_i$ is the estimated value. For this thesis all weighting functions has been set to 1.0 as a start value by user.
2. Compute the *adjusted residuals*, and standardize them. The adjusted residuals are given by eq. (8.5)

$$r_{adj} = \frac{r_i}{\sqrt{1-h_i}} = \frac{y_i - \hat{y}_i}{\sqrt{1-h_i}} \tag{8.5}$$

   where h_i are *leverages* which down- weight the large residuals, and thus reducing the effect of outliers. The leverages are given by eq.(8.6)

$$h = diag\left(X \left(X^t X \right)^{-1} X^t \right) \tag{8.6}$$

   where *X* is the predictor matrix containing all the independent variable observations (i.e. speed and ice thickness), and *diag* indicates diagonal elements in a square matrix. This procedure was suggested by [20], and will not be discussed in depth. After the residuals are adjusted, they are *standardized* by eq. (8.7)

$$u = \frac{r_{adj}}{K \cdot s} = \frac{r_{adj}}{K \cdot MAD / 0.6745} \tag{8.7}$$

where MAD is the *Median Absolute Deviation* of the residuals, s is the *robust variance* of the residuals and K is a *turning constant*, equal to 4.685.

3. Calculate new weighting function, and compare with the one used in eq. (8.4). The new weights are calculated by eq. (8.8)

$$w_i = \begin{cases} \left(1-(u_i)^2\right)^2 & |u_i| < 1 \\ 0 & |u_i| \geq 1 \end{cases} \tag{8.8}$$

4. If convergence is not achieved, repeat from step 1 using new weights.

The goodness of fit parameters (see Table 8-1 and Table 8-3) are based on the same parameters as the iteration, and are shortly described below. For detailed explanations, see [21].

1.1.1.1 Sum of squares due to error (SSR)

This is a measure of the difference between the fit and the measured response, and is given by eq. (8.4) above. This value is often denoted SSR.

1.1.1.2 R-Square

This statistic measures how well the fit explains the variation in the data set. R-square is the square of the correlation between the true response value and the response value predicted by the fit, and is defined by eq.(8.9), where $\bar{y}$ is the mean true response.

$$R^2 = \frac{\sum_{i=1}^{n} w_i \left(\hat{y}_i - \bar{y}\right)}{\sum_{i=1}^{n} w_i \left(y_i - \bar{y}\right)} \tag{8.9}$$

It is important to note that the R^2 value calculation includes the weights from eq.(8.8), meaning that the R^2 value cannot be compared to R^2 values from ordinary least square regression.

1.1.1.3 Root mean square error

This is an estimate for the standard deviation of the random component of the data (i.e. the part of the data not explained by the regression), and is given by

$$RMSE = \sqrt{E\left(\left(\hat{y} - y\right)^2\right)} = \sqrt{\frac{1}{n}\sum_{i=1}^{n}\left(\hat{y}_i - y_i\right)^2} \tag{8.10}$$

8.1.4 Model errors

As discussed in chapter 4, the resistance predicted by the analytical formulations is dependent on not only ice thickness and vessel speed. Both the mechanical properties of ice (flexural

strength and density) and the friction between ship and ice have significant influence on the resistance prediction. As these parameters are unknown for the time series in question, they have not been accounted for in the regression model. As this is a rather large simplification, it may account for some of the discrepancy between the analytical models and the resistance estimated from measurements. Another source of error is the simplifications used when estimating the resistance from measurements. This is discussed in section 5.2

8.1.5 Section conclusions

The ratio between resistance estimated from measurements and resistance estimated by selected analytical formulations does not appear to be well described by a second- order surface in the vessel speed/ ice thickness domain. The discrepancy between the estimated and predicted resistance may be caused by parameters not accounted for or by an unknown dependency of speed and thickness, which will be investigated in the next sections.

8.2 Dividing the data into subgroups

Based on the discussions in section 8.1 it appears that it may be beneficial to divide the data into smaller subgroups, depending on vessel speed and ice thickness. This will enable fitting of statistical distributions to the data, with the statistical parameters being dependent on speed and ice thickness. It will also make it possible to present the results in 2D, which is more suitable on paper. The division into subgroups is done using Matlab, and the number of subgroups in both speed and ice thickness domain can be specified by the user. This procedure regarding parameter specification for the Matlab script is described in appendix A

Six subgroups in both speed and ice thickness domain has been found to give the desired data stability, while maintaining relatively large data sets. Each data set should contain at least 20 observations in order to be useful for statistical analysis. Scatterplots of the data in each subgroup is produced in order to visually check if any trends occur in the divided data. These plots can be found in appendix A. The number of observations in each subgroup is given by Table 8-5.

Table 8-5: Number of observations in each subgroup.
Subgroups excluded from further analysis are marked with gray background color. Row and column labels in SI units

	h =[0.0,0.5]	h =[0.5,1.0]	h =[1.0,1.5]	h =[1.5,2.0]	h =[2.0,2.5]	h =[2.5,3.0]
V =[0.0,0.7]	41	39	17	6	2	0
V =[0.7,1.3]	21	36	44	22	2	2
V =[1.3,2.0]	37	105	59	13	8	0
V =[2.0,2.7]	119	163	74	9	2	0
V =[2.7,3.3]	222	188	28	2	0	0
V =[3.3,4.0]	54	31	10	0	0	0

8.3 Lognormal statistical distribution

Based on the nature of the data (ratio between two variables that may be normal distributed), a lognormal distribution is a natural first approach. By assuming that the ratio between estimated resistance from measurements and analytical estimates in a subgroup is lognormal distributed with a true mean value μ and standard deviation σ , *maximum likelihood estimators* for mean

value $\hat{\mu}$ and standard deviation $\hat{\sigma}$ can be found. This is done using built-in functions in Matlab, and the procedure is covered in most statistical handbooks, for instance [22].

The assumption of lognormal distribution is tested both by plotting the ratio on a lognormal distribution paper, and by a chi-square test. In order to easily interpret the results, a number of plots are generated, as shown in Figure 8-5. This allows for visual inspection of both the lognormal paper plot and the histogram with lognormal *probability density function (PDF)* curves. A Weibull line is also fitted to the probability plot. This is further discussed in section 8.4.

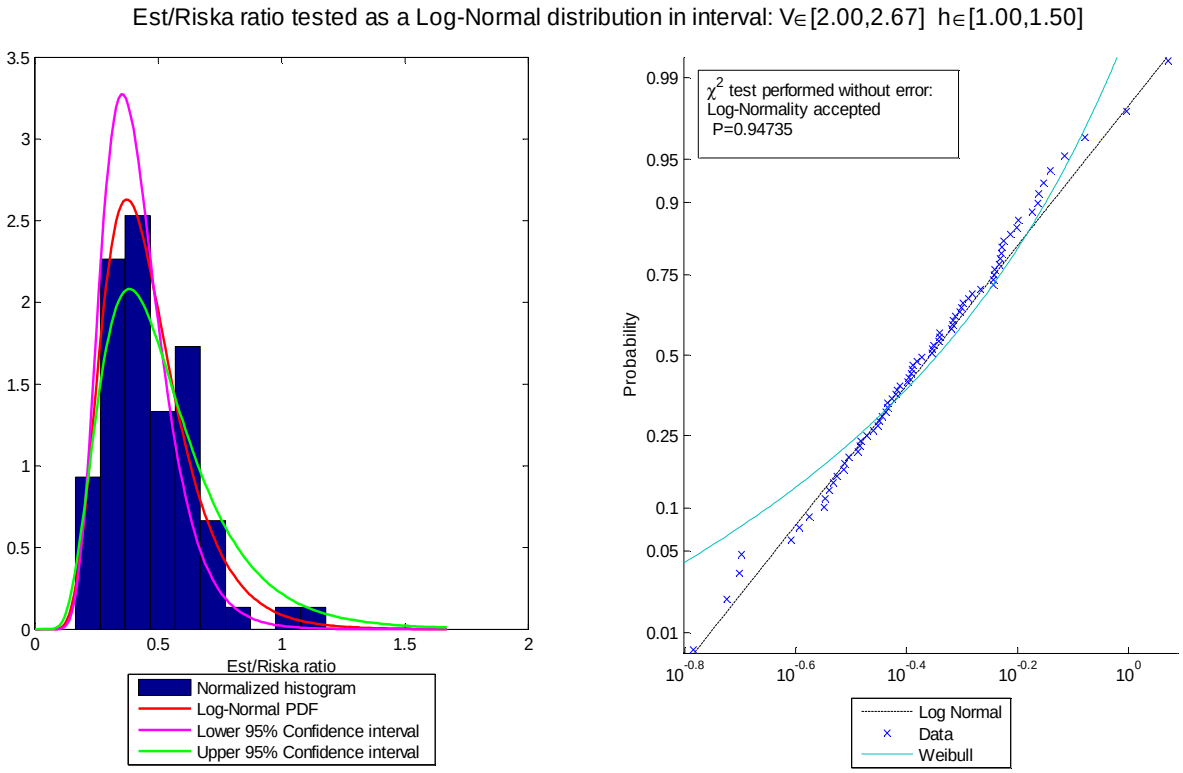

Figure 8-5: Lognormal test for ratio between estimated resistance from measurements and Riska estimate. Vessel speed between 2 and 2.67 m/s, ice thickness between 1.0 and 1.5 m. Lognormal distribution is accepted with 95% confidence for the given data set partition.

As the total number of plots become rather high, some effort has been put into plotting a "residual plot" for the probability fit. This is shown in Figure 8-6 and Figure 8-7. These plot are useful when trying to determine whether or not all data sets are well fitted to the distribution, and to identify trends in goodness of fit (e.g. if all data sets with same ice thickness has poor fit, this is easily identified). For increased readability, all data sets with the same speed interval have the same line color, while all data sets with matching ice thickness have the same line style.

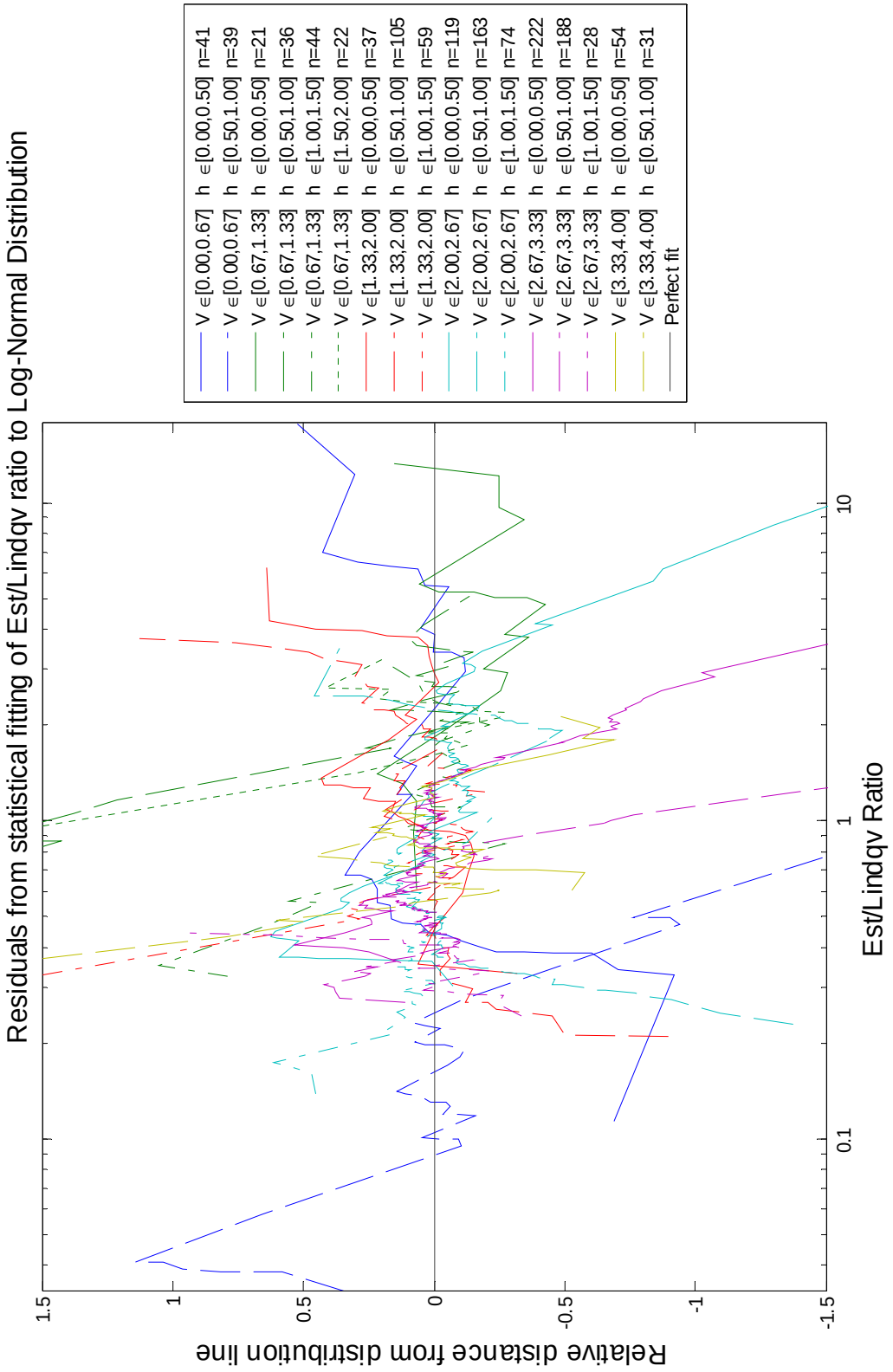

Figure 8-6: Residuals from statistical fitting of the Lindqvist ratio to Log-Normal distribution.
The values on the Y-axis indicate relative distance from the perfect fit line. The plot clarifies data set where the distribution fit is poor (large deviance from zero)

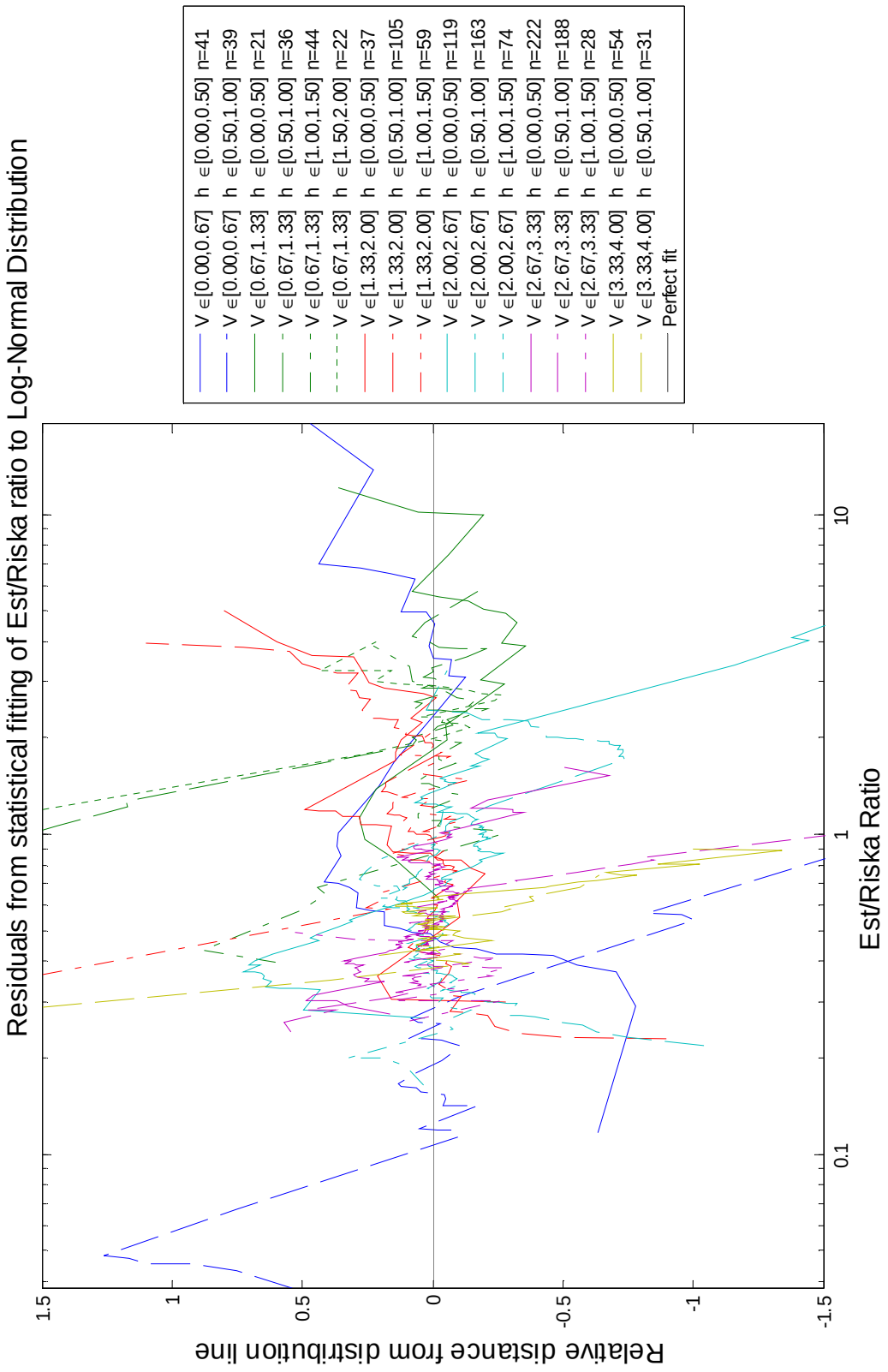

Figure 8-7: Residuals from fitting of the Riska ratio to Log-Normal distribution.
The values on the Y-axis indicate relative distance from the perfect fit line. The plot clarifies data set where the distribution fit is poor (large deviance from zero)

8.3.1 Chi square goodness of fit test

While it is possible to use the residual plots in Figure 8-6 and Figure 8-7 together with all the probability plots (see Figure 8-5 and appendices E and F) to determine if the data follows a lognormal distribution, it is normally recommended to perform a statistical test, called a *goodness of fit test*. The *Chi square test* is one of the most common goodness of fit tests. The idea behind the test is to perform a *hypothesis* test, where the H_0 hypothesis in question is *"this data follows a Lognormal distribution with μ and σ estimated by maximum likelihood estimators"*, while the H_1 hypothesis is *"this data cannot be described by the Lognormal distribution"* The procedure is described in detail in most statistical handbooks, for instance [22]. For the benefit of the reader, a short summary is provided below.

1. Divide the sample space into k separate bins, and calculate the expected number of observations in each bin (denoted e_i) using estimated mean and standard deviation.
2. Count the number of observations in each bin, denoted o_i.
3. Calculate χ^2, which is a random variable whose sampling distribution is chi-squared with *k-m-1* degrees of freedom, where k is number of bins and m is number of parameters estimated from the data.

$$\chi^2 = \sum_{i=1}^{k} \frac{(o_i - e_i)^2}{e_i} \tag{8.11}$$

4. Compare the obtained χ^2 with a tabulated value for desired degree of freedom, and accept the hypothesis if the tabulated value is larger than the calculated value.

The results from the chi square tests on both the Riska and the Lindqvist ratio are given below, in Table 8-6 and Table 8-7. Data sets marked with red background color is rejected as lognormal distribution with 95% confidence, while the data sets with green background color are accepted.

Table 8-6 Chi-square test results for Riska ratio fitted to lognormal distribution.
***Reject* is a logical value, where 1 is true and 0 is false. The cells are also color coded according to this (red and green). *P* is the probability of obtaining the data set in question (or more extreme) if the data comes from a lognormal distribution with the estimated parameters. Subgroups not analyzed according to discussion in section 8.2 are marked with gray.**

	h =[0.0,0.5]		h =[0.5,1.0]		h =[1.0,1.5]		h =[1.5,2.0]		h =[2.0,2.5]		h =[2.5,3.0]	
	Reject	P	Reject	P	Reject	P	Reject	P	Reject	P	Reject	P
V =[0.0,0.7]	1	0,0003	1	0,0009	To few points		To few points		To few points		To few points	
V =[0.7,1.3]	0	0,1524	0	0,0534	0	0,6029	1	2E-05	To few points		To few points	
V =[1.3,2.0]	1	0,024	0	0,2657	1	0,0311	To few points		To few points		To few points	
V =[2.0,2.7]	0	0,0713	1	0	0	0,9474	To few points		To few points		To few points	
V =[2.7,3.3]	0	0,0932	1	7E-05	0	0,1506	To few points		To few points		To few points	
V =[3.3,4.0]	0	0,0992	1	0,0006	To few points		To few points		To few points		To few points	

Table 8-7 Chi-square test results for Lindqvist ratio fitted to lognormal distribution
For explanation, see Table 8-6.

	h =[0.0,0.5]		h =[0.5,1.0]		h =[1.0,1.5]		h =[1.5,2.0]		h =[2.0,2.5]		h =[2.5,3.0]	
	Reject	P	Reject	P	Reject	P	Reject	P	Reject	P	Reject	P
V =[0.0,0.7]	1	0,001	1	0,0015	To few points		To few points		To few points		To few points	
V =[0.7,1.3]	0	0,1524	0	0,0534	0	0,714	1	2E-05	To few points		To few points	
V =[1.3,2.0]	0	0,3073	0	0,5167	0	0,0894	To few points		To few points		To few points	
V =[2.0,2.7]	1	0,0216	1	0	0	0,7432	To few points		To few points		To few points	
V =[2.7,3.3]	1	0,034	1	0,0013	0	0,4398	To few points		To few points		To few points	
V =[3.3,4.0]	0	0,1557	0	0,1339	To few points		To few points		To few points		To few points	

The results are inconclusive. For some of the data sets a lognormal distribution describes the data rather well, while for other data sets the chi square test rejects the lognormal hypothesis. To see if the number of observations influenced the result, Figure 8-8 was created using the information in Table 8-5, Table 8-6 and Table 8-7. This figure shows that the lognormal fit is poor most of the data sets, with a P-value above 0.20 for only 8 of 34 data sets. It does not seem to be a clear relationship between the number of observations and the probability of lognormal distribution. The difference between the Riska and the Lindqvist ratios does not appear to be systematic.

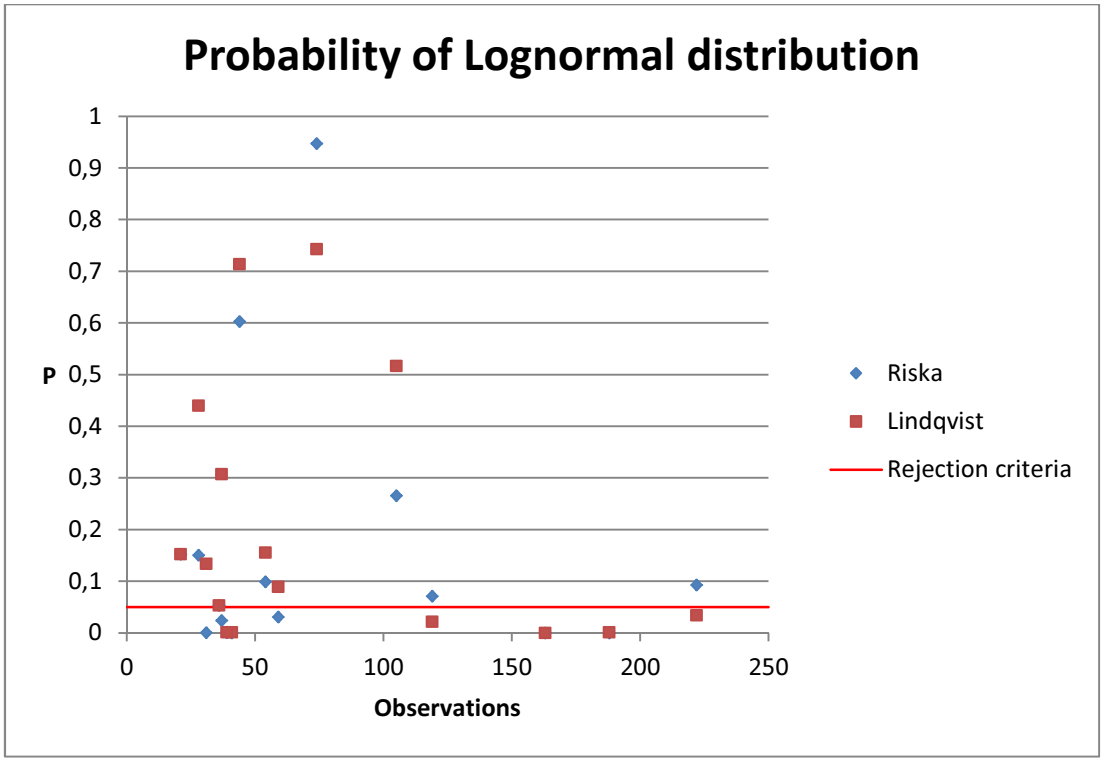

Figure 8-8: Probability of lognormal distribution as function of number of observations

8.3.2 Sources of error

When the ratio is modeled as a statistical distribution, it implies the assumption that the ratio between resistance estimated from measurements and resistance estimated from analytical formulations does not depend on speed and ice thickness (in a limited range of speeds/ ice thicknesses). This is assumed to be valid if the range of speed and ice thickness is sufficiently small. For the data in question this is checked by inspecting the scatter plots provided in

appendix A. There does not appear to be any trends in the divided data, and all data points in a subset have an apparently random distribution.

8.3.3 Section Conclusion

There is not clear evidence to support the hypothesis that the Riska and Lindqvist ratios can be modeled by lognormal distribution. The distribution fit is good for some combinations of ice thickness and vessel speed, but not for all combinations. There is no clear connection between a rejection of the hypothesis for a given dataset and the characteristics of the dataset (number of observations, vessel speed or ice thickness).

8.4 Weibull distribution

Visual inspection of the probability plots (see Figure 8-5 and appendices E and F), and in particular the tails, indicates that a Weibull distribution can model the data. This *hypothesis* is tested both visually and by chi-square tests. The visual tests include both residual plots and a series of Weibull probability plots (se Figure 8-9). To reduce the number of plots that has to be investigated, a *Weibull line* was fitted to the existing lognormal plots, as seen in Figure 8-5. If the data points were perfectly Weibull- distributed, they would follow this line.

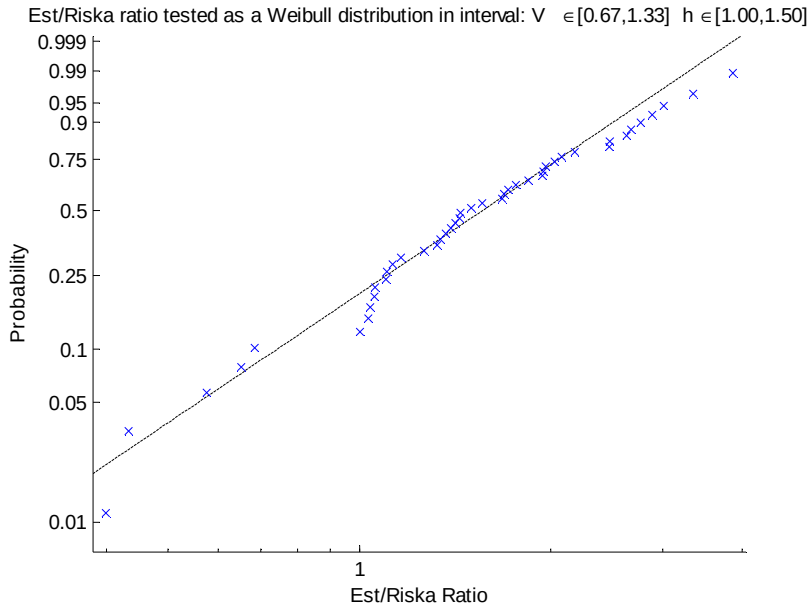

Figure 8-9: Probability plot of the Riska ratio for speeds between 0.67 and 1.33 [m/s] and ice thickness between 1.0 and 1.5 [m]

8.4.1 Chi-square test of Weibull distribution

The chi-square test is a way of estimating the likelihood of obtaining the given data set if the hypothesis of probability distribution (in this case, Weibull) is correct. The procedure is briefly described in section 8.3.1, and described in detail in most statistical handbooks, for instance [22].

The results from the Chi-square test are shown in Table 8-8 and Table 8-9. It is seen that the Weibull distribution has a rather good fit for ice thicknesses above 1.0 [m], while it does not fit the data for lower ice thicknesses. It does not appear to be any significant difference between the two ratios.

Table 8-8: Chi-square test results for Lindqvist ratio fitted to Weibull distribution

	h =[0.0,0.5]		h =[0.5,1.0]		h =[1.0,1.5]		h =[1.5,2.0]		h =[2.0,2.5]		h =[2.5,3.0]	
	Reject	P	Reject	P	Reject	P	Reject	P	Reject	P	Reject	P
V =[0.0,0.7]	1	7E-05	1	0	To few points		To few points		To few points		To few points	
V =[0.7,1.3]	0	0,0937	0	0,1116	0	0,7696	0	0,1573	To few points		To few points	
V =[1.3,2.0]	1	0,0204	1	0,0409	0	0,4724	To few points		To few points		To few points	
V =[2.0,2.7]	1	1E-05	1	0	0	0,4743	To few points		To few points		To few points	
V =[2.7,3.3]	1	0,0008	1	0	0	0,6286	To few points		To few points		To few points	
V =[3.3,4.0]	1	0,0042	0	0,1865	To few points		To few points		To few points		To few points	

Table 8-9 Chi-square test results for Lindqvist ratio fitted to Weibull distribution

	h =[0.0,0.5]		h =[0.5,1.0]		h =[1.0,1.5]		h =[1.5,2.0]		h =[2.0,2.5]		h =[2.5,3.0]	
	Reject	P	Reject	P	Reject	P	Reject	P	Reject	P	Reject	P
V =[0.0,0.7]	1	4E-05	1	0	To few points		To few points		To few points		To few points	
V =[0.7,1.3]	0	0,4692	0	0,343	0	0,658	0	0,1573	To few points		To few points	
V =[1.3,2.0]	1	0,024	0	0,0851	0	0,4012	To few points		To few points		To few points	
V =[2.0,2.7]	1	0	1	0	0	0,5736	To few points		To few points		To few points	
V =[2.7,3.3]	1	0	1	0	0	0,0882	To few points		To few points		To few points	
V =[3.3,4.0]	1	0,0024	0	0,3535	To few points		To few points		To few points		To few points	

As for the Lognormal distribution, residual plots have been created to visually check the distribution fits. The residual plots from the Weibull distribution fitting are shown in Figure 8-10 and Figure 8-11. It is seen from the plots that the Weibull distribution fits rather well for the middle quartile, but is unable to describe the data in the tails to a satisfactory level. This may be caused by some outlier phenomena, where the outliers are a result of an unknown process. It may also be caused by the fact that most of the data points are in the middle quartile, and hence the maximum likelihood estimators will be mostly influenced by this data.

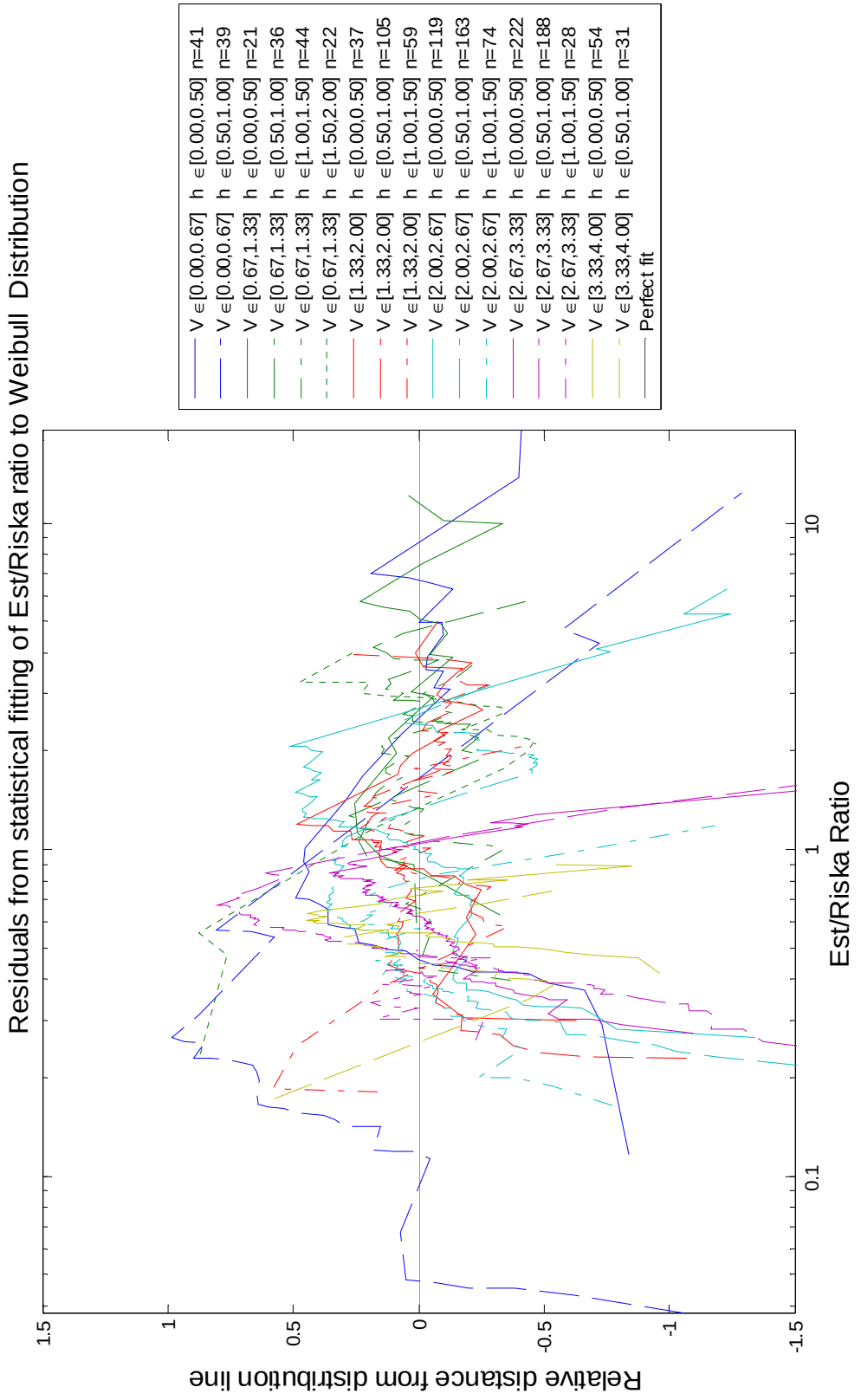

Figure 8-10: Residual plot from fitting of Riska ratio to Weibull distribution.
The values on the Y-axis indicate relative distance from the perfect fit line. The plot clarifies data set where the distribution fit is poor (large deviance from zero)

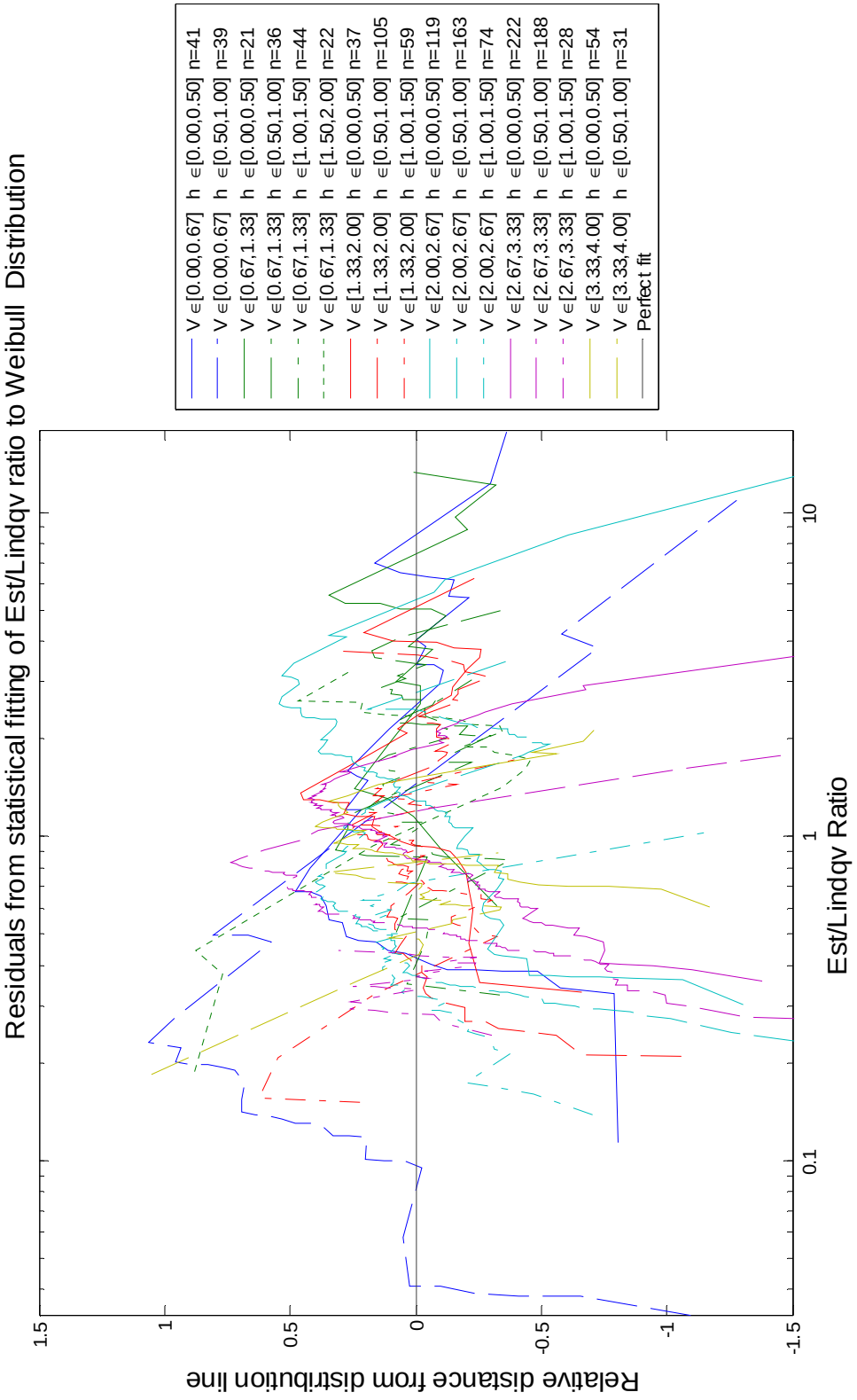

Figure 8-11: Residual plot from fitting of Lindqvist ratio to Weibull distribution.
The values on the Y-axis indicate relative distance from the perfect fit line. The plot clarifies data set where the distribution fit is poor (large deviance from zero)

8.5 Sources of discrepancy

As all attempts to describe the Riska and Lindqvist ratios as functions of speed and ice thickness has not provided satisfactory results, sources of discrepancy has been investigated. Both time dependency and measurement errors are discussed.

8.5.1 Systematic measurement errors

As discussed in section 3.2.1, the ice thickness sensor has some weaknesses that may influence the result. Both the interpretation of snow cover as ice and the reduced accuracy in broken ice will give inaccurate ice thickness measurements. This means that the ice thickness may be systematically overestimated in periods with snow cover, and systematically underestimated in periods with broken ice (which may be caused by ridging).

8.5.2 Assumption of continuous ice

The resistance calculations are based on the assumption that the ice has to be broken. As the ice thickness sensor is unable to properly distinguish between large and small ice sheets, it is difficult to know if the ice is broken in relatively small pieces before the ship encounters it. This would naturally influence the resistance, as the breaking part of the resistance is significant.

8.5.3 Time dependency

As shown in section 4.4, the resistance is highly dependent on the mechanical properties of the ice, which are unknown. One may suspect that the ice resistance encountered during the voyage may be varying as a function of time. This has been investigated by plotting the Riska and Lindqvist ratios against the sampling time, to see if there may be a trend. This plot is shown in Figure 8-12, which also shows the ice thickness and vessel speed.

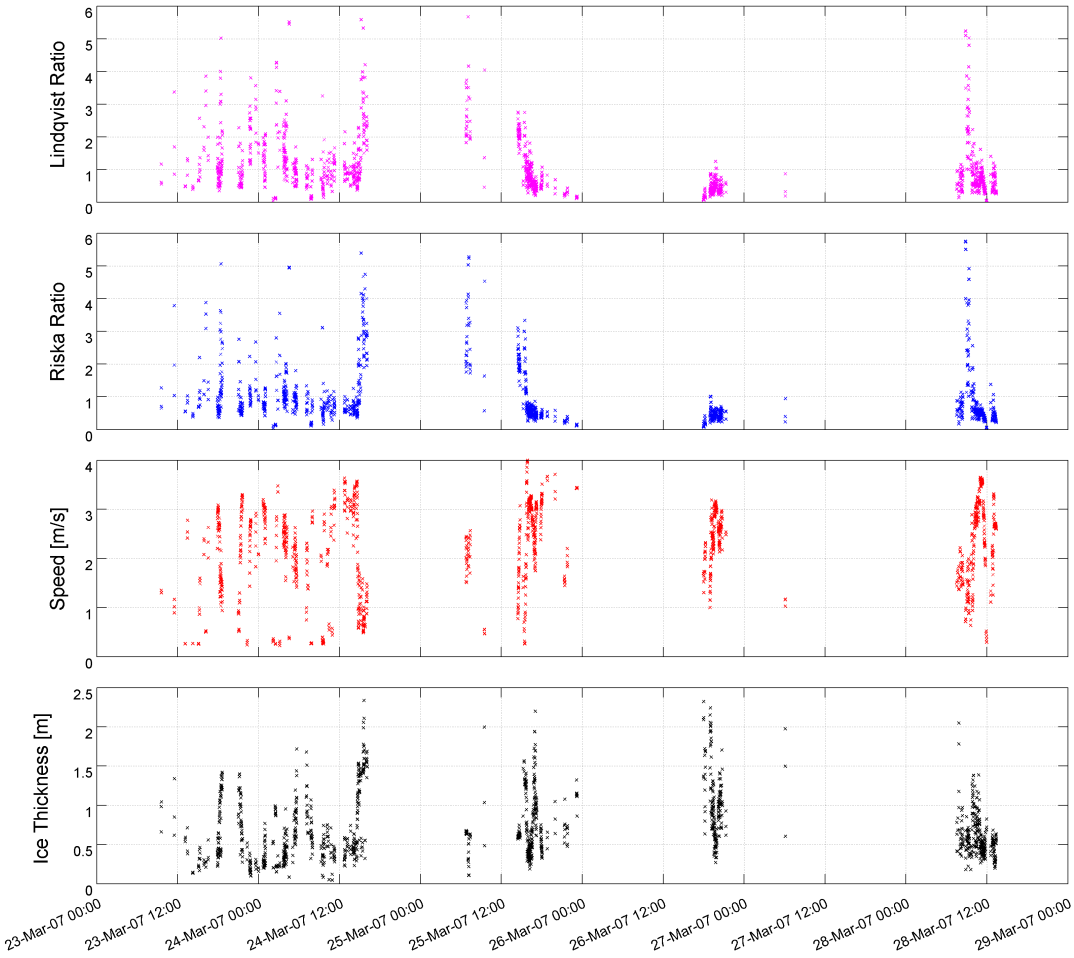

Figure 8-12: Lindqvist and Riska ratios, vessel speed and ice thickness plotted against sampling time

It is seen from Figure 8-12 that most of the selected data has an apparently random difference between estimated resistance from measurements and estimated resistance from analytical formulations. The data points sampled on 26.03.07 has however a relatively stable ratio between resistance estimated from measurements and resistance estimated from analytical formulations, while the variation in both ice thickness and vessel speed is significant. This change from large variance to small variance and back again is taken as a sign of a change in unknown parameters, or systematic measurement errors. The data selected on 26.03.07 is analyzed in section 8.6**.**

8.6 Data selected on 26th March 2007

As discussed in section 8.5.1, the resistance data selected on 26.3.07 has significantly less scatter compared to the rest of the data set. As more stable data may be an indication of higher data quality, additional analysis has been performed on this data.

8.6.1 Riska and Lindqvist ratios as function of speed

Figure 8-13 and Figure 8-14 shows the Lindqvist and Riska ratios as function of vessel speed. The data appears to be randomly distributed around a linear trend, indicated by the red line in the plots (a linear least square line). The residuals from a linear regression support this assumption, as they are randomly distributed around zero without any obvious correlation as opposed to the fitted surfaces discussed in section 8.1.

The only difference between the two ratios with regard to speed dependency is that the Riska ratio is less sensitive to changes in speed, as indicated by eq. (8.12) and Table 8-10**.** When examining the confidence intervals, it is found that the Riska ratio as a function of vessel speed may be modeled as a constant value with a random variation (the confidence interval for p_1 includes zero). The Lindqvist ratio must however be modeled with a linear dependency in addition to the random variation.

$$Line_{LeastSquares} = p_1 \cdot v + p_2 \tag{8.12}$$

Table 8-10: Coefficients for least square lines fitted to Lindqvist and Riska ratios. Line equation is given in eq.(8.12)

	Coefficient	Value	Lower 95% confidence interval	Upper 95% confidence interval
Lindqvist	p_1	0.1593	0.1037	0.2149
	p_2	0.03983	0.1003	0.18
Riska	p_1	0.03048	-0.01693	0.07789
	p_2	0.3522	0.2327	0.4716

As both the Riska and the Lindqvist resistance estimates are linear functions of vessel velocity, these findings indicate that the Lindqvist resistance estimate would be able to better describe resistance from Arctic sea ice if a second order velocity term was introduced.

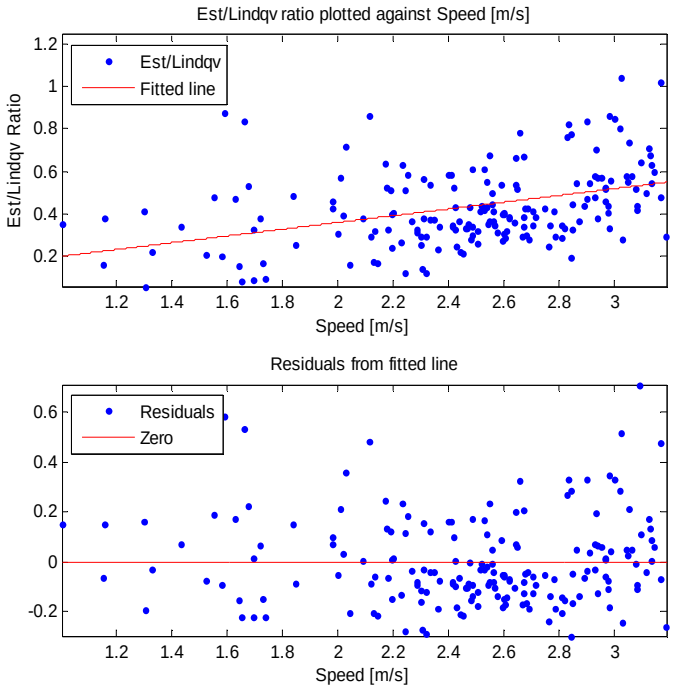

Figure 8-13: Ratio between resistance estimated from measurements and Lindqvist estimate plotted against vessel speed for data collected 26.3.07

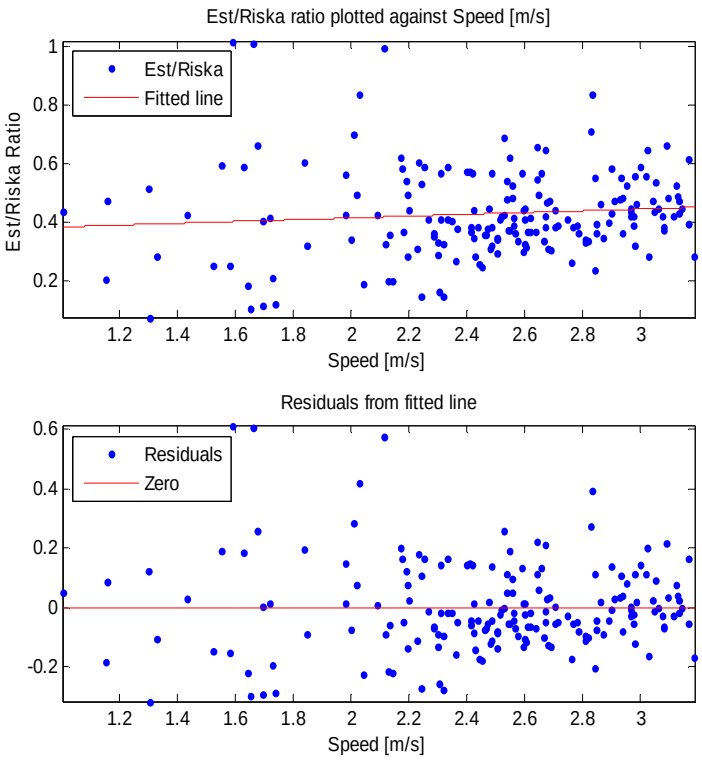

Figure 8-14: Ratio between resistance estimated from measurements and Riska estimate plotted against vessel speed for data collected 26.3.07

8.6.2 Lindqvist and Riska ratios as function of ice thickness

When plotting the ratios against ice thickness, a quite different result appears. A clear limit for the lower limit is found, as illustrated by Figure 8-15 and Figure 8-16. The physical reasons for this limit are unclear, but it indicates that the ice thickness dependency of the Riska and Lindqvist formulations are not able to accurately describe the resistance. Equations for the lower limits are given below.

$$LowerBoundary_{Riska} = 0.4281 \cdot h^{-0.5237} - 0.1686$$
$$LowerBoundary_{Lindqvist} = 0.256 \cdot h^{-1.228} - 0.00893 \quad (8.13)$$

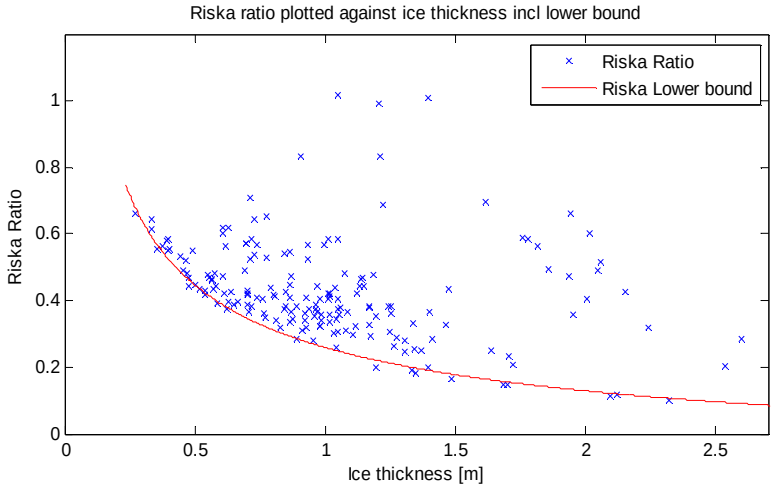

Figure 8-15: Riska ratio plotted against ice thickness for data collected 26.3.07. The lower limit for the data is indicated by the red line.

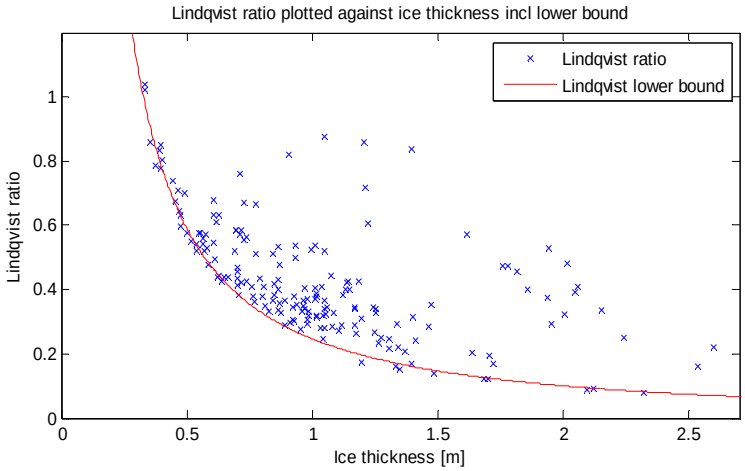

Figure 8-16: Lindqvist ratio plotted against vessel speed for data collected 26.3.07. The lower limit for the data is indicated by the red line.

These results indicate that the formulations are either applied outside their area of applicability, or that the mechanical properties of ice used in the formulations are incorrect.

8.6.3 Section conclusions

For a carefully selected data set there are clear trends in the ratio between resistance estimated from measurements and resistance estimated from analytical formulations. The speed dependency of the Riska ratio may be modeled as constant with a random variation, while the speed dependency of the Lindqvist ratio is best modeled as linear with a random variation. The deviance of mean value from 1.0 is believed to be caused by the simplifications made in the estimation of resistance based on measurements (further discussed in section 5.2). For the ice thickness dependency there are clear lower limits for the ratios, which can be well described by a power line. The physical background for this lower limit is unclear, and has not been investigated further. This indicates that the ice thickness dependency in the formulations (which have both linear and second-order terms) may be incorrect.

It is however important to be aware of the fact that these data sets were chosen because they had better consistency with the analytical models than the rest of the selected observations. One should therefore use caution when using this data set to verify the existing analytical formulations.

8.7 Chapter summary

There has not been found any clear trends or relations in the data selected by the method discussed in chapter 6. A second order surface has been fitted to the ratio between resistance estimated from measurements and resistance estimated from analytical formulations in the vessel speed/ice thickness domain without obtaining an acceptable fit. The data has been divided into subset depending on ice thickness and vessel speed, and an attempt to fit statistical distributions to this data has been made. For the Lognormal distribution one is able to fit the data to the distribution for some of the data sets, but not for all. There are no clear connection between the goodness of the fit and the nature of the data (speed, ice thickness and number of observations). For the Weibull distribution there is a reasonably good match between the data and the distributions for relatively high ice thickness (between 1.0 and 1.5 [m]), but the overall fit is considered to be poor.

As a consequence of the lack of consistency between the selected data and statistical models, the selection of data points has been reviewed. After investigating the sampling time dependency of the data, it was found that the data selected on 26.3.07 showed far less variation in the resistance ratio compared to the rest of the data, while still having considerable variantion of speed and ice thickness. Taking this as an indication of higher data quality the data was selected for further analysis. The speed dependency of the Lindqvist ratio obtained in this data set was found to have a clear linear trend, while the trend was constant for the Riska ratio. This indicates that the speed dependency of the Lindqvist formulation is not able to describe the true speed dependency of the resistance. The ice thickness dependency of both ratios has a clear lower limit that can be expressed as a power function. As the ice thickness dependency in the analytical models contains both linear and power terms, this is taken as a signal of inaccuracy in the power terms in both the Riska and Lindqvist models.

9 Result discussion

In this thesis the ratio between ice resistance estimated from onboard measurements on KV Svalbard and estimates from analytical formulations presented by Riska et al. [2] and Lindqvist [1] has been analyzed.

9.1.1 Data selected by automated routine

Most of the data analyzed in this thesis is considered to be of low quality, as the variance of the found resistance ratios is not constant for varying ice thicknesses and vessel speeds. This is an indication of unknown variation of variables, for instance flexural strength of the ice. This strongly indicates that it is not sufficiently to only use the vessel speed and ice thickness as resistance predictors, additional information about the material properties of the ice is also needed.

Both the Lindqvist and Riska ratio has been fitted to a surface, but the residuals from the fit are not randomly distributed, which indicates that there are other variables that influence the result. Attempts to fit the data to Lognormal and Weibull distributions have not been successful, even if some parts of the data fits rather well. It may be beneficial to fit the data to other distributions, but that has not been prioritized in this thesis.

For the Lindqvist formulation it is possible to specify the values for all material properties, while the Riska formulation has combined material constants into a set of equation constants. This makes it difficult to investigate how changes in the ice properties would influence the resulting Riska estimated resistance.

9.1.2 Data selected manually

The results obtained from measurements performed the 23rd of March 2007 are considered to be of high quality, and are believed by the author to be a contribution to the ongoing research on the subject.

The results indicate that the speed dependency of the formulation presented by Riska et al. is likely to be correct. There may be need for a correction of the mean level, but this cannot be determined without further information regarding the propeller efficiency of the vessel in question. The speed dependency of the Lindqvist ratio is showing a linear trend for the data presented in this thesis. This indicates that the Lindqvist formulation should include a second order velocity term. The problem with this simple conclusion is that the speed dependency of ice resistance should have the same order of velocity terms in all formulations (e.g. as the linear relationship in the Riska formulation is assumed to be correct, then the linear relationship in the Lindqvist formulation should also be correct). The error in the Lindqvist formulation is therefore believed to be caused by a correlation between the speed and an unknown parameter.

The ice thickness dependency is found to be inaccurate for both formulations. Both the Riska and Lindqvist ratios have a clear lower bound, which can be expressed as a power function. This indicates that the ice thickness variation is unable to properly describe the resistance for the vessel in question.

9.1.3 Sources of discrepancy

The data sets selected by the automated routine have a significant variation in the resistance estimated from measurements of vessel speed and power which cannot be predicted only by the known parameters. This variation in resistance is believed to be caused by variation of the ice parameters. As discussed in chapters 2 (ice characteristics) and 1 (resistance models), sea ice is not a constant material, and the resistance models proposed in literature are sensitive to changes in the mechanical properties. It is therefore reasonable to also assume that the true ice resistance is sensitive to changes in mechanical properties (e.g. flexural strength). It is believed that this variation in ice strength is one of the causes for the variation of the results

Another source of variation of the resistance may be the relationship between loading speed and the compressive strength of ice. Several experimental studies have shown a relationship between the stain rate $\left(\partial\epsilon/\partial t\right)$ and maximum compressive strength. It is unclear how large influence this will have on the flexural strength, and this should be further investigated.

The ice thickness sensor is an instrument that measures the average distance to the sea surface over approximately 12 m^2 and the distance to the ice/ snow surface as an instantaneous value. This will give inaccurate measurements in cases without almost perfect level ice conditions, which are relatively rare. It is unclear how this will affect the results, but it may explain some of the apparently random variation in ice resistance for similar ice thickness and vessel speed.

The ratio between two different estimates of the same quantity is expected to be distributed around 1.0. The clear deviance from this value for the ratios examined in this thesis is believed to be caused by the simplifications introduced in the resistance model developed by the author. The assumption of a propeller efficiency of 1.0 is clearly a large simplification, which introduces a significant error. As estimation of this efficiency is outside the author's field of education and experience, there has been made no attempt on performing such estimate.

9.2 Conclusions

Both the Riska and Lindqvist resistance formulations are unable to fully describe the ice resistance for the vessel KV Svalbard in Arctic sea ice using the selected ice properties. The Riska formulation appears to be able to predict the resistance as a function of vessel speed, but the ice thickness dependency is inaccurate. As the Riska formulation has no mechanical properties to select, it is less flexible to applications outside the original area of application (The Baltic Sea). The Lindqvist formulation is unable to describe the resistance both in the speed and ice thickness domain. This may be caused by incorrect values for the mechanical properties of the Arctic Sea Ice.

10 Further work

During the work with this thesis, several tasks have arisen that has not been performed due to lack or information, time or knowledge. These are listed below, in a systematic manner.

10.1 Further work on the data from KV Svalbard

- The propeller curves should be obtained, or the propeller efficiency estimated in some other way. This is necessary to improve the accuracy of the resistance model.
- It is possible to develop a model for the ice strength as function of ice thickness and temperature. This would ideally require a model relating weather data and ice temperature, but it may be sufficient to use a linear interpolation of air temperature and freezing temperature for sea water.
- The ice properties may be varied in order to see if changed properties may improve the accuracy of the Lindqvist formulation.

10.2 Further work on ice resistance in general

- Additional full-scale test data should be analyzed. This would enable validation of the hull shape parameters in the resistance formulations.
- Full-scale test data which includes measurements of the mechanical properties of ice (flexural strength and density) should be obtained.
- If additional full scale test are not available, it may be beneficial to compare resistance predicted by the use of Finite Element Methods with the present analytical formulations.
- Kai Riska and his team may be approached in order to get the resistance formulation with ice material constants. The formulation is widely used, and it would be of scientific interest to investigate how this formulation is able to describe ice resistance with different ice characteristics.
- The effect of strain rate on flexural strength should be investigated (a thorough literature search may be sufficient).

11 References

1. Lindqvist, G. *A straightforward method for calculation of ice resistance of ships.* in *The 10th International Conference on Port and Ocean Engineering under Arctic Conditions*. 1989. Luleå.
2. Riska, W., Englund, Leiviskä, *Performance of merchant vessels in ice in the Baltic.* Helsinki university of technology - Ship Laboratory, 1997.
3. Valanto, *Resistance of ships in Level ice.* SNAME Transactions, 2001. **109**: p. 53-83.
4. Su, B., K. Riska, and T. Moan, *A numerical method for the prediction of ship performance in level ice.* Cold Regions Science and Technology, 2010. **60**(3): p. 177-188.
5. Timco, G.W. and W.F. Weeks, *A review of the engineering properties of sea ice.* Cold Regions Science and Technology, 2010. **60**(2): p. 107-129.
6. Furnes, G., *Ice 1 - Lecture notes*. 2010, NTNU.
7. Riska, K., *Ice 2 - Lecture Notes*. 2010, NTNU.
8. Kovacs, A., *Sea Ice Part 1. Bulk salinity versus ice floe thickness.* CRREL Report 96-7, Hanover, NH, USA, 1996.
9. Timco, G.W., Frederking, R.M.W., *A review of sea ice density.* Cold Regions Science and Technology, 1996. **24**: p. 1-6.
10. Frankenstein, G.E., Garner, R., *Equations for determining the brine volume of se ice from -0,5 to -22,9 deg C.* Journal of Glaciology, 1967. **6**(48): p. 943 - 944.
11. Sinha, N., *Rate sensitivity of compressive strength of columnar-grained ice.* Experimental Mechanics, 1981. **21**(6): p. 209-218.
12. Leira, B., Espeland, Amdahl, *Ice-load estimation for a ship hull based on continuous response monitoring.* Proceedings of the Institution of Mechanical Engineers; Part M; Journal of Engineering for the Maritime Environment [1475-0902], 2009. **223**(4): p. 529-540.
13. Madsen, A., *Estimation of Ice Resistance of Ships based on Measurements of Ice Thickness, Speed and Power*, in *Department of Marine Technology*. 2010, Norwegian University of Science and Technology.
14. Riska, *Design of Ice Breaking Ships*, H. Shen, Editor. 2010.
15. Pfaffling, A., *Ship-borne sea ice thickness electromagnetic measurements*. 2007, PFAFFLING geophysics.
16. Gow, A.J.W., W. F. ; Kosloff, Pekka ; Carsey, Susan, *Petrographic and Salinity Characteristics of Brackish Water Ice in the Bay of Bothnia.* Cold Regions Research And Engineering Lab Hanover Nh, 1992: p. 45.
17. Hietala, R. *The Baltic Sea Portal - Hydrography of the Baltic Sea* [cited 2010 19.12.2010]; Available from: http://www.itameriportaali.fi/en/tietoa/veden_liikkeet/en_GB/hydrografia/.
18. Riska, K., A. Suyuthi, Editor. 2011.
19. Mathworks, *Matlab 2010b Help*. 2011.
20. DuMouchel, W.H., and F. L. O'Brien *Integrating a Robust Option into a Multiple Regression Computing Environment.* in *American Statistical Association, Computer Science and Statistics: Proceedings of the 21st Symposium on the Interface*. 1989.: Alexandria, VA.
21. Mathworks. *Residual Analysis: Curve fitting technique*. 2011 [cited 2011 30.04]; Available from: http://www.mathworks.com/help/toolbox/curvefit/bq_5ka6-1_1.html.
22. Warpole, M., Myers, Ye, *Probability and Statistics for Engineers and Scientists*. 2007: Pearson Education.
23. Suyuthi, A., *Selection of data points for ice resistance estimation*. 2011, NTNU.

12 Appendix

A Matlab calculations

Having used Matlab as the main computational tool in this thesis, a large program structure has been developed. The first figure in this appendix shows the main flowchart of the program, indicating the main operations and decisions that are performed. As the statistical analysis has been focused upon, the flowchart for this subroutine is also provided in the second figure in this appendix. The Matlab code is also provided electronically on the attached CD. Both *Statistics Toolbox* and *Curve Fitting Toolbox* are required in order to run the program properly.

This section is intended as a reference to help the reader understand the structure of the Matlab code. As a consequence, some information may be duplicated in order to improve readability (it should not be necessary to read the entire section to understand one subsection).

A.1 Input file

The input file *input.txt* is read by Matlab, and controls all relevant parameters in the program. The structure of the file should be self-explanatory, but some comments are provided.

A.1.1 Time length

If a nonzero time length is chosen, a new file containing necessary data with the selected time length will be created, which may be used as input file in subsequent runs (the construction of this file is the most time-consuming part of the analysis). The file is used for *data selection* when it is created

A.1.2 File names

File for data selection is used to identify time intervals with sufficiently stable conditions, while *File for resistance calculation* is used to calculate the resistance in previously found time intervals. This allows for selection of data based on stability over relatively long time periods, while the resistance is calculated for shorter time periods, increasing the number of data points without decreasing the quality of the data. File names for input files must be provided without single quotation marks

A.1.3 Data selection method

There are two main ways of selecting data points, namely *automated selection* and *manual selection*. The automated selection is based on the method described in chaper 6, while the manual selection is based on previous works on the data sets previously performed by either Madsen[13] or Suyuthi[23]. The manual selection is implemented in order to be able to compare the results from this thesis with the results from [13] and [23].

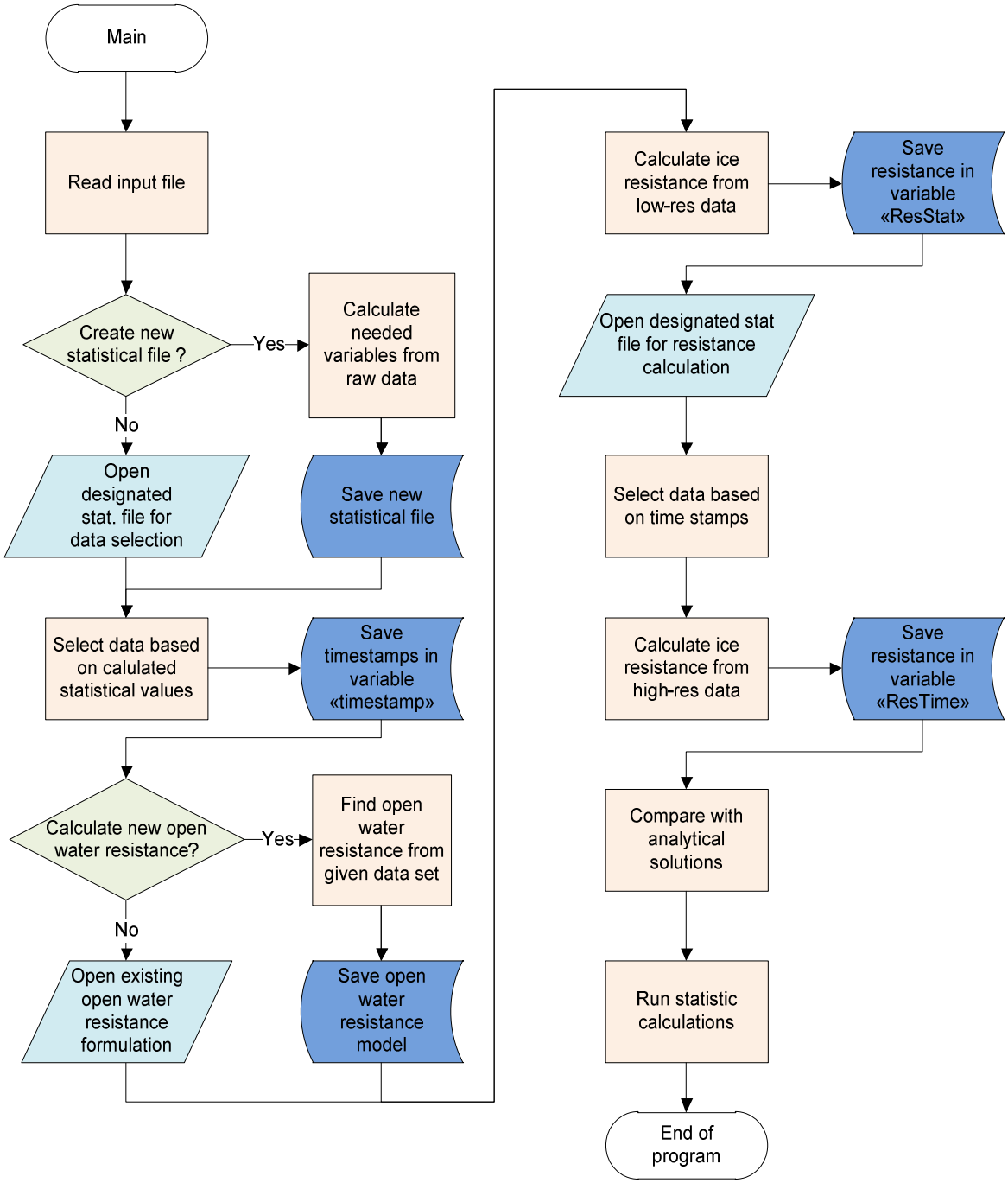

Main Matlab flowchart

A.1.4 Selection of plotting parameters

All plots can be activated or deactivated in the input file, by use of true or false statements, where 1 is taken as true and 0 as false. If the *save to file* option is active, plots will be closed after they are saved. This is done to avoid memory errors (with all plots activated, the program will generate around 100 plots).

A.1.5 Fitting of additional probability distributions

The program is designed to fit the ratio between resistance estimated from measurements and resistance estimated from analytical formulas to a *lognormal distribution.* As this fit may not be accurate, there is an option of fitting additional distributions to the data, which may be specified in

the input file. The specification is done by Matlab distribution names, which can be found either in the end of the file *regression.m*, or in the Matlab documentation. The program only accepts two-parameter distributions. If no additional distributions are to be fitted to the data, remove the line completely.

A.1.6 Files saved to disk

If the *save files* option is active, the program will create the folder *Plots* which will contain all plots generated by the program. This operation requires the user to have write permission to the current folder, which may be a problem if the program is run from e.g. a CD. If save is activated, most plots will be closed after they are saved.

A.2 Statistical analysis

The statistical analysis subroutine performs two main tasks, *calculations of statistical properties* and *plotting of results*. The subroutine has been continuously developed throughout the thesis work, meaning that not all of the functionality is equally relevant. All graphical output from this subroutine is controlled by the input file, and can be automatically saved to disk. In this subroutine both *struct arrays* and *cell arrays* are used to a large extent. If the reader is not familiar with these variable types, a Google search is recommended if the code is to be investigated in detail.

The flowchart for the statistical analysis is shown in the last figure in this appendix.

A.2.1 Division of data into subgroups

In order to investigate if the ratio between resistance estimated from measurements and resistance estimated from analytical formulaitons is dependent on speed and ice thickness, the data is divided in separate bins. These bins are placed in a *cell array* which simplifies the process. Similar cell arrays are used to handle statistical values for the different bins.

A.2.2 Modifications of internal Matlab functions

In order to plot the residuals from the fitting of statistical distributions, the residuals have to be retrieved from the internal subroutine that plots the probability plot (*probplot*). The modification is rather simple, and involves a *global struct variable*:

1. Open the Matlab file *probplot* (type *edit probplot* in command window)
2. In line 80, insert
   ```
   global Torstein;
   ```
3. In line 178, insert
   ```
   Torstein.linefun=linefun;
   ```
4. In line 278, insert
   ```
   global Torstein; Torstein.mainy=q; Torstein.mainx=x;
   ```
5. In line 492, insert
   ```
   global Torstein; Torstein.fity=fx;Torstein.fitx=x;
   ```

The variable name is chosen to ensure that it is unique in the entire Matlab environment, a necessity since it is a global variable.

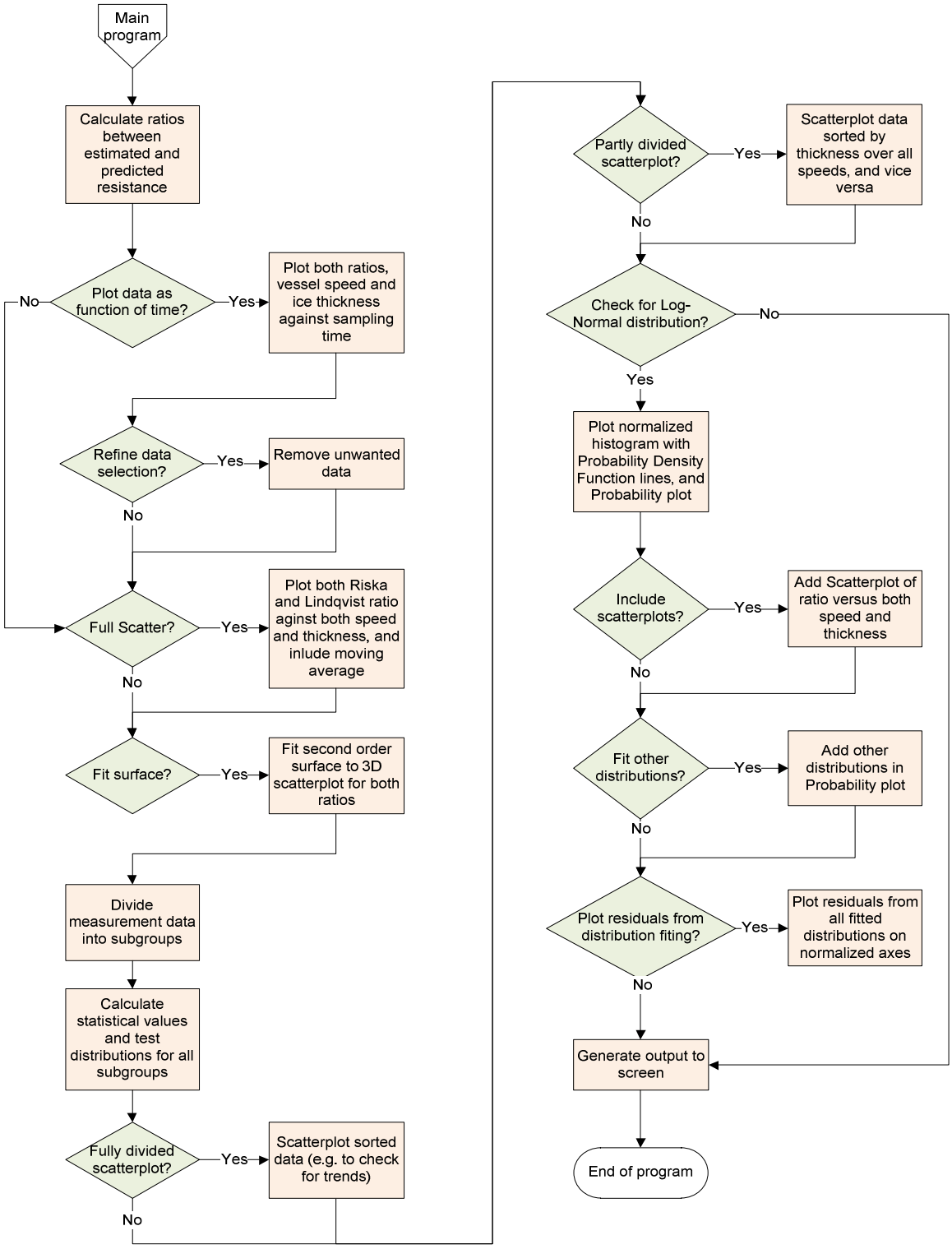

Flowchart for statistical analysis

B Contents on CD

B.1 Matlab

All files used to run the Matlab script, including raw data and statistical analysis data

B.2 Report

The report, in PDF format.

B.3 Cited work

Selected references which have proven hard to find are enclosed.

C Sensitivity of parameters in resistance formulation

C.1 Bow angle φ

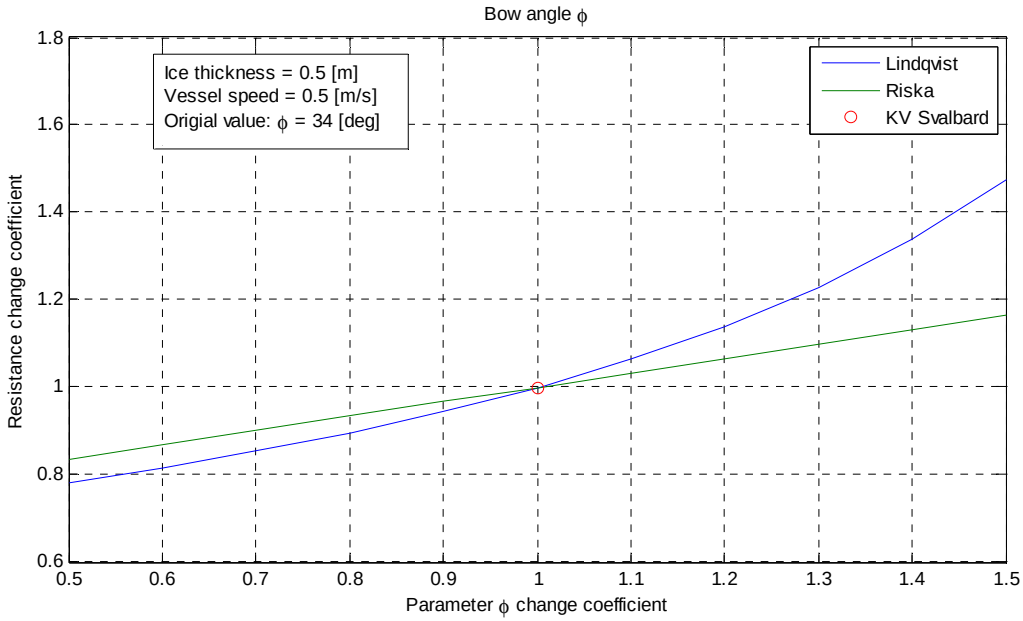

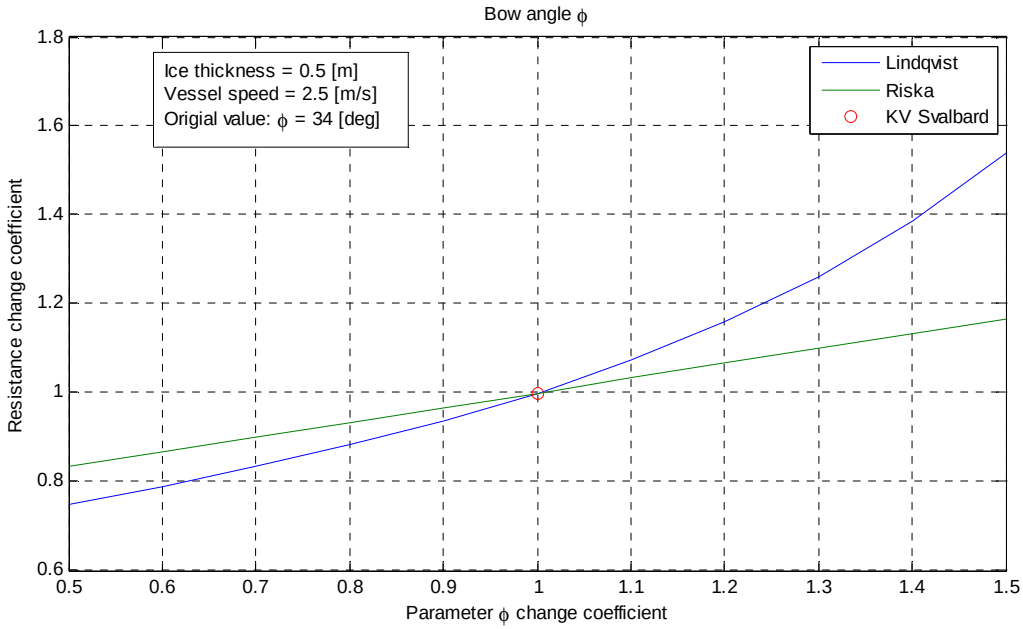

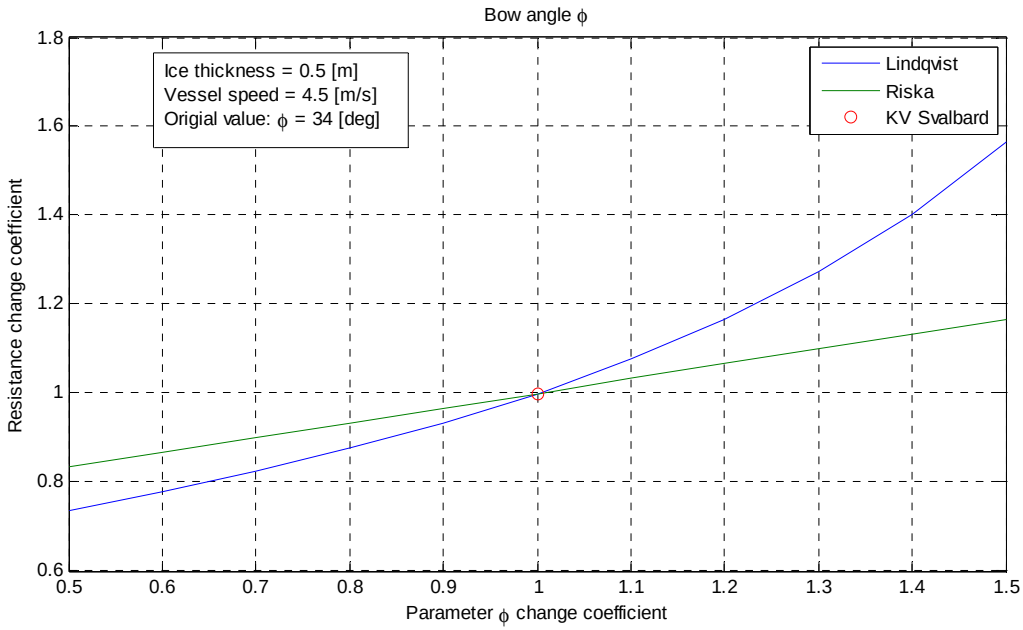
Bow angle ϕ
Ice thickness = 0.5 [m]
Vessel speed = 4.5 [m/s]
Origial value: ϕ = 34 [deg]
Lindqvist
Riska
KV Svalbard
Resistance change coefficient
Parameter ϕ change coefficient
1.8
1.6
1.4
1.2
1
0.8
0.6
0.5
0.6
0.7
0.8
0.9
1
1.1
1.2
1.3
1.4
1.5

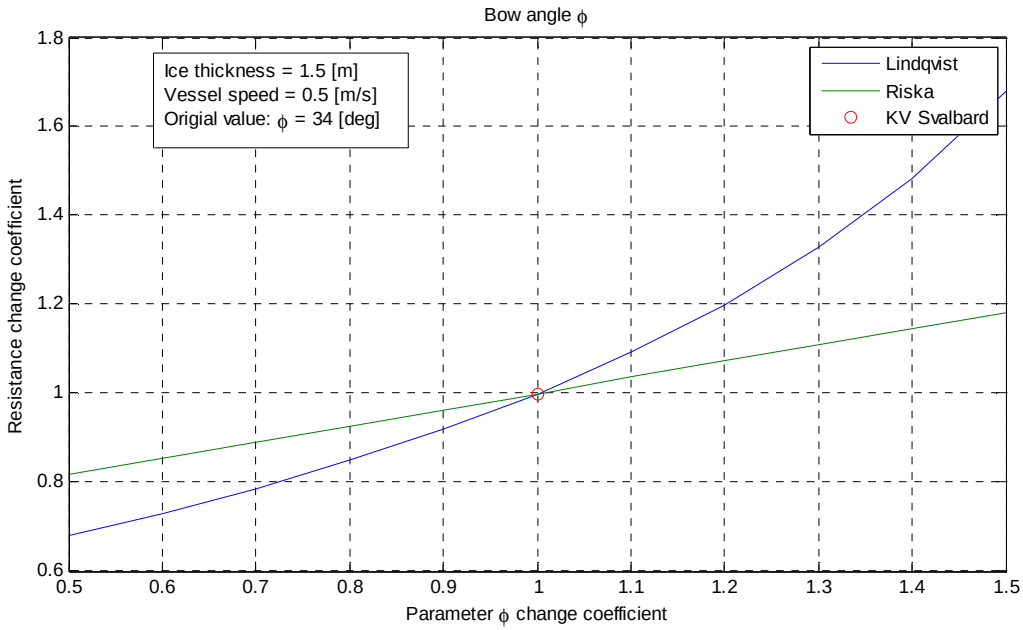
Bow angle ϕ
Ice thickness = 1.5 [m]
Vessel speed = 0.5 [m/s]
Origial value: ϕ = 34 [deg]
Lindqvist
Riska
KV Svalbard
Resistance change coefficient
Parameter ϕ change coefficient
1.8
1.6
1.4
1.2
1
0.8
0.6
0.5
0.6
0.7
0.8
0.9
1
1.1
1.2
1.3
1.4
1.5

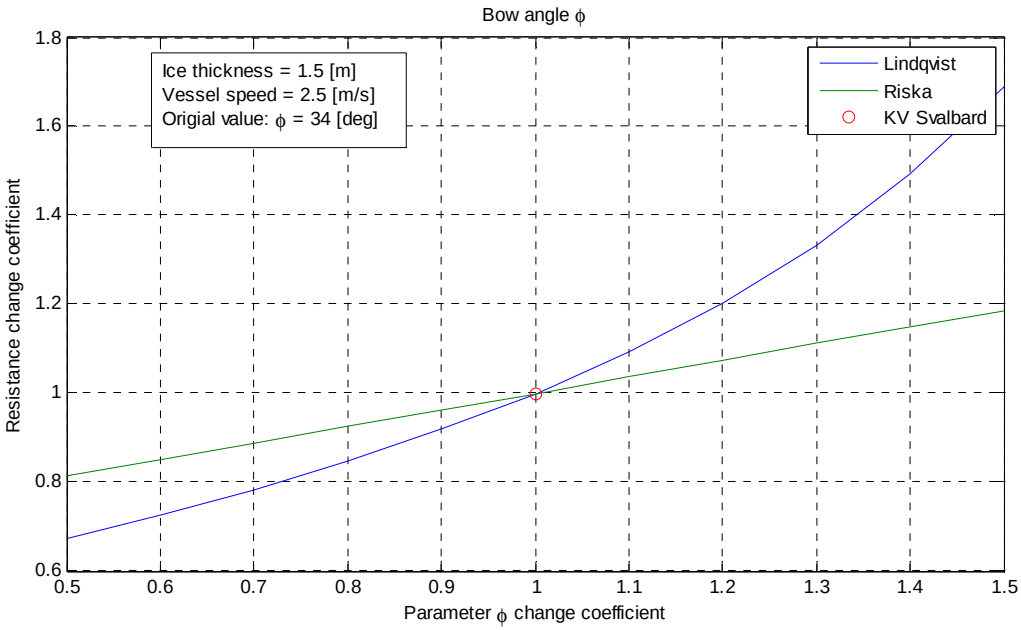
Bow angle ϕ
Ice thickness = 1.5 [m]
Vessel speed = 2.5 [m/s]
Origial value: ϕ = 34 [deg]
Lindqvist
Riska
KV Svalbard
Resistance change coefficient
Parameter ϕ change coefficient
1.8
1.6
1.4
1.2
1
0.8
0.6
0.5
0.6
0.7
0.8
0.9
1
1.1
1.2
1.3
1.4
1.5

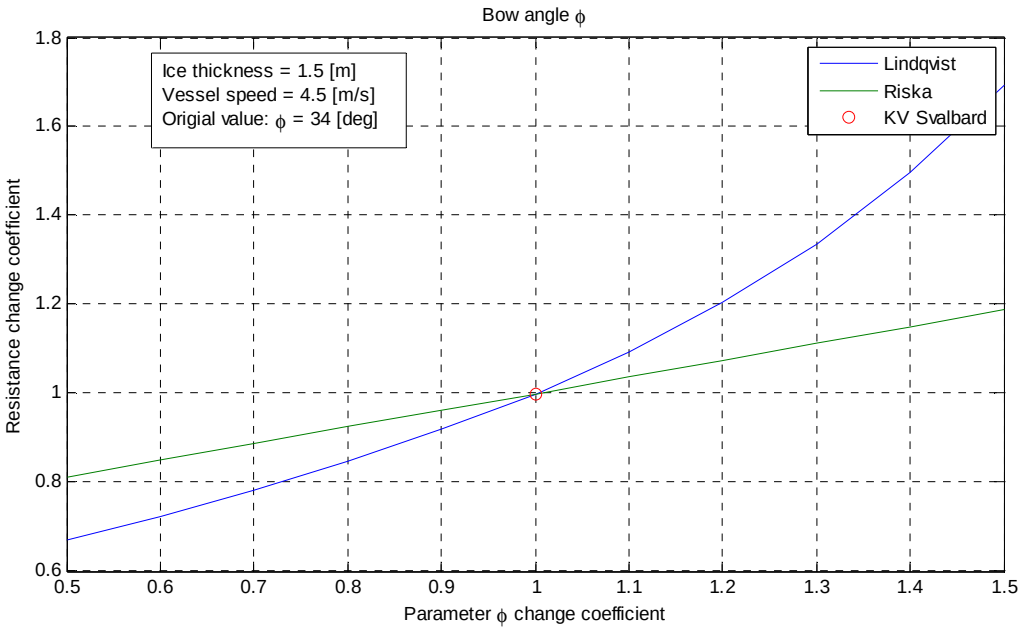
Bow angle ϕ
Ice thickness = 1.5 [m]
Vessel speed = 4.5 [m/s]
Origial value: ϕ = 34 [deg]
Lindqvist
Riska
KV Svalbard
Resistance change coefficient
Parameter ϕ change coefficient
1.8
1.6
1.4
1.2
1
0.8
0.6
0.5
0.6
0.7
0.8
0.9
1
1.1
1.2
1.3
1.4
1.5

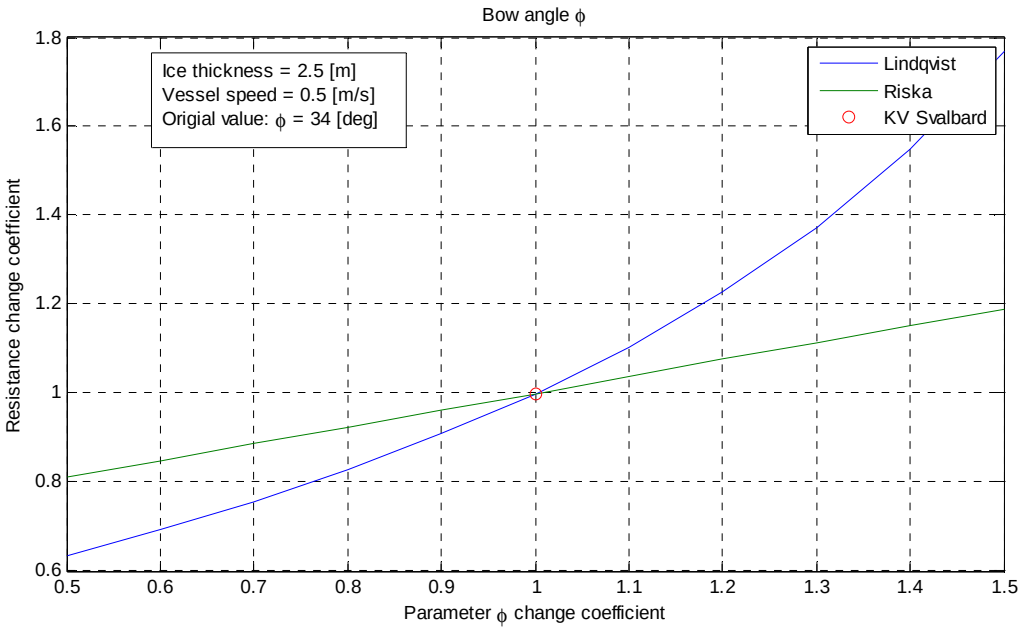
Bow angle ϕ
Ice thickness = 2.5 [m]
Vessel speed = 0.5 [m/s]
Origial value: ϕ = 34 [deg]
Lindqvist
Riska
KV Svalbard
Resistance change coefficient
Parameter ϕ change coefficient
1.8
1.6
1.4
1.2
1
0.8
0.6
0.5
0.6
0.7
0.8
0.9
1
1.1
1.2
1.3
1.4
1.5

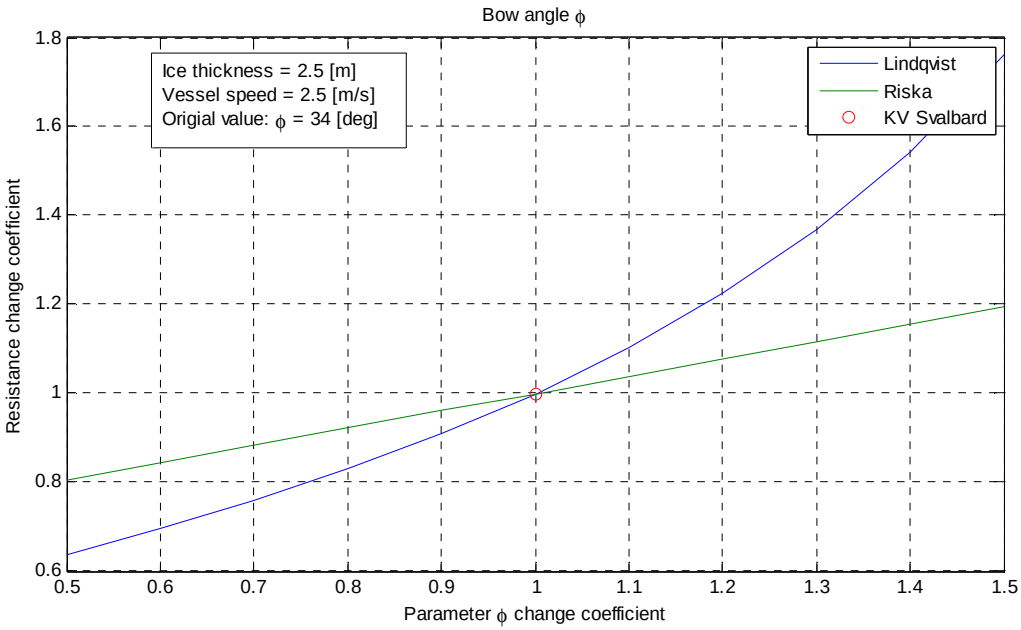
Bow angle ϕ
Ice thickness = 2.5 [m]
Vessel speed = 2.5 [m/s]
Origial value: ϕ = 34 [deg]
Lindqvist
Riska
KV Svalbard
Resistance change coefficient
Parameter ϕ change coefficient
1.8
1.6
1.4
1.2
1
0.8
0.6
0.5
0.6
0.7
0.8
0.9
1
1.1
1.2
1.3
1.4
1.5

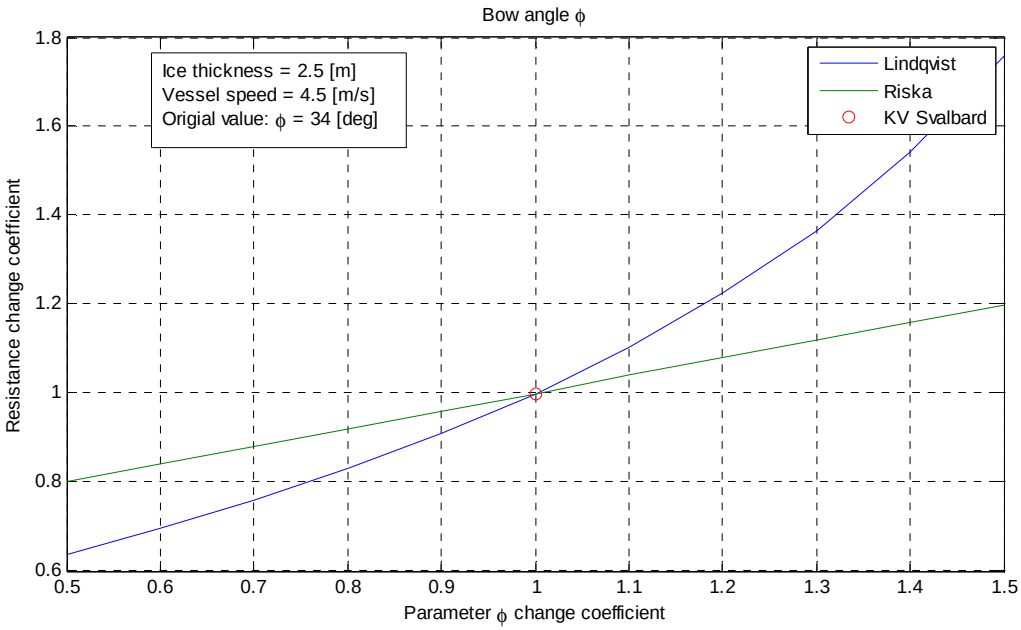
Bow angle ϕ
Ice thickness = 2.5 [m]
Vessel speed = 4.5 [m/s]
Origial value: ϕ = 34 [deg]
Lindqvist
Riska
KV Svalbard
Resistance change coefficient
Parameter ϕ change coefficient
1.8
1.6
1.4
1.2
1
0.8
0.6
0.5
0.6
0.7
0.8
0.9
1
1.1
1.2
1.3
1.4
1.5

C.2 Waterplane entrance angle α

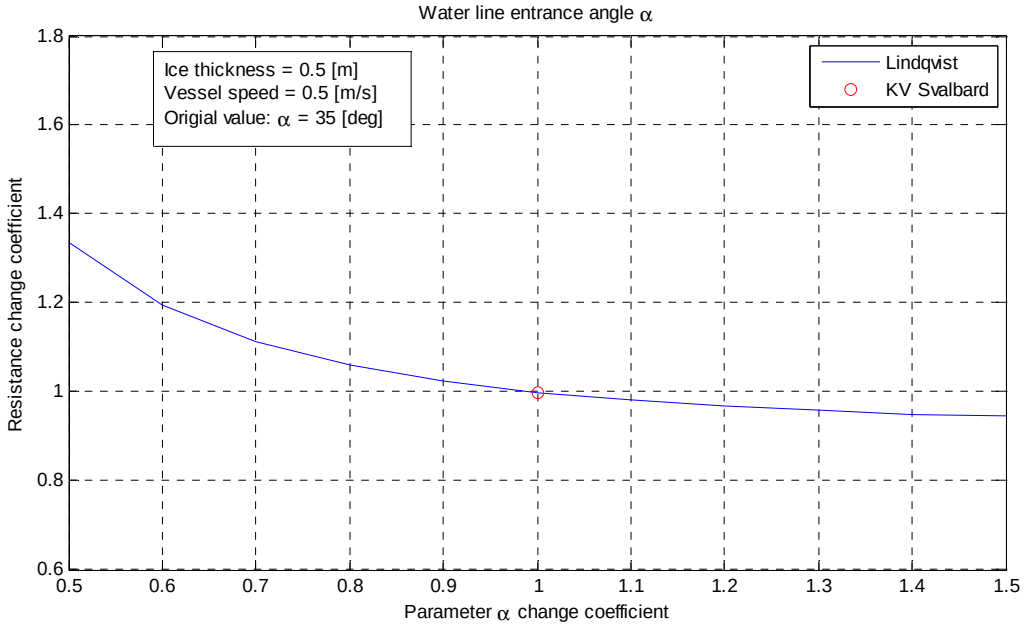

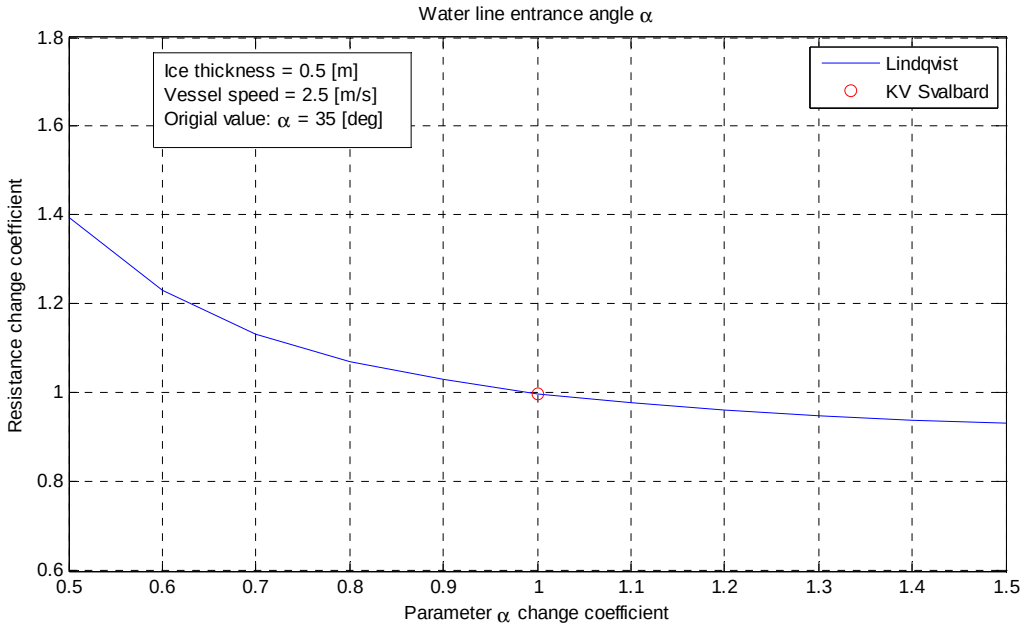

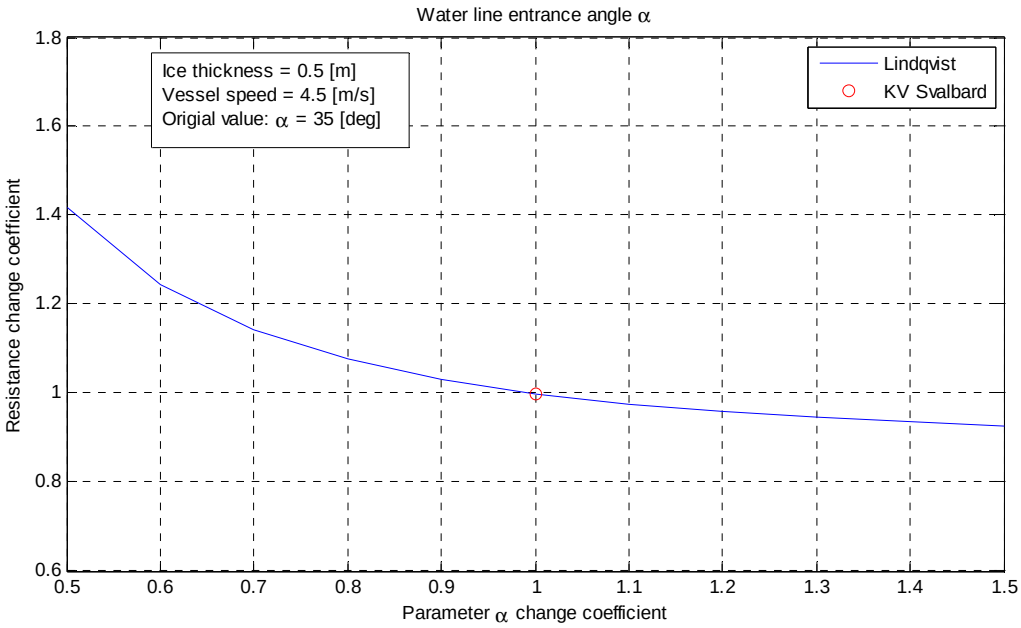
Water line entrance angle α
Ice thickness = 0.5 [m]
Vessel speed = 4.5 [m/s]
Origial value: α = 35 [deg]
Lindqvist
KV Svalbard
Resistance change coefficient
Parameter α change coefficient
1.8
1.6
1.4
1.2
1
0.8
0.6
0.5
0.6
0.7
0.8
0.9
1
1.1
1.2
1.3
1.4
1.5

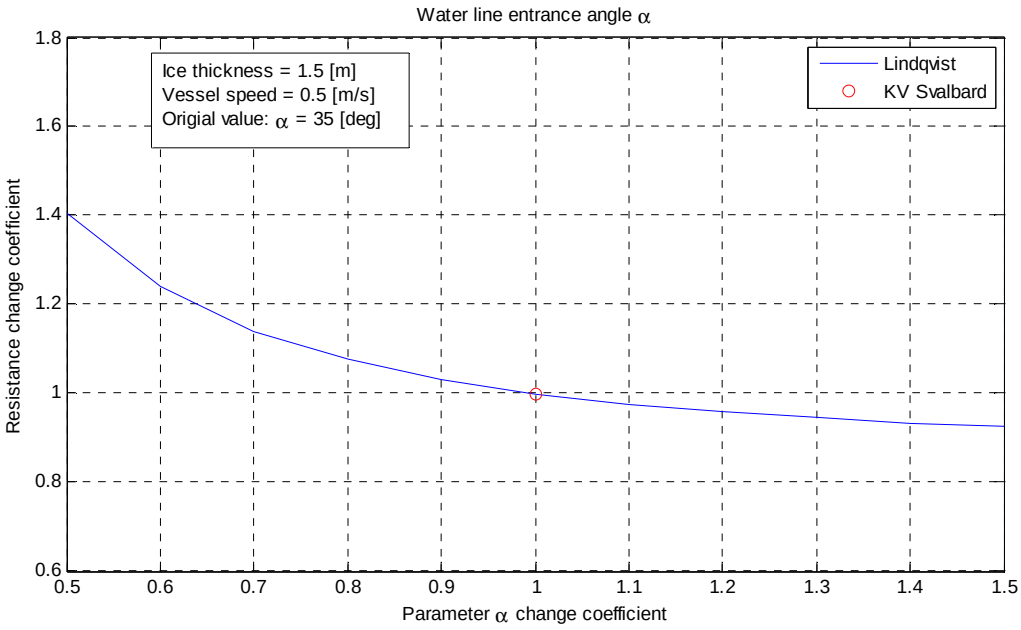
Water line entrance angle α
Ice thickness = 1.5 [m]
Vessel speed = 0.5 [m/s]
Origial value: α = 35 [deg]
Lindqvist
KV Svalbard
Resistance change coefficient
Parameter α change coefficient
1.8
1.6
1.4
1.2
1
0.8
0.6
0.5
0.6
0.7
0.8
0.9
1
1.1
1.2
1.3
1.4
1.5

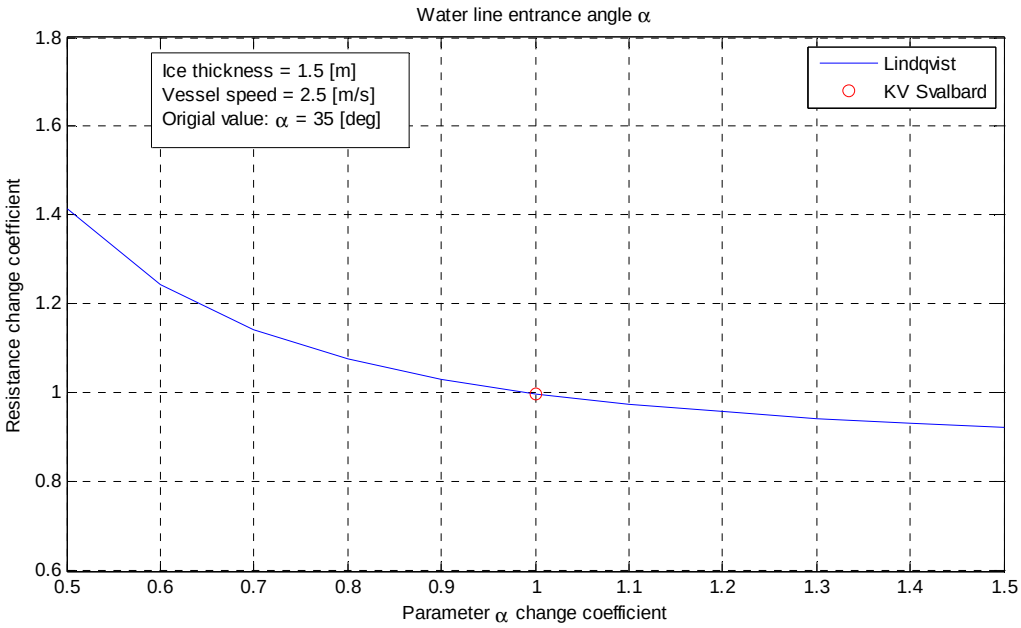
Water line entrance angle α
Ice thickness = 1.5 [m]
Vessel speed = 2.5 [m/s]
Origial value: α = 35 [deg]
Lindqvist
KV Svalbard
Resistance change coefficient
Parameter α change coefficient
1.8
1.6
1.4
1.2
1
0.8
0.6
0.5
0.6
0.7
0.8
0.9
1
1.1
1.2
1.3
1.4
1.5

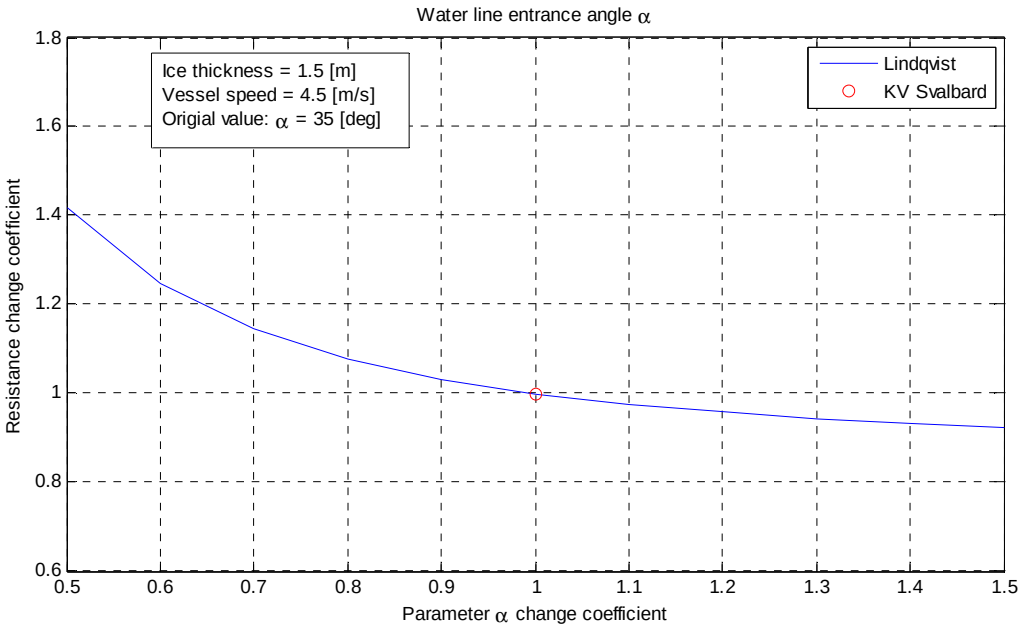
Water line entrance angle α
Ice thickness = 1.5 [m]
Vessel speed = 4.5 [m/s]
Origial value: α = 35 [deg]
Lindqvist
KV Svalbard
Resistance change coefficient
Parameter α change coefficient
1.8
1.6
1.4
1.2
1
0.8
0.6
0.5
0.6
0.7
0.8
0.9
1
1.1
1.2
1.3
1.4
1.5

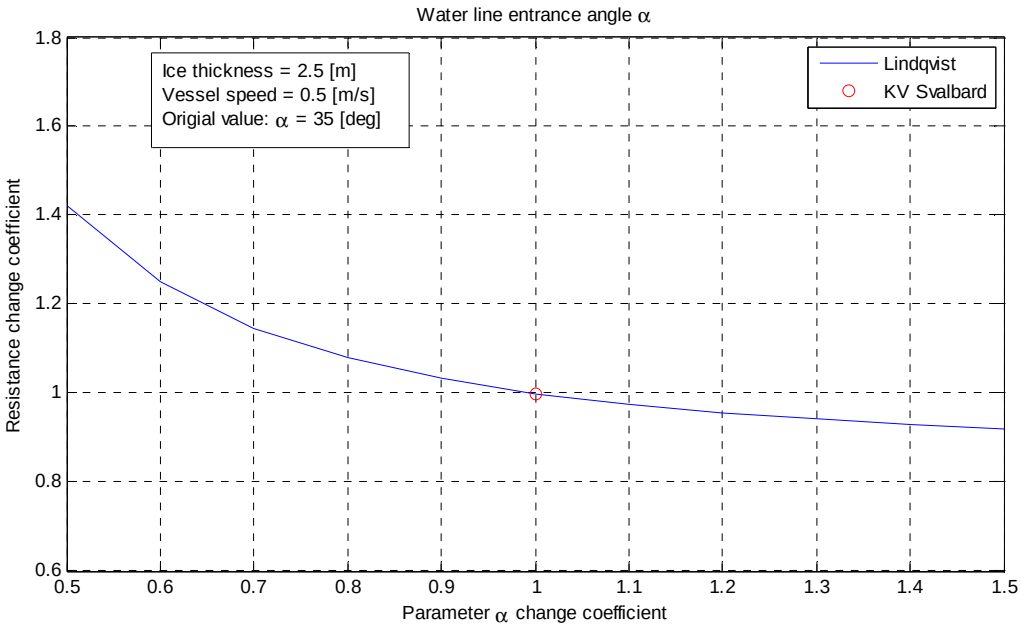
Water line entrance angle α
Ice thickness = 2.5 [m]
Vessel speed = 0.5 [m/s]
Origial value: α = 35 [deg]
Lindqvist
KV Svalbard
Resistance change coefficient
Parameter α change coefficient
1.8
1.6
1.4
1.2
1
0.8
0.6
0.5
0.6
0.7
0.8
0.9
1
1.1
1.2
1.3
1.4
1.5

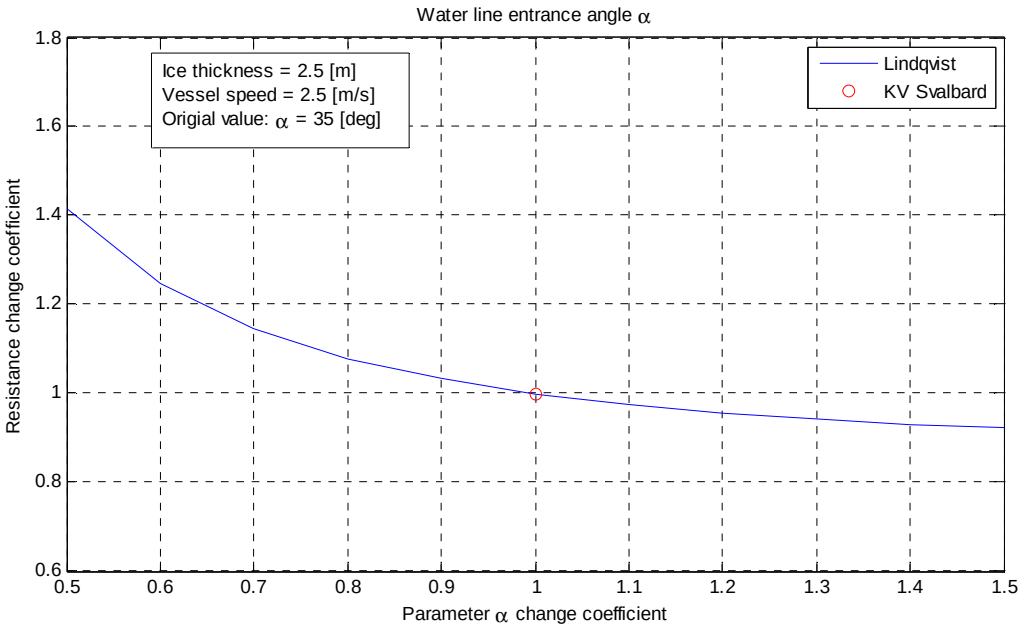
Water line entrance angle α
Ice thickness = 2.5 [m]
Vessel speed = 2.5 [m/s]
Origial value: α = 35 [deg]
Lindqvist
KV Svalbard
Resistance change coefficient
Parameter α change coefficient
1.8
1.6
1.4
1.2
1
0.8
0.6
0.5
0.6
0.7
0.8
0.9
1
1.1
1.2
1.3
1.4
1.5

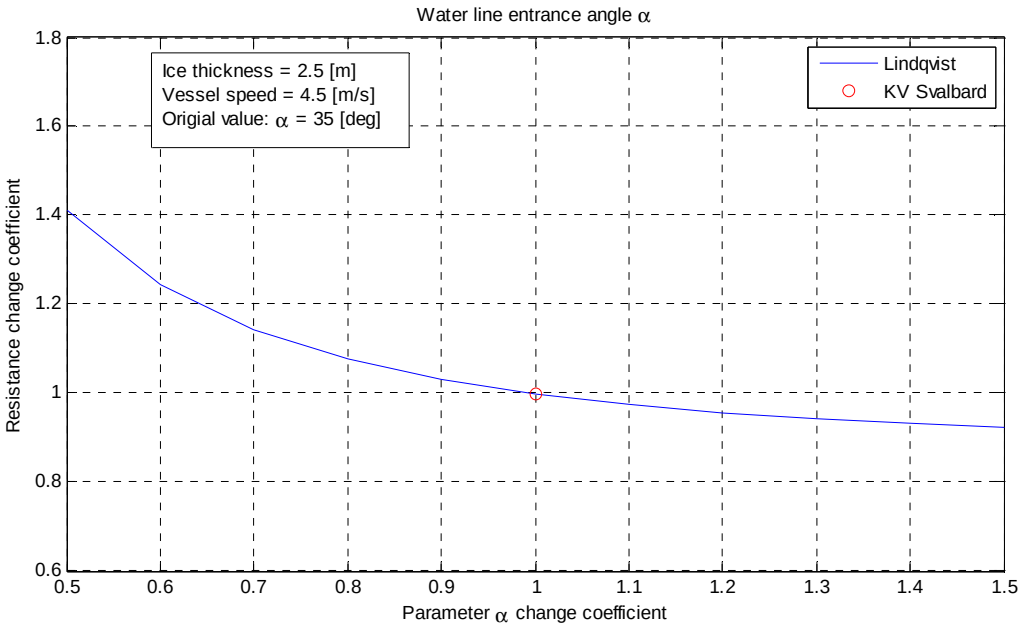
Water line entrance angle α
Ice thickness = 2.5 [m]
Vessel speed = 4.5 [m/s]
Origial value: α = 35 [deg]
Lindqvist
KV Svalbard
Resistance change coefficient
Parameter α change coefficient
1.8
1.6
1.4
1.2
1
0.8
0.6
0.5
0.6
0.7
0.8
0.9
1
1.1
1.2
1.3
1.4
1.5

C.3 Ice bending strength σ

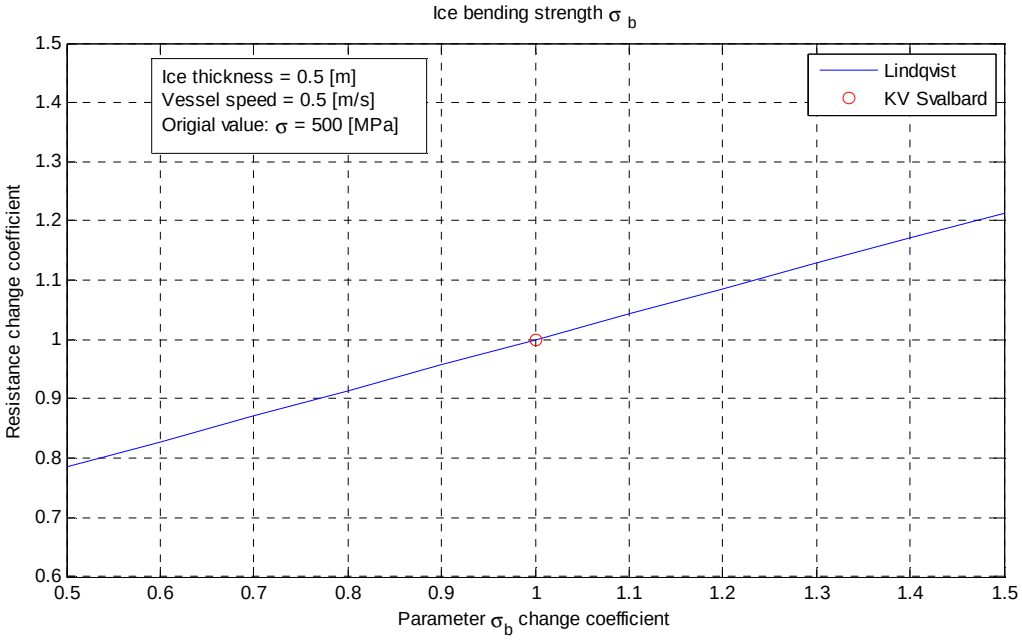

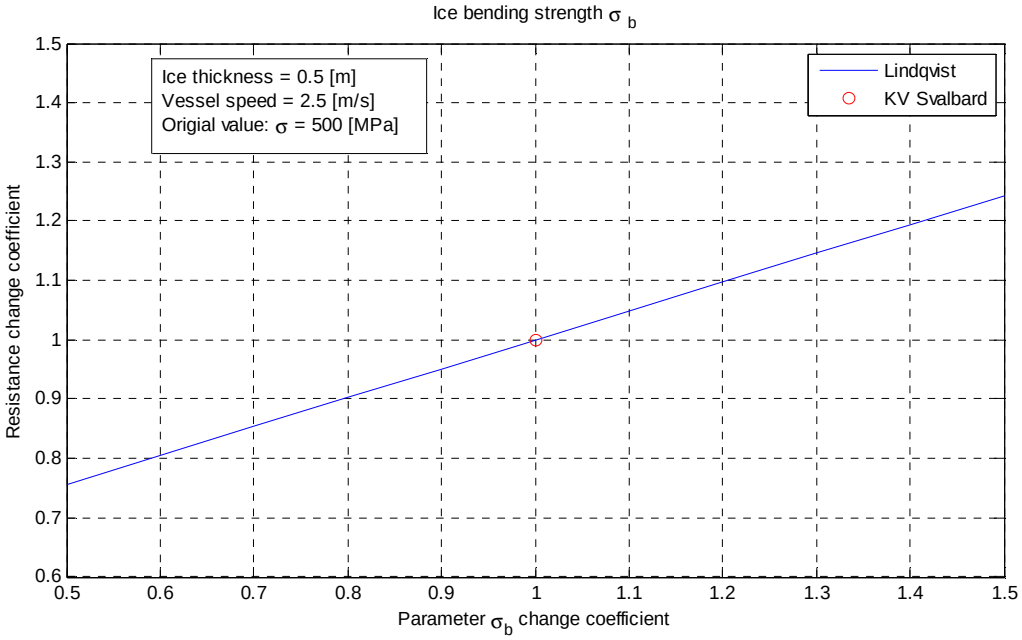

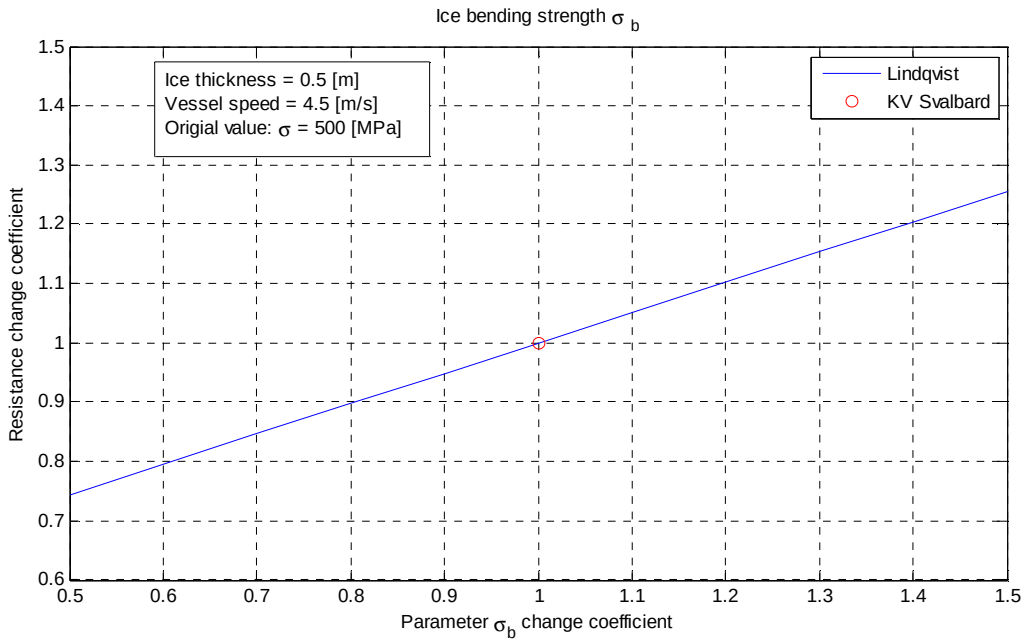
Ice bending strength σ b
Ice thickness = 0.5 [m]
Vessel speed = 4.5 [m/s]
Origial value: σ = 500 [MPa]
Lindqvist
KV Svalbard
Resistance change coefficient
Parameter σb change coefficient
0.5
0.6
0.7
0.8
0.9
1
1.1
1.2
1.3
1.4
1.5

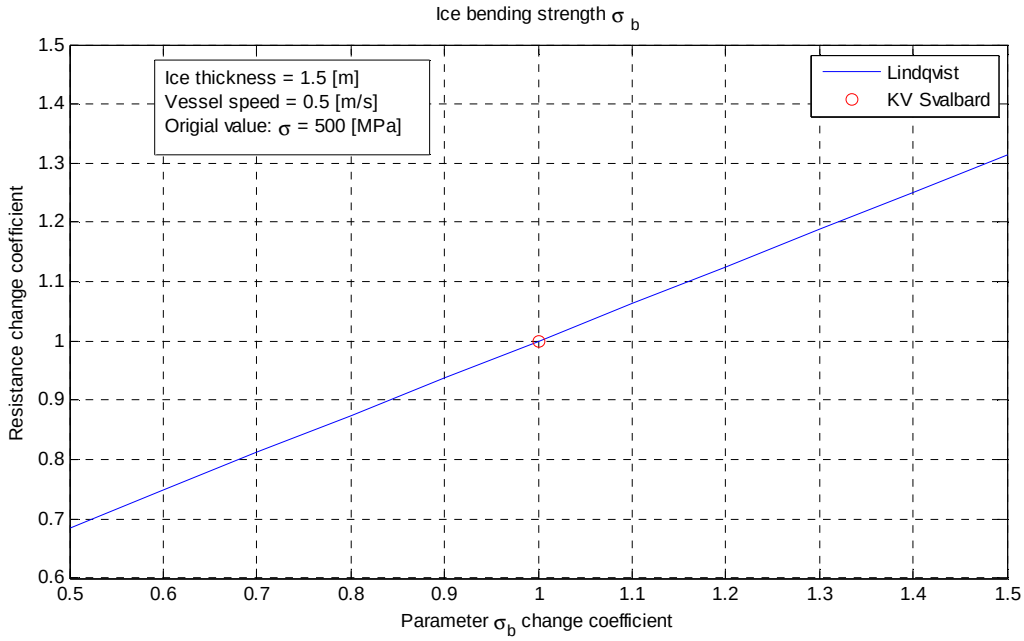
Ice bending strength σ b
Ice thickness = 1.5 [m]
Vessel speed = 0.5 [m/s]
Origial value: σ = 500 [MPa]
Lindqvist
KV Svalbard
Resistance change coefficient
Parameter σb change coefficient
0.5
0.6
0.7
0.8
0.9
1
1.1
1.2
1.3
1.4
1.5

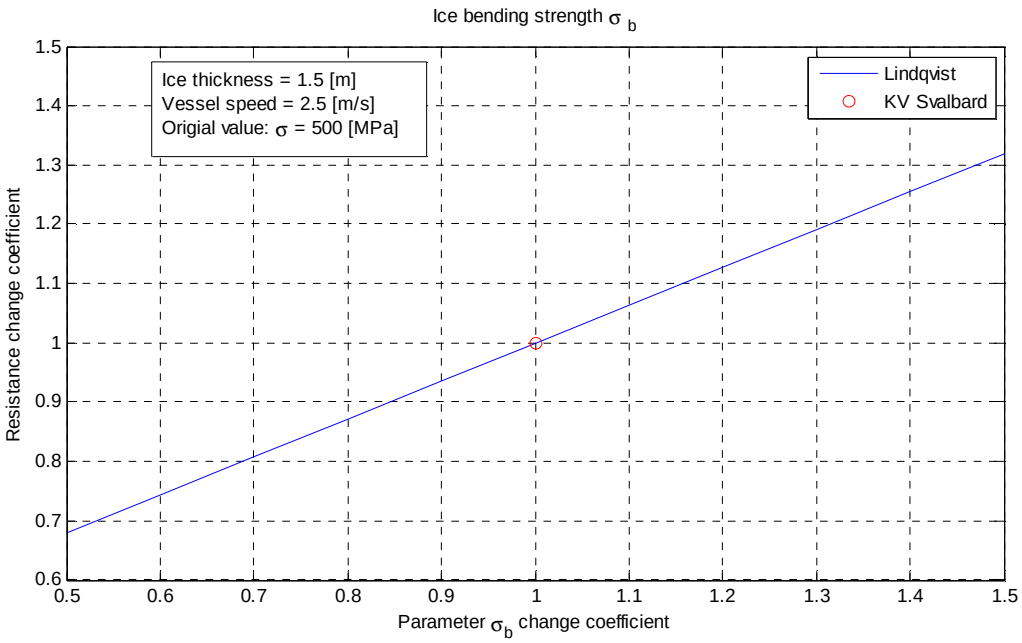
Ice bending strength σ b
Ice thickness = 1.5 [m]
Vessel speed = 2.5 [m/s]
Origial value: σ = 500 [MPa]
Lindqvist
KV Svalbard
Resistance change coefficient
Parameter σb change coefficient
0.5 0.6 0.7 0.8 0.9 1 1.1 1.2 1.3 1.4 1.5
0.6 0.7 0.8 0.9 1 1.1 1.2 1.3 1.4 1.5

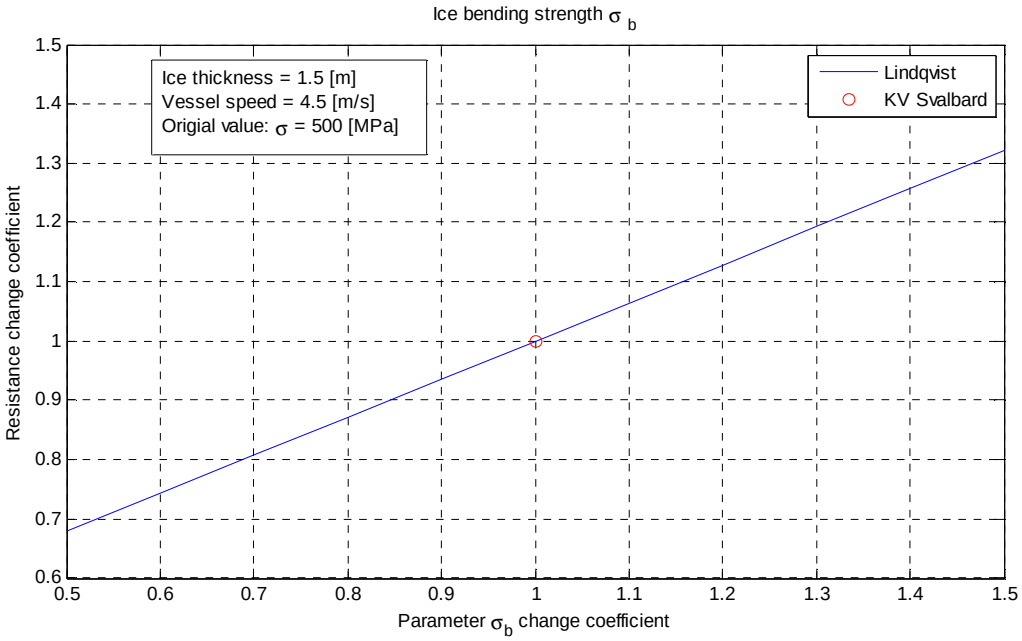
Ice bending strength σ b
Ice thickness = 1.5 [m]
Vessel speed = 4.5 [m/s]
Origial value: σ = 500 [MPa]
Lindqvist
KV Svalbard
Resistance change coefficient
Parameter σb change coefficient
0.5 0.6 0.7 0.8 0.9 1 1.1 1.2 1.3 1.4 1.5
0.6 0.7 0.8 0.9 1 1.1 1.2 1.3 1.4 1.5

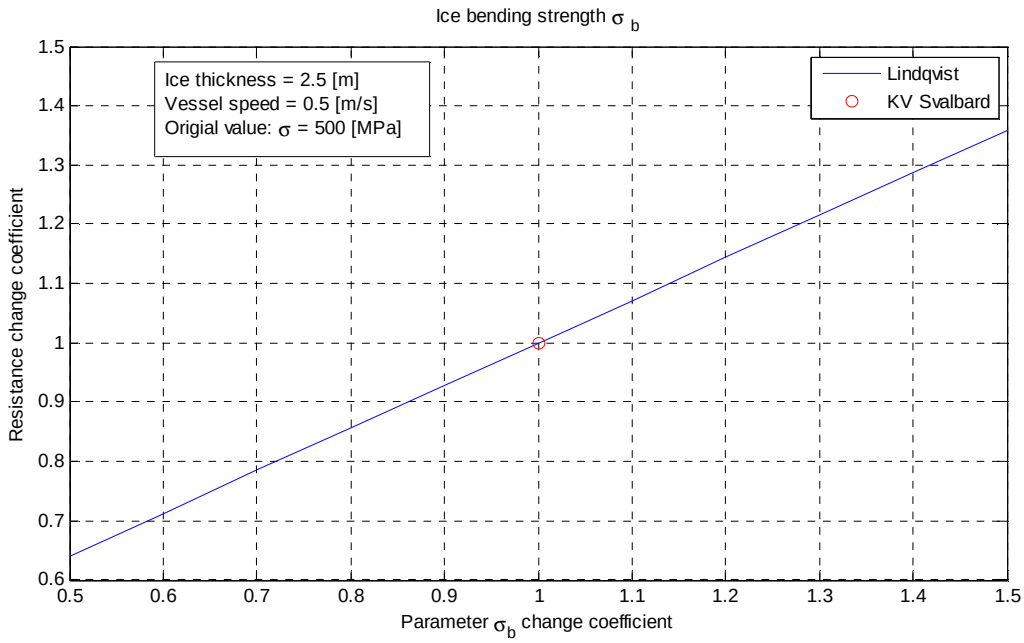
Ice bending strength σ b
Ice thickness = 2.5 [m]
Vessel speed = 0.5 [m/s]
Origial value: σ = 500 [MPa]
Lindqvist
KV Svalbard
Resistance change coefficient
Parameter σb change coefficient
0.5
0.6
0.7
0.8
0.9
1
1.1
1.2
1.3
1.4
1.5

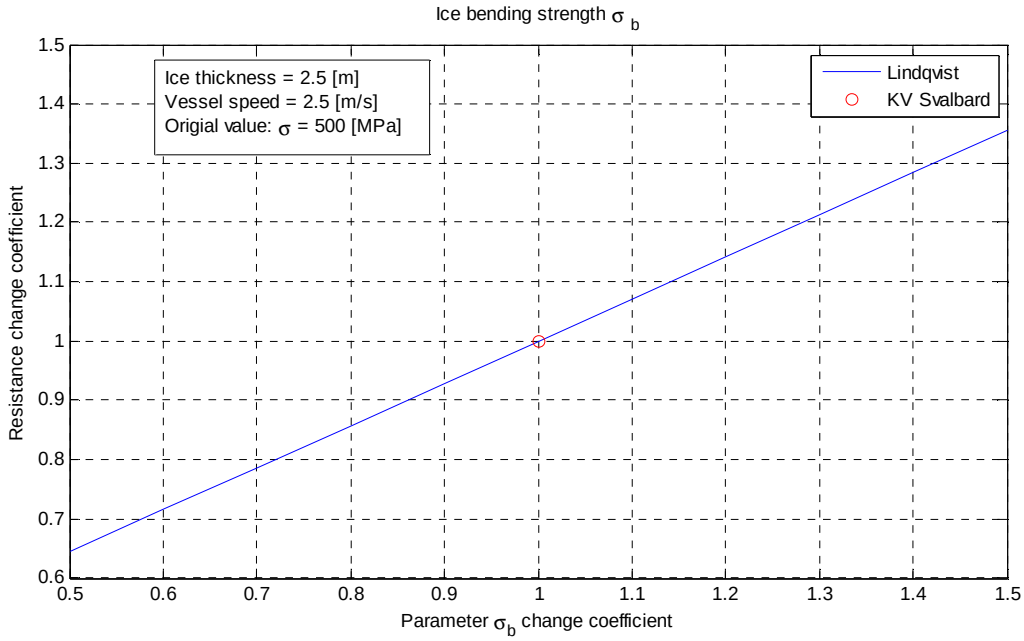
Ice bending strength σ b
Ice thickness = 2.5 [m]
Vessel speed = 2.5 [m/s]
Origial value: σ = 500 [MPa]
Lindqvist
KV Svalbard
Resistance change coefficient
Parameter σb change coefficient
0.5
0.6
0.7
0.8
0.9
1
1.1
1.2
1.3
1.4
1.5

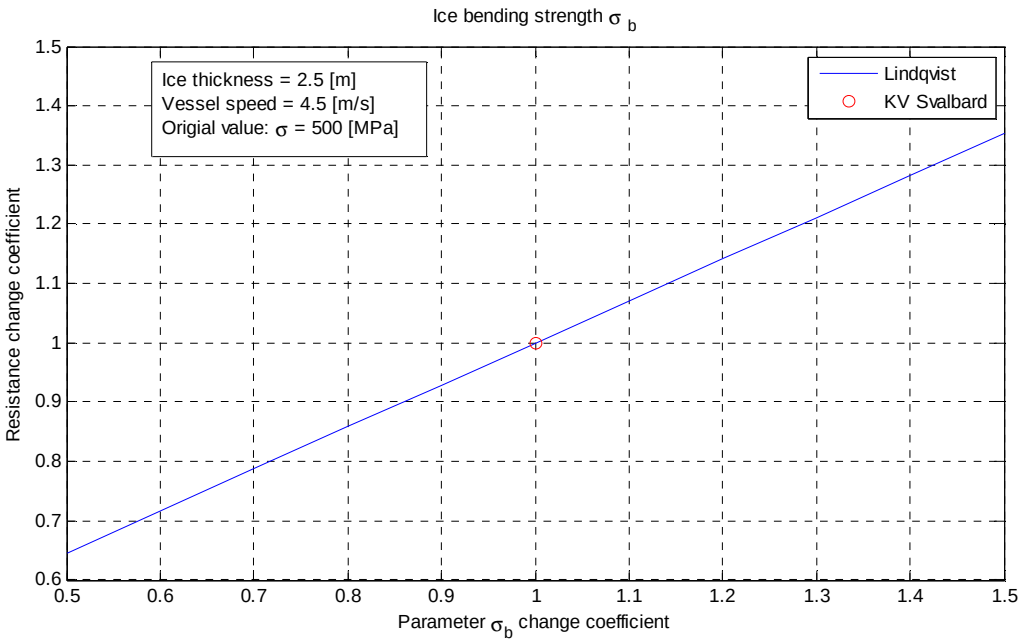
Ice bending strength σ b
Ice thickness = 2.5 [m]
Vessel speed = 4.5 [m/s]
Origial value: σ = 500 [MPa]
Lindqvist
KV Svalbard
Resistance change coefficient
Parameter σb change coefficient
1.5
1.4
1.3
1.2
1.1
1
0.9
0.8
0.7
0.6
0.5
0.6
0.7
0.8
0.9
1
1.1
1.2
1.3
1.4
1.5

C.4 Friction coefficient μ

The friction coefficient sensitivity is not dependent on speed, therefore only one speed case is shown.

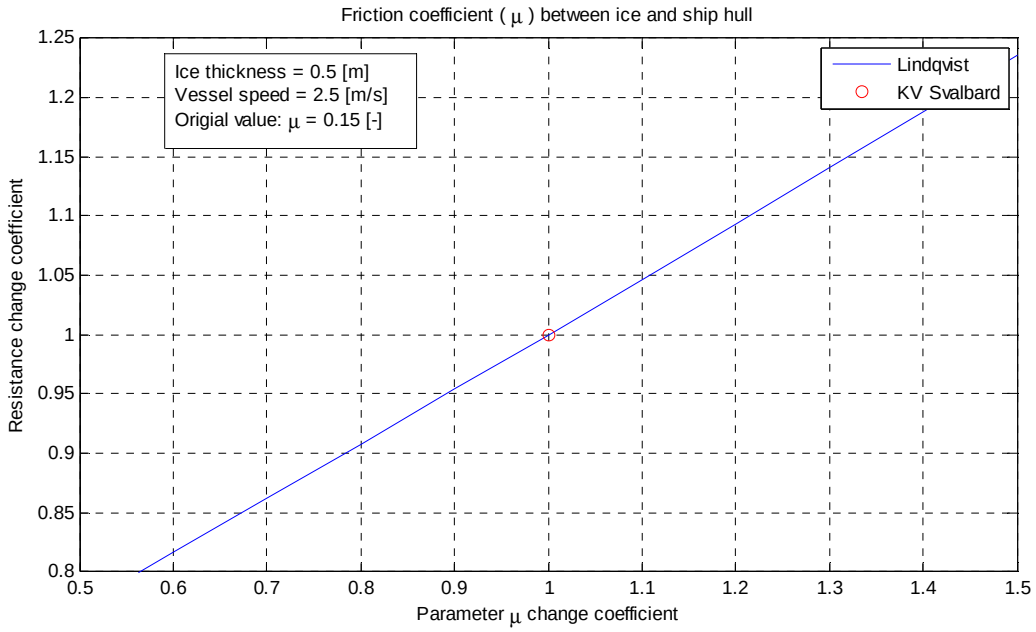

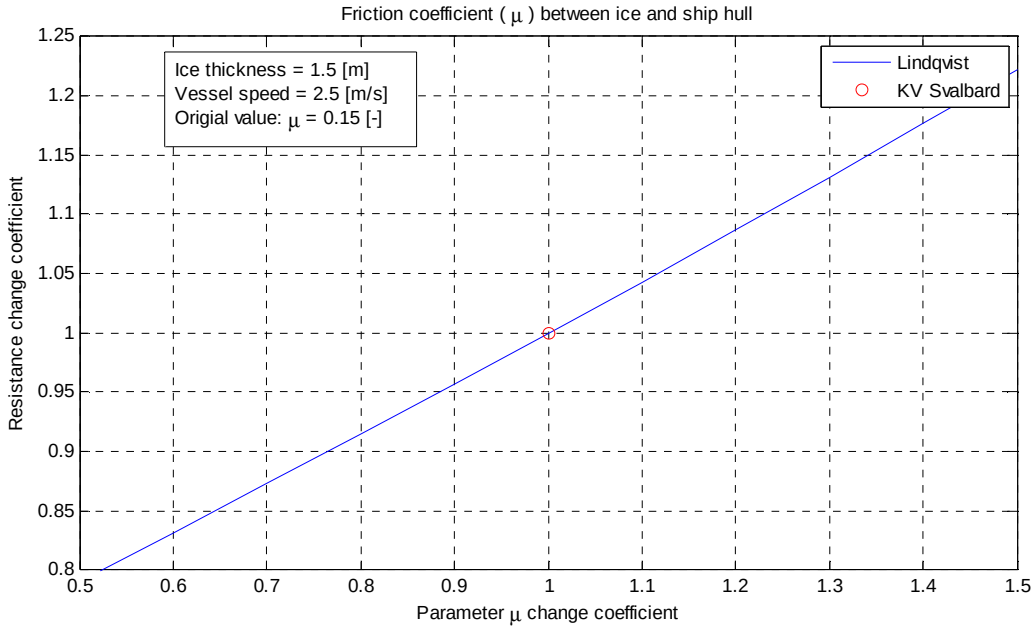

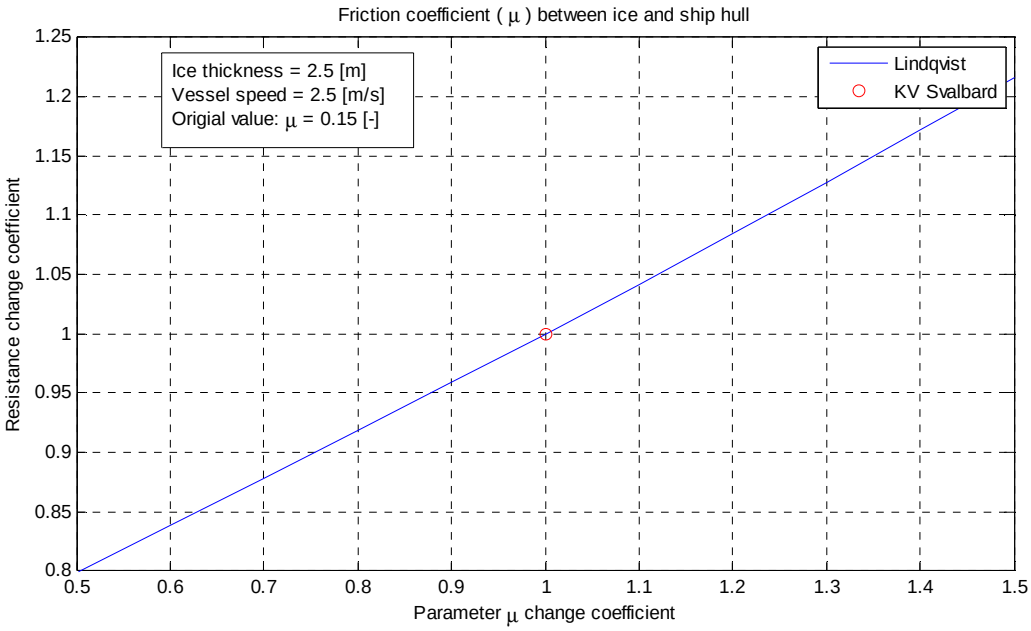
Friction coefficient (μ) between ice and ship hull
Ice thickness = 2.5 [m]
Vessel speed = 2.5 [m/s]
Origial value: μ = 0.15 [-]
Lindqvist
KV Svalbard
Resistance change coefficient
Parameter μ change coefficient
1.25
1.2
1.15
1.1
1.05
1
0.95
0.9
0.85
0.8
0.5
0.6
0.7
0.8
0.9
1
1.1
1.2
1.3
1.4
1.5

C.5 Bow section length

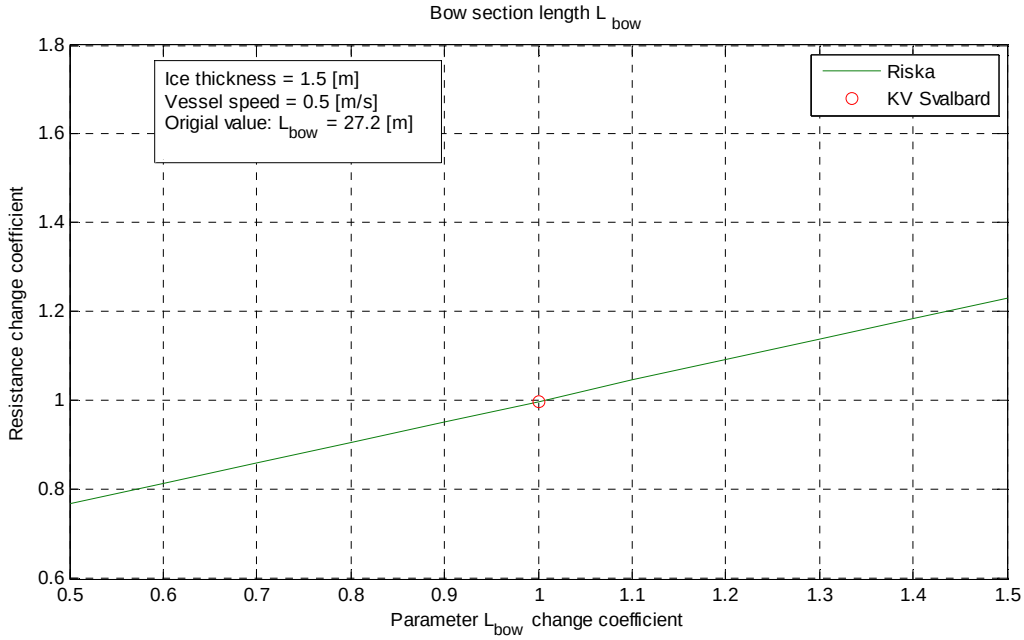

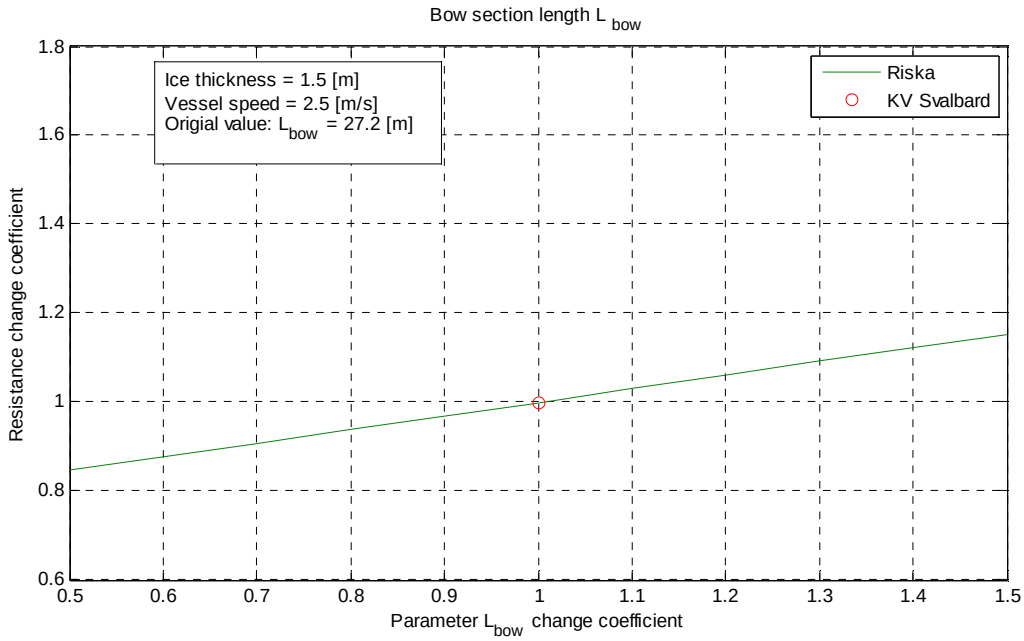

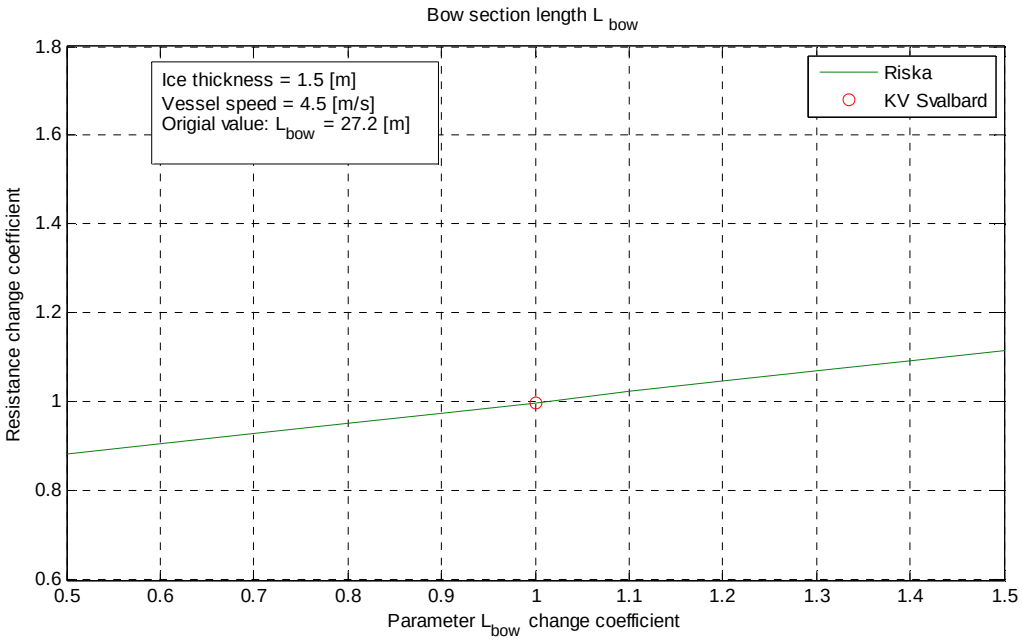
Bow section length L bow
Ice thickness = 1.5 [m]
Vessel speed = 4.5 [m/s]
Origial value: L bow = 27.2 [m]
Riska
KV Svalbard
Resistance change coefficient
Parameter L bow change coefficient
1.8
1.6
1.4
1.2
1
0.8
0.6
0.5
0.6
0.7
0.8
0.9
1
1.1
1.2
1.3
1.4
1.5

C.6 Length of section with parallel sides

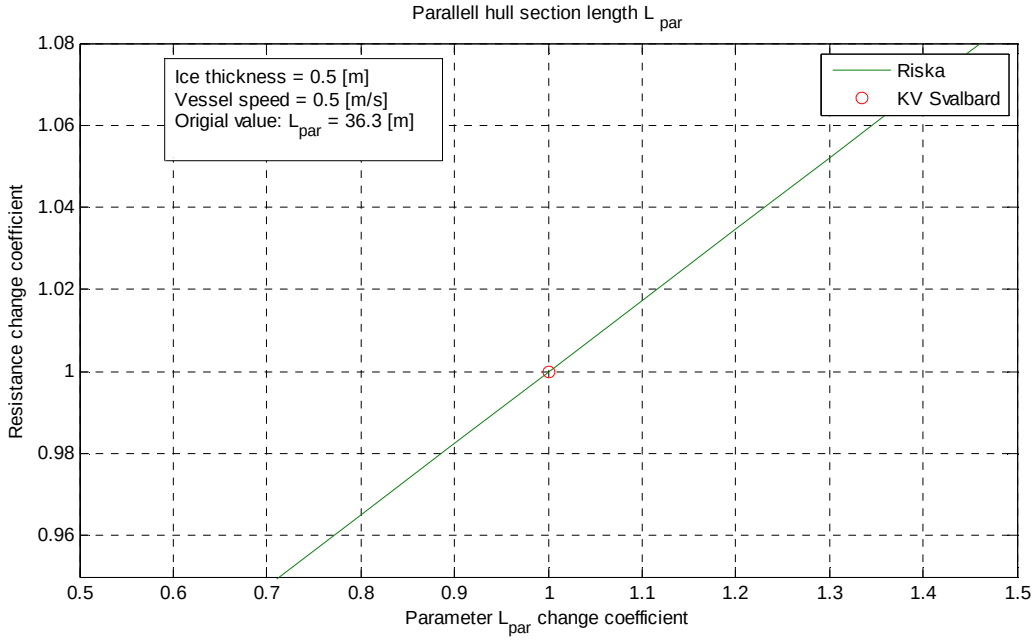

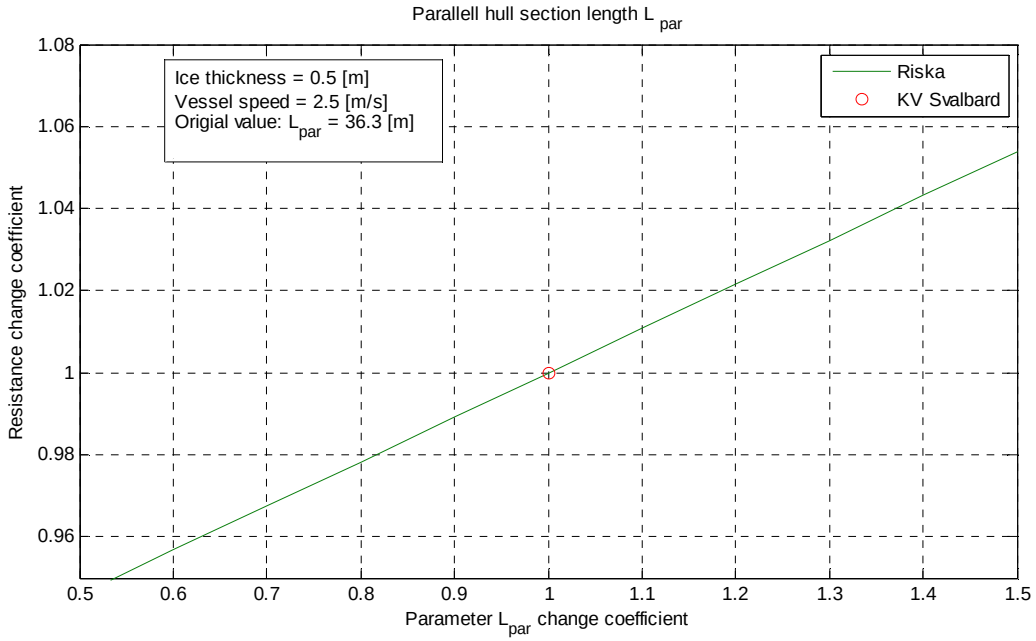

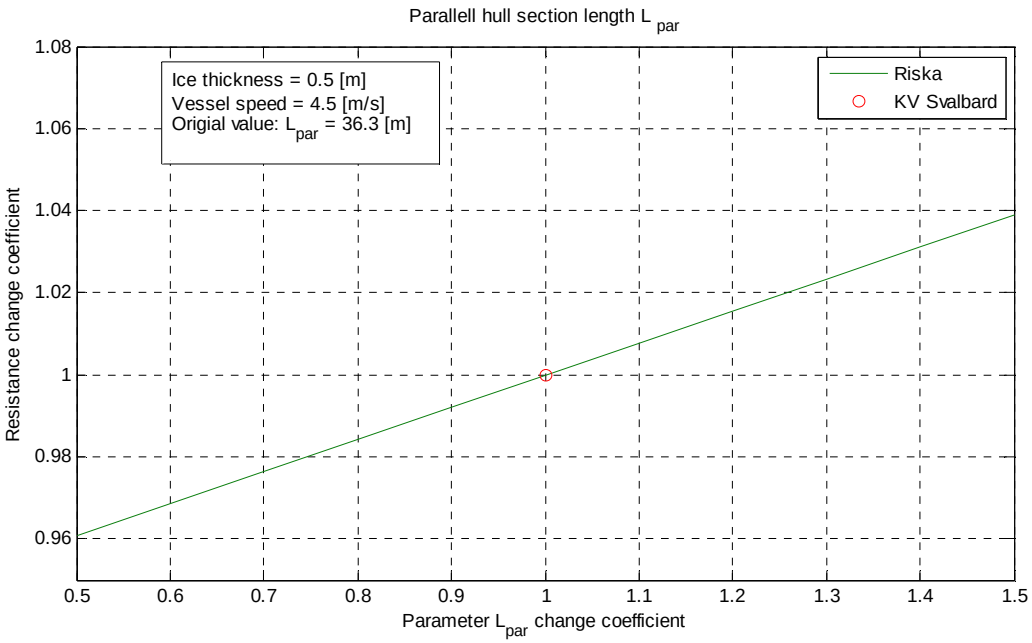
Parallell hull section length L par
Ice thickness = 0.5 [m]
Vessel speed = 4.5 [m/s]
Origial value: L par = 36.3 [m]
Riska
KV Svalbard
Resistance change coefficient
Parameter L par change coefficient
1.08
1.06
1.04
1.02
1
0.98
0.96
0.5
0.6
0.7
0.8
0.9
1
1.1
1.2
1.3
1.4
1.5

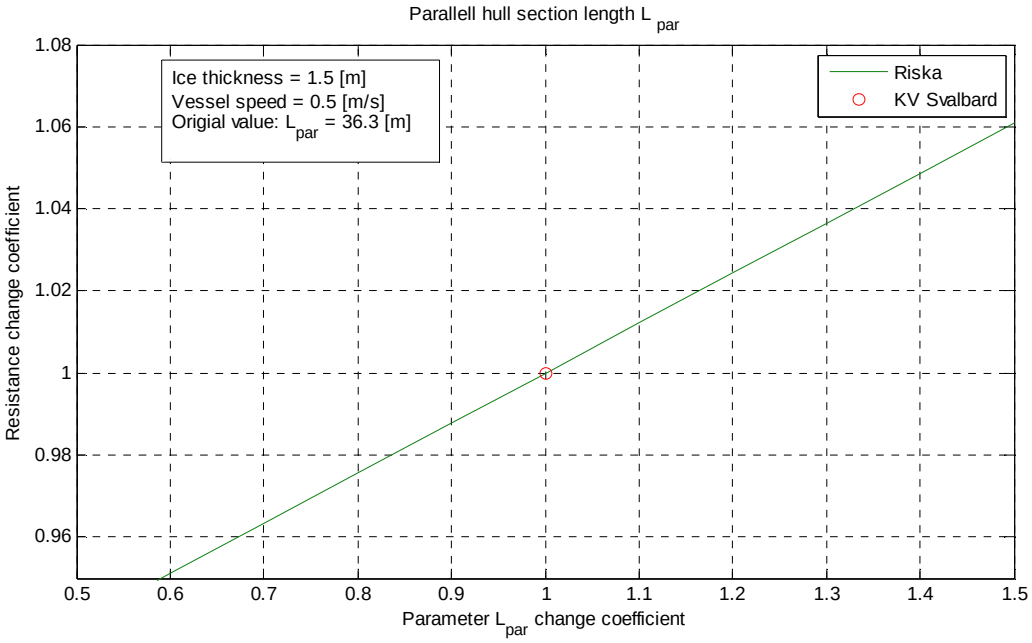
Parallell hull section length L par
Ice thickness = 1.5 [m]
Vessel speed = 0.5 [m/s]
Origial value: L par = 36.3 [m]
Riska
KV Svalbard
Resistance change coefficient
Parameter L par change coefficient
1.08
1.06
1.04
1.02
1
0.98
0.96
0.5
0.6
0.7
0.8
0.9
1
1.1
1.2
1.3
1.4
1.5

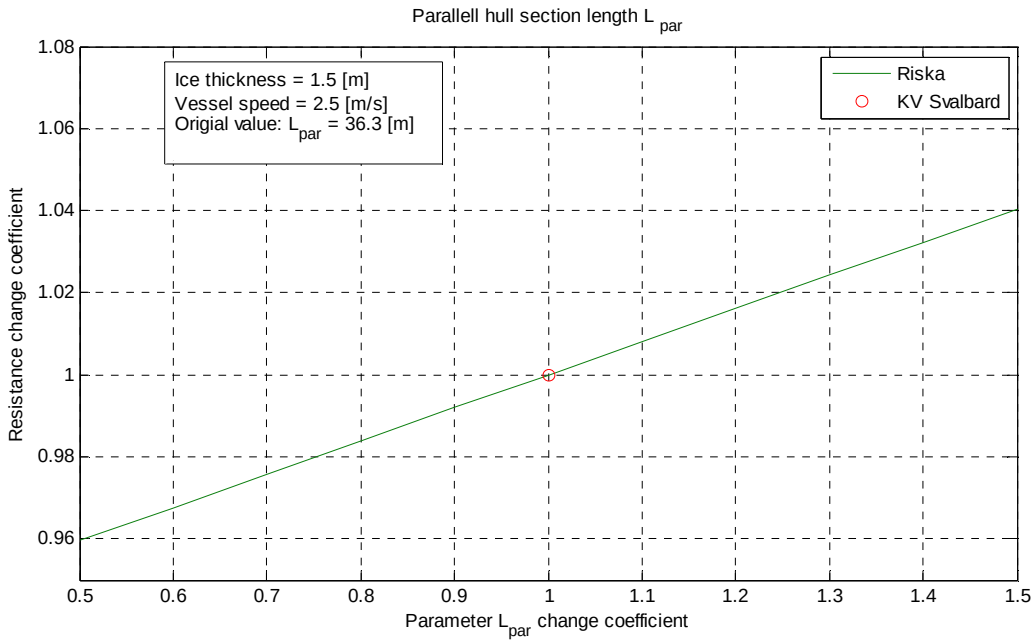
Parallell hull section length L par
Ice thickness = 1.5 [m]
Vessel speed = 2.5 [m/s]
Origial value: L par = 36.3 [m]
Riska
KV Svalbard
Resistance change coefficient
Parameter L par change coefficient
1.08
1.06
1.04
1.02
1
0.98
0.96
0.5
0.6
0.7
0.8
0.9
1
1.1
1.2
1.3
1.4
1.5

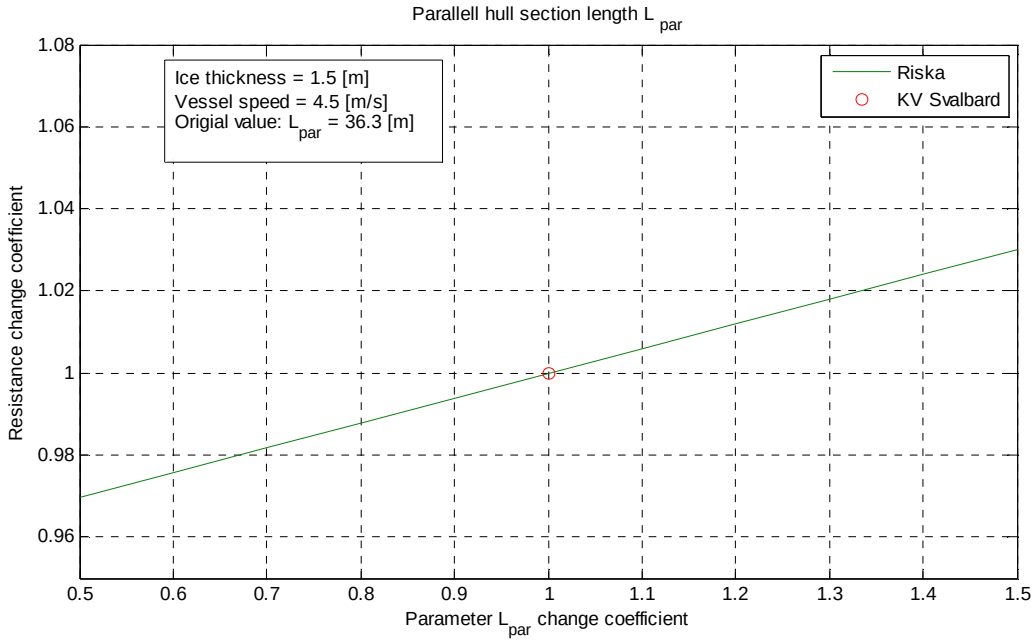
Parallell hull section length L par
Ice thickness = 1.5 [m]
Vessel speed = 4.5 [m/s]
Origial value: L par = 36.3 [m]
Riska
KV Svalbard
Resistance change coefficient
Parameter L par change coefficient
1.08
1.06
1.04
1.02
1
0.98
0.96
0.5
0.6
0.7
0.8
0.9
1
1.1
1.2
1.3
1.4
1.5

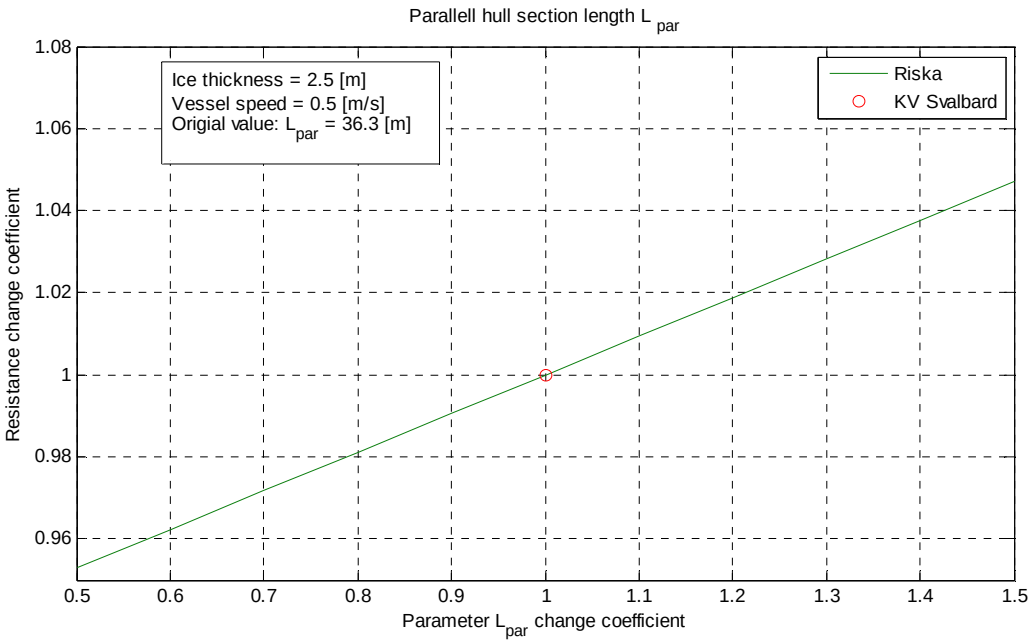
Parallell hull section length L par
Ice thickness = 2.5 [m]
Vessel speed = 0.5 [m/s]
Origial value: L par = 36.3 [m]
Riska
KV Svalbard
Resistance change coefficient
Parameter L par change coefficient
1.08
1.06
1.04
1.02
1
0.98
0.96
0.5
0.6
0.7
0.8
0.9
1
1.1
1.2
1.3
1.4
1.5

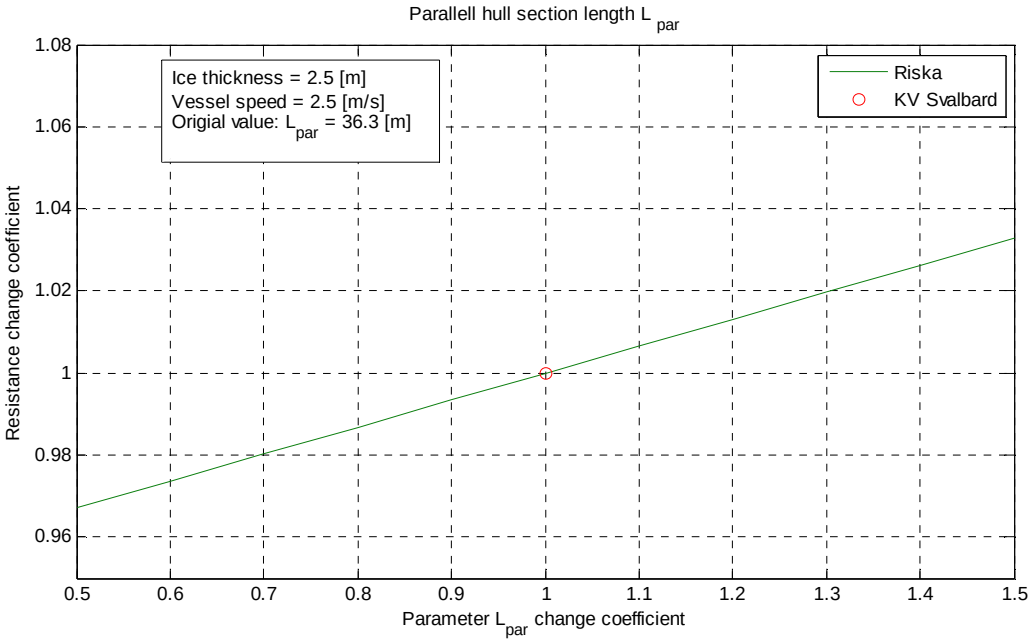
Parallell hull section length L par
Ice thickness = 2.5 [m]
Vessel speed = 2.5 [m/s]
Origial value: L par = 36.3 [m]
Riska
KV Svalbard
Resistance change coefficient
Parameter L par change coefficient
1.08
1.06
1.04
1.02
1
0.98
0.96
0.5
0.6
0.7
0.8
0.9
1
1.1
1.2
1.3
1.4
1.5

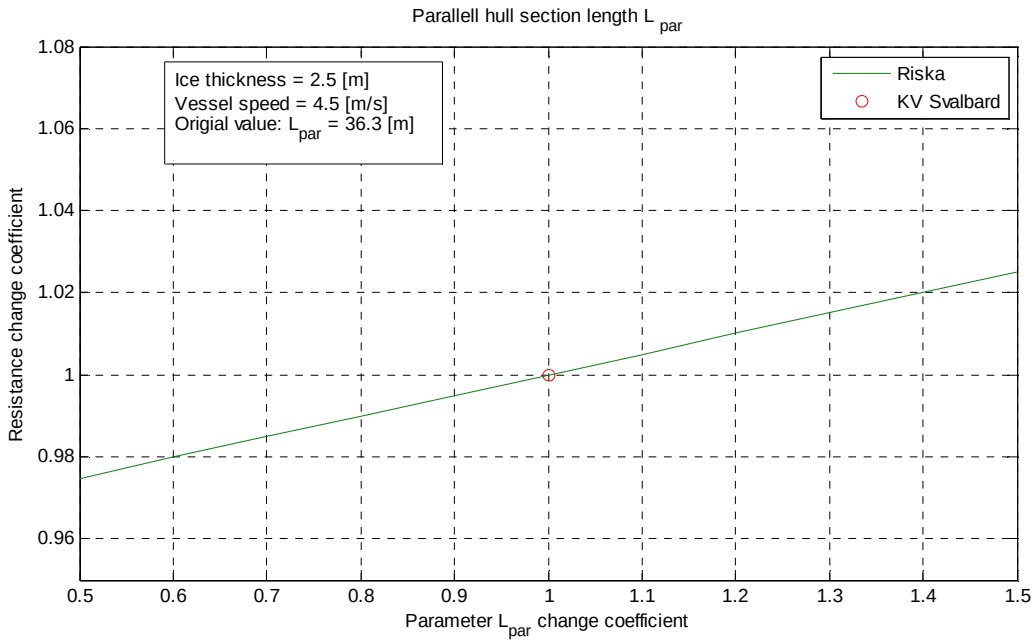
Parallell hull section length L par
Ice thickness = 2.5 [m]
Vessel speed = 4.5 [m/s]
Origial value: L par = 36.3 [m]
Riska
KV Svalbard
Resistance change coefficient
Parameter L par change coefficient
1.08
1.06
1.04
1.02
1
0.98
0.96
0.5
0.6
0.7
0.8
0.9
1
1.1
1.2
1.3
1.4
1.5

D Scatterplots of divided data

Ratio between resistance estimated from measurements and Lindqvist estimate, plotted against ice thickness.

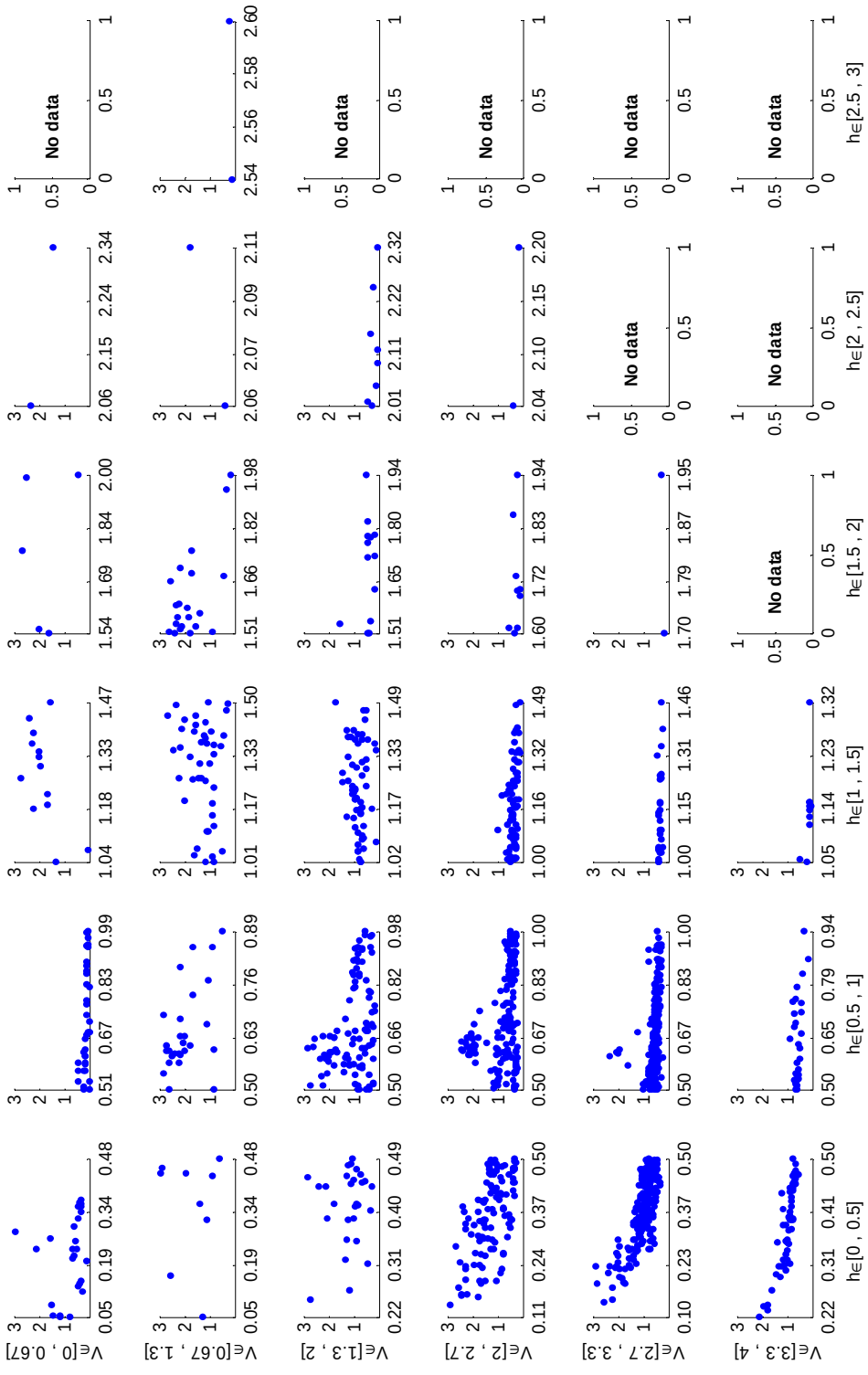

Ratio between resistance estimated from measurements and Lindqvist estimate, plotted against ice speed

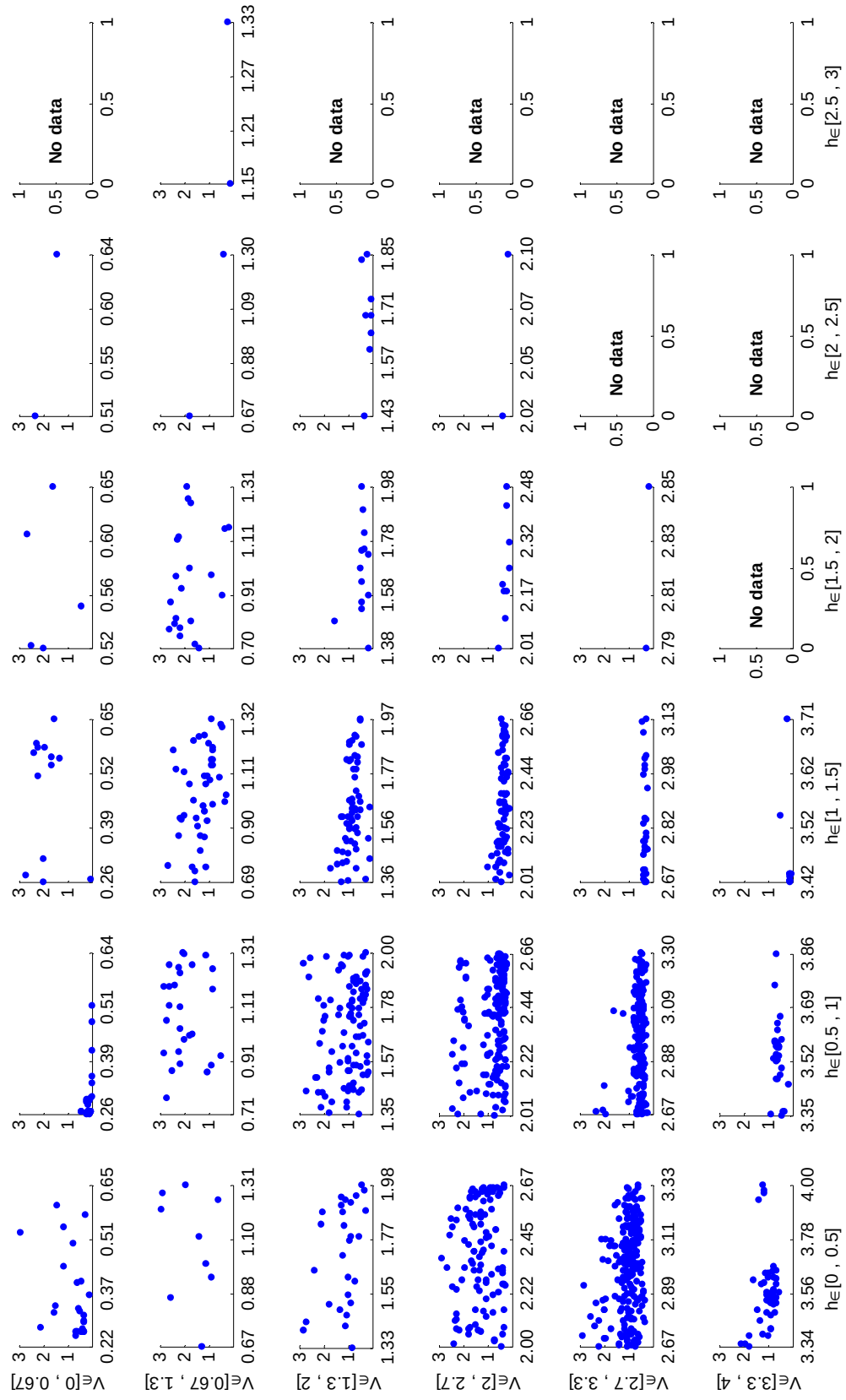

Ratio between resistance estimated from measurements and Riska estimate, plotted against ice thickness

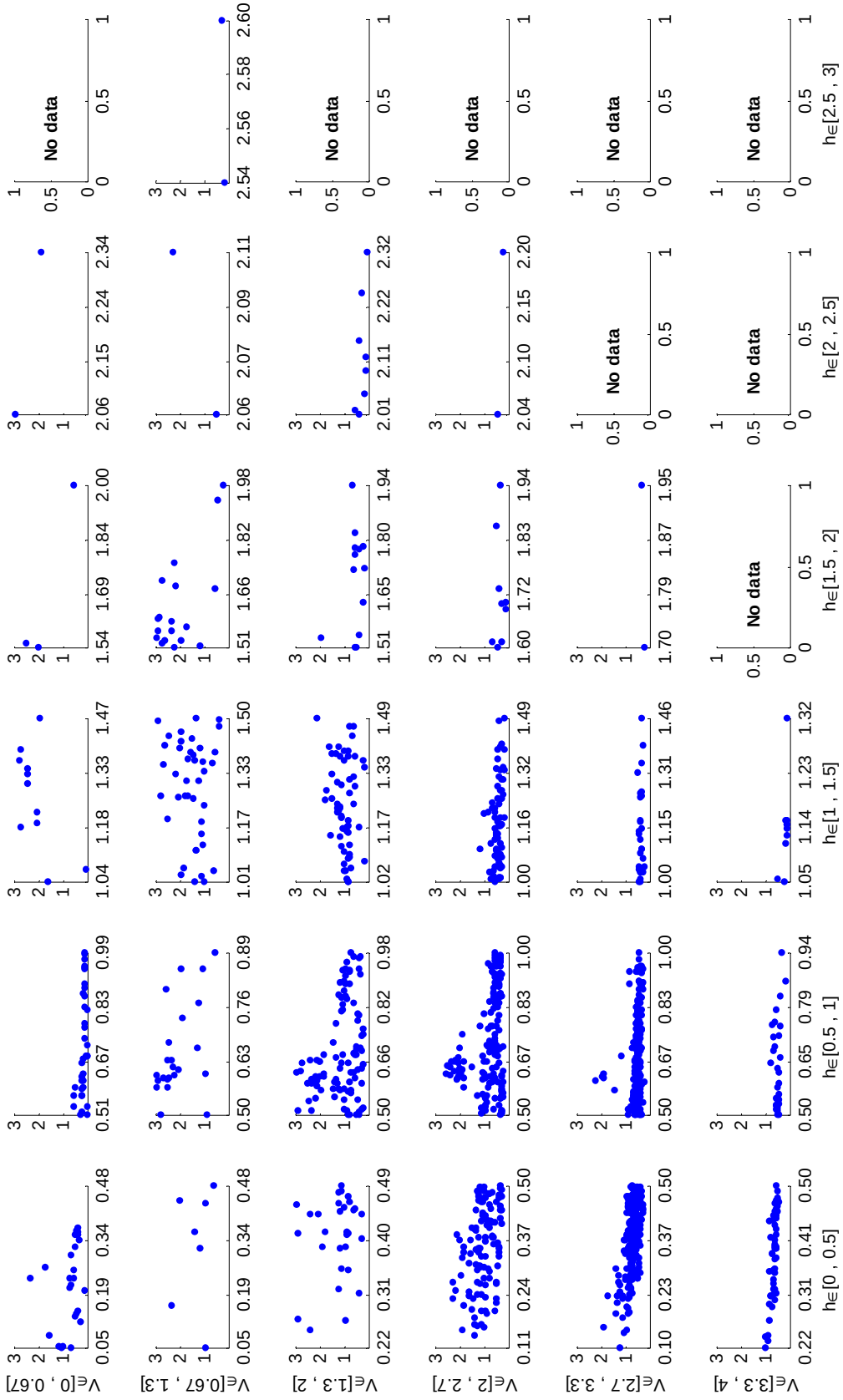

Ratio between resistance estimated from measurements and Riska estimate, plotted against speed

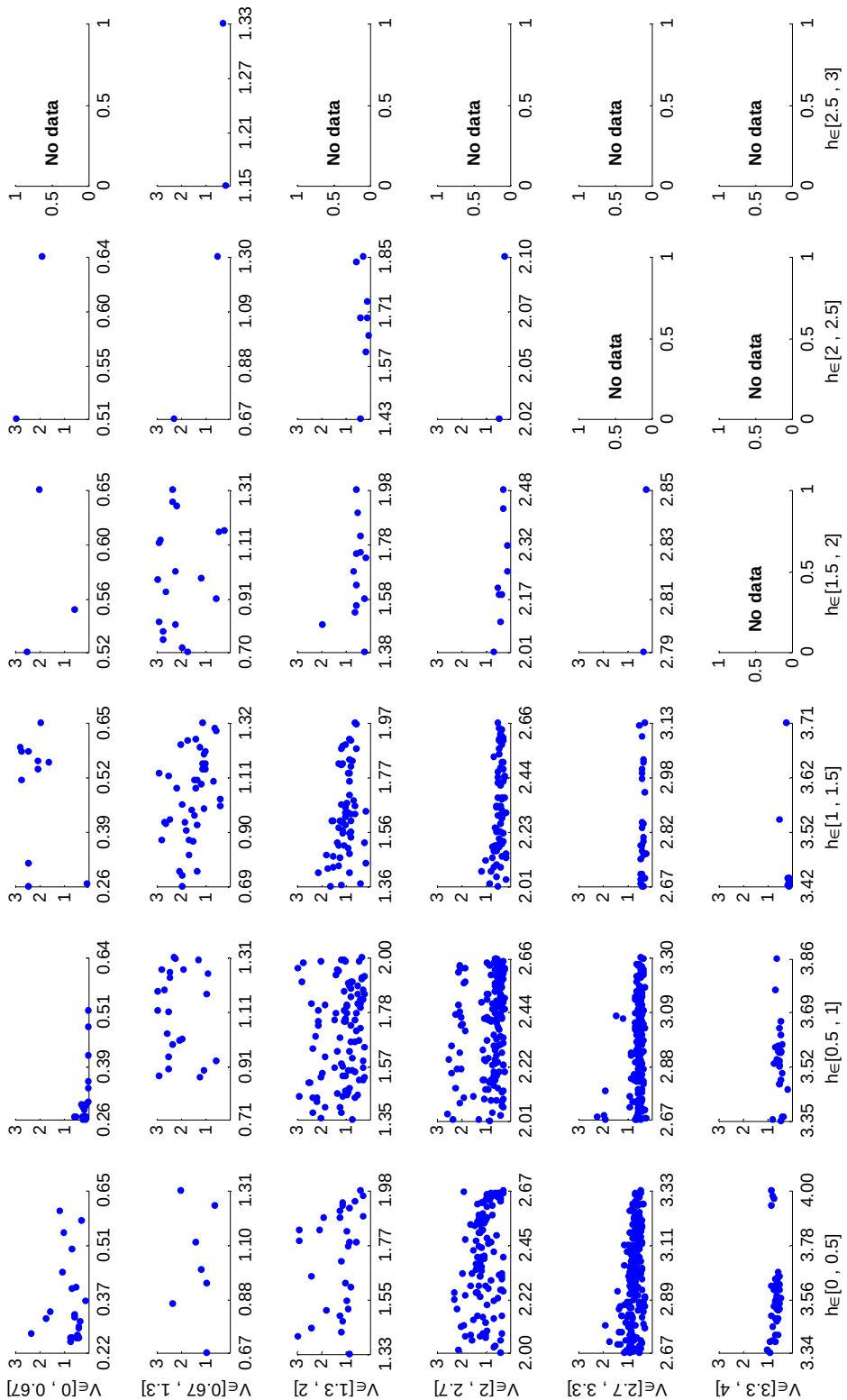

E Lognormal probability plots for Lindqvist formulation

E.1 Speed ∈[0,0.67]

Est/Lindqv ratio tested as a Log-Normal distribution in interval: V∈[0.00,0.67] h∈[0.00,0.50]

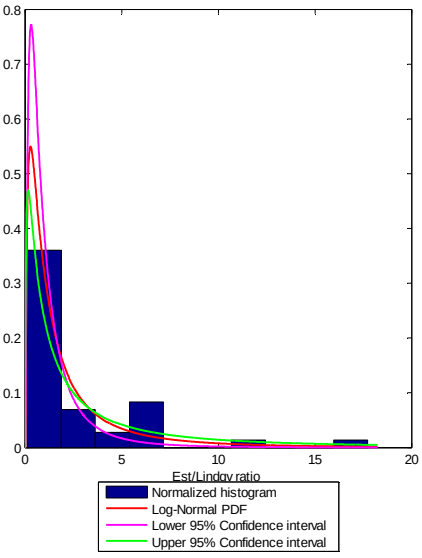

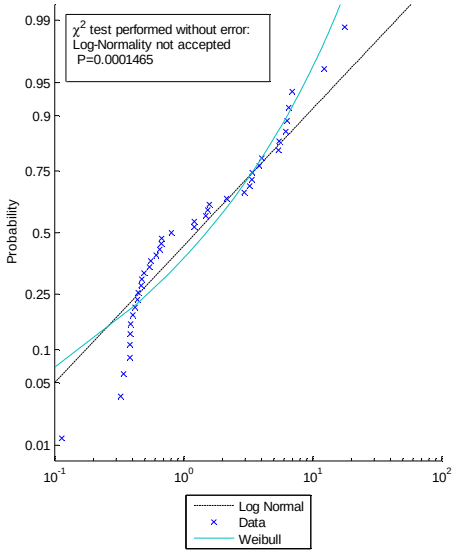

Est/Lindqv ratio tested as a Log-Normal distribution in interval: V∈[0.00,0.67] h∈[0.50,1.00]

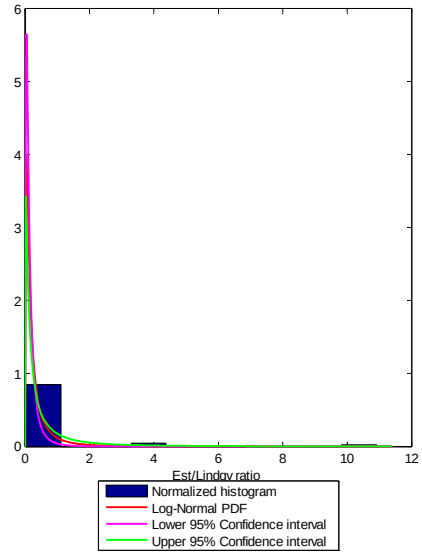

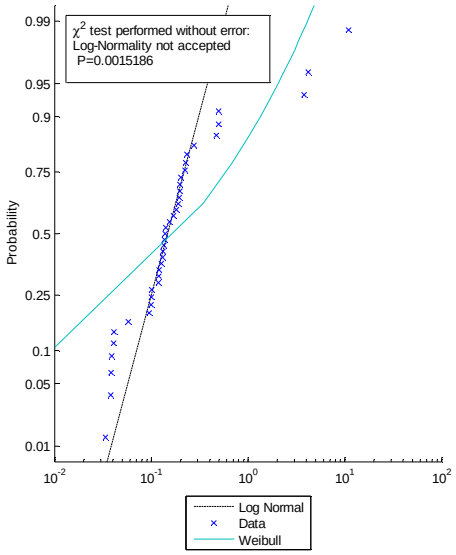

E.2 Speed ∈[0.67,0.67]

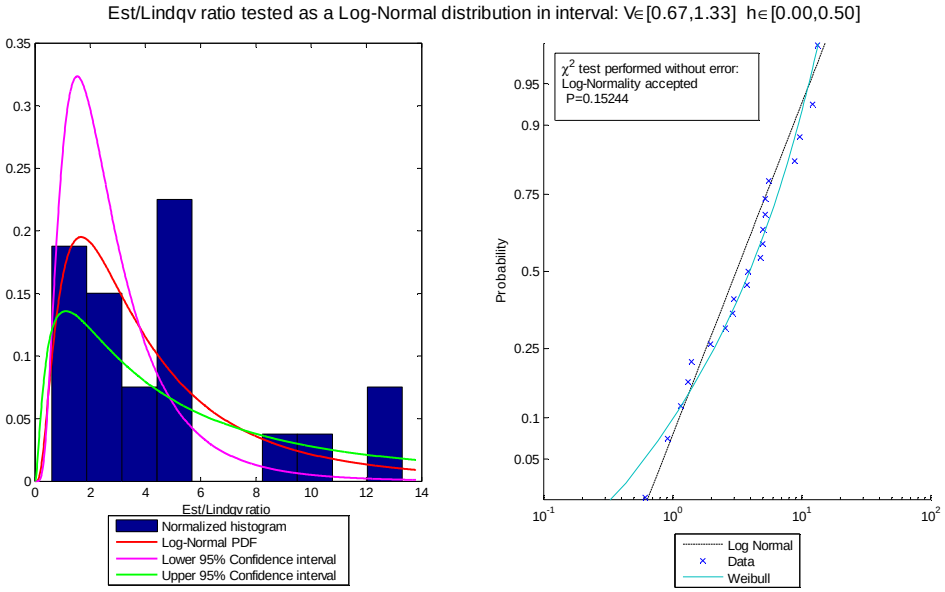

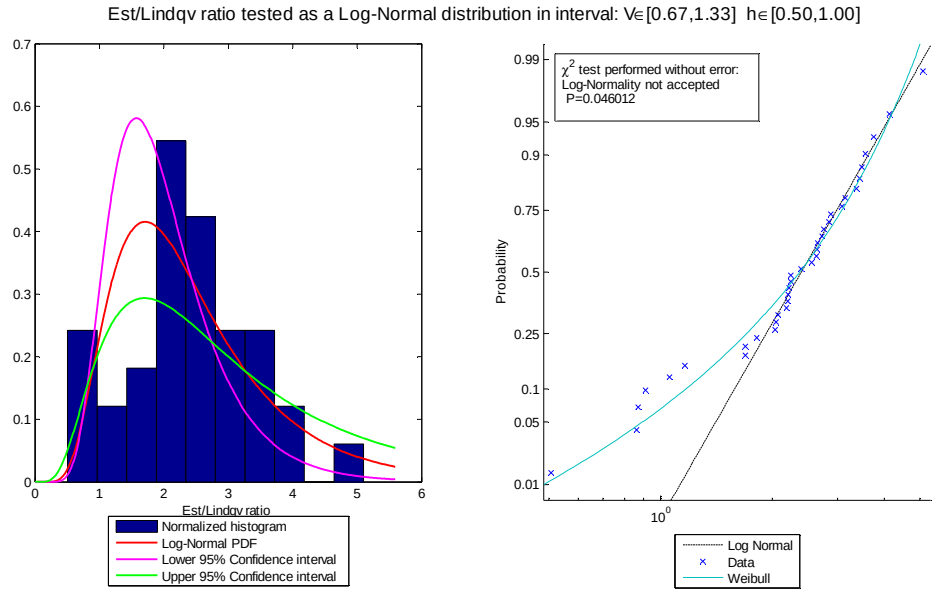

Est/Lindqv ratio tested as a Log-Normal distribution in interval: V∈[0.67,1.33] h∈[1.00,1.50]

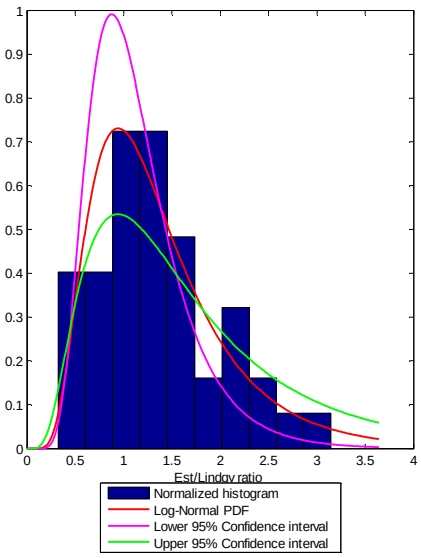

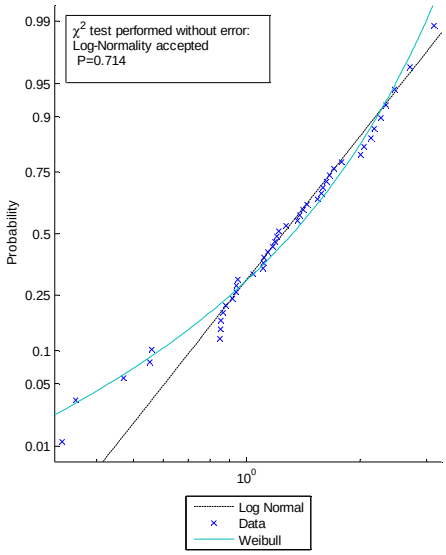

Est/Lindqv ratio tested as a Log-Normal distribution in interval: V∈[0.67,1.33] h∈[1.50,2.00]

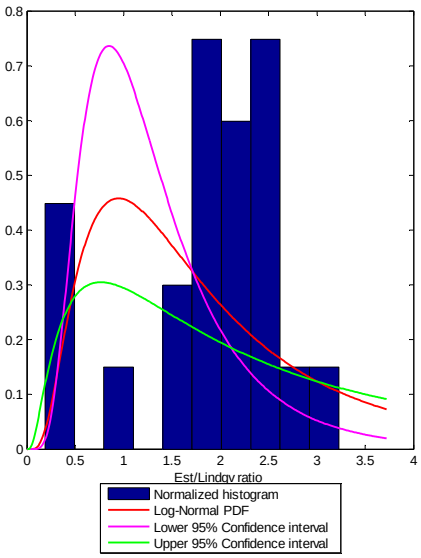

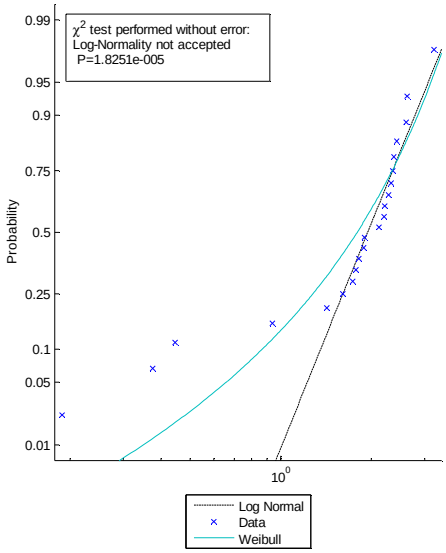

E.3 Speed ∈[1.33,2.0]

Est/Lindqv ratio tested as a Log-Normal distribution in interval: V∈[1.33,2.00] h∈[0.00,0.50]

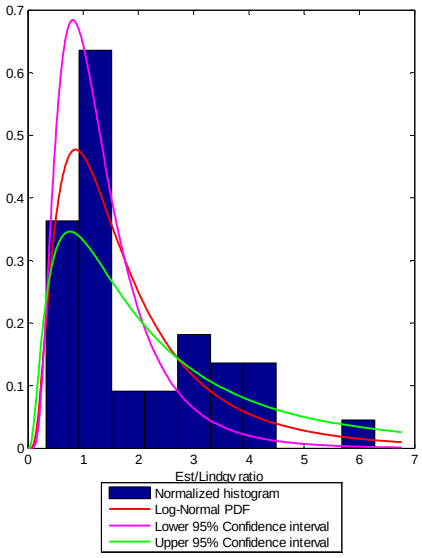

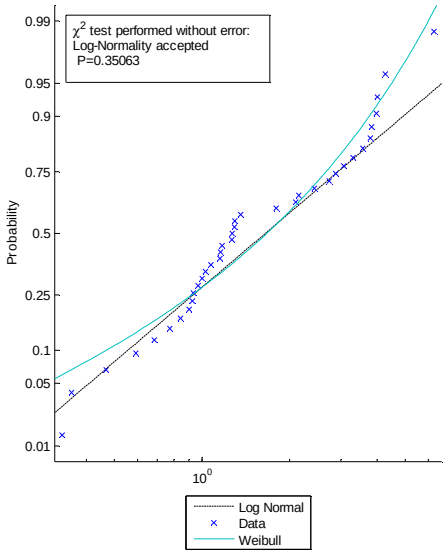

Est/Lindqv ratio tested as a Log-Normal distribution in interval: V∈[1.33,2.00] h∈[0.50,1.00]

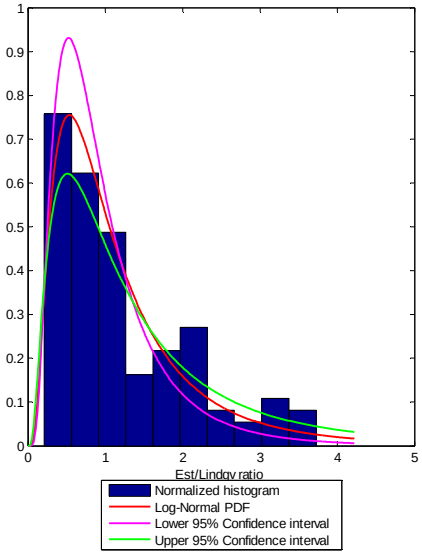

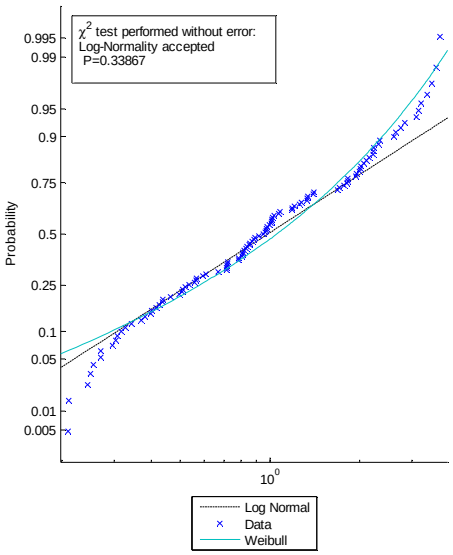

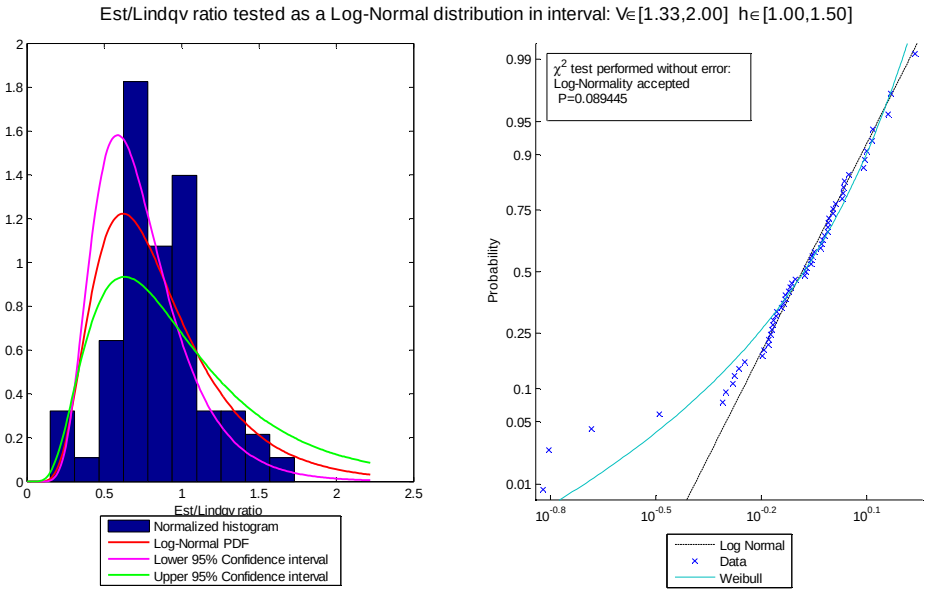

E.4 Speed ∈[2.0,2.67]

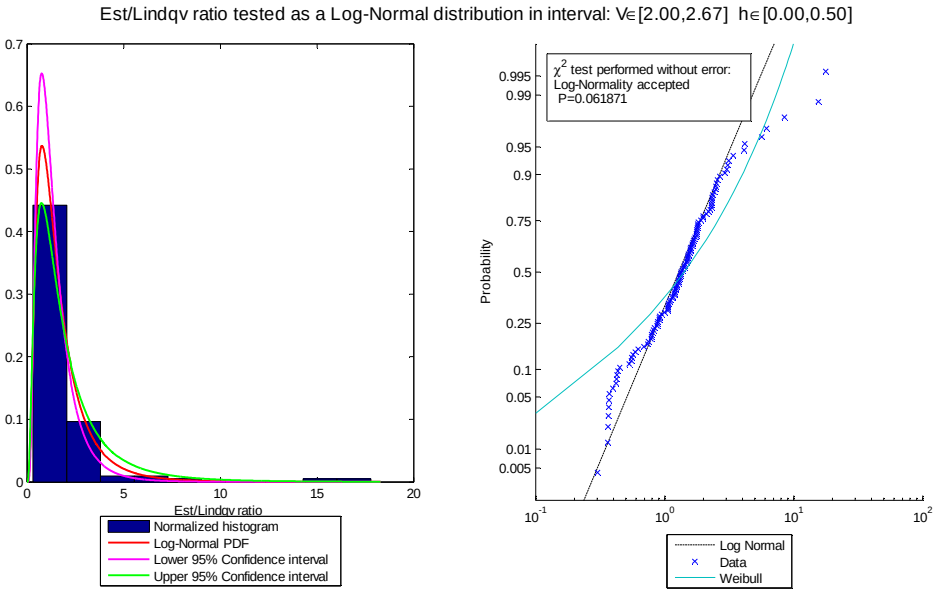

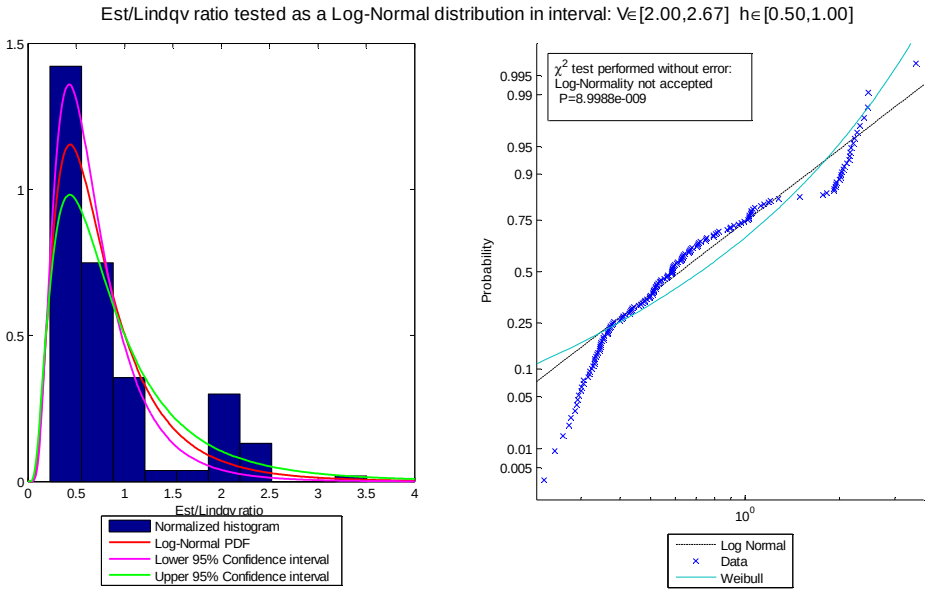
Est/Lindqv ratio tested as a Log-Normal distribution in interval: V∈[2.00,2.67] h∈[0.50,1.00]
χ² test performed without error:
Log-Normality not accepted
P=8.9988e-009
Probability
Est/Lindqv ratio
Normalized histogram
Log-Normal PDF
Lower 95% Confidence interval
Upper 95% Confidence interval
Log Normal
Data
Weibull

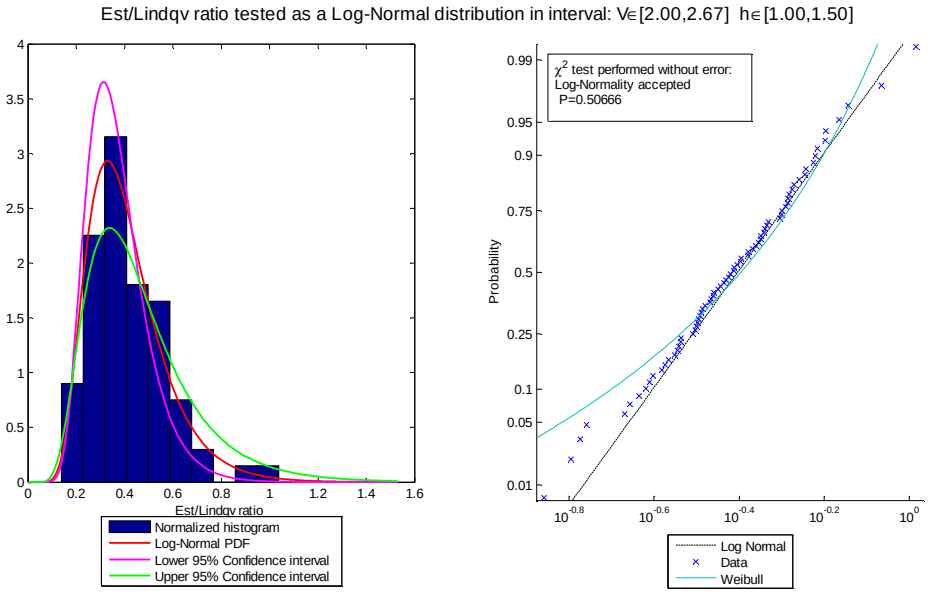
Est/Lindqv ratio tested as a Log-Normal distribution in interval: V∈[2.00,2.67] h∈[1.00,1.50]
χ² test performed without error:
Log-Normality accepted
P=0.50666
Probability
Est/Lindqv ratio
Normalized histogram
Log-Normal PDF
Lower 95% Confidence interval
Upper 95% Confidence interval
Log Normal
Data
Weibull

E.5 Speed ∈[2.67,3.33]

Est/Lindqv ratio tested as a Log-Normal distribution in interval: V∈[2.67,3.33] h∈[0.00,0.50]

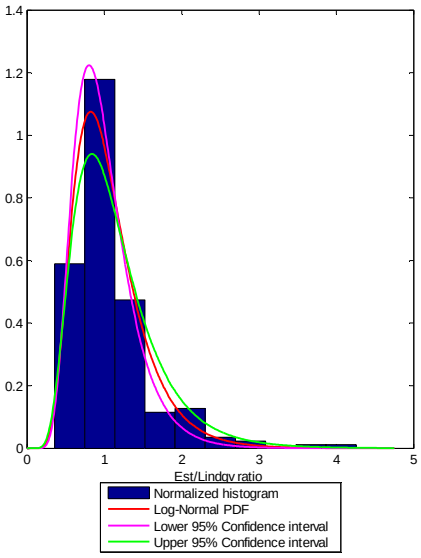

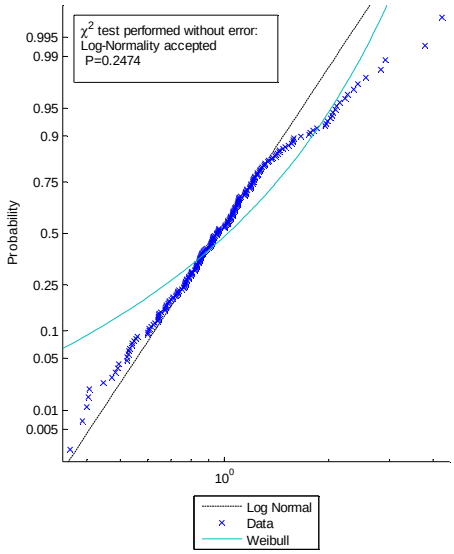

Est/Lindqv ratio tested as a Log-Normal distribution in interval: V∈[2.67,3.33] h∈[0.50,1.00]

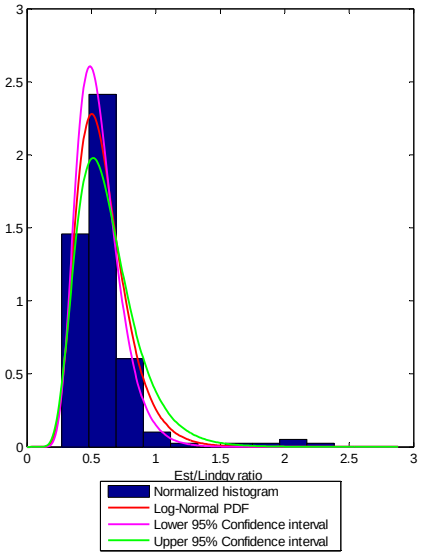

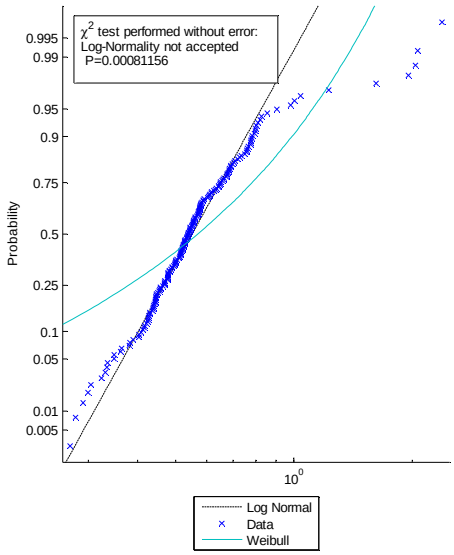

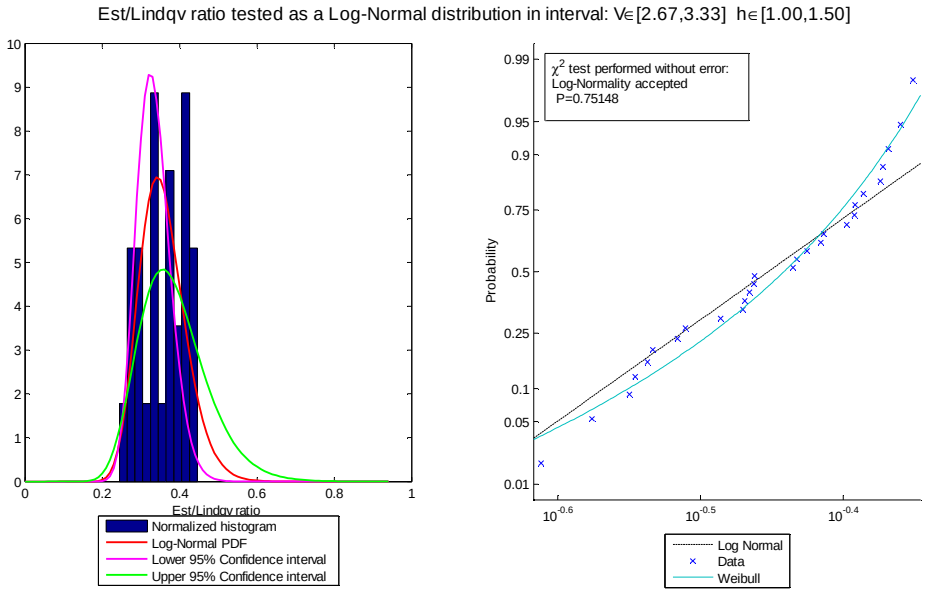

E.6 Speed ∈[3.33,4.00]

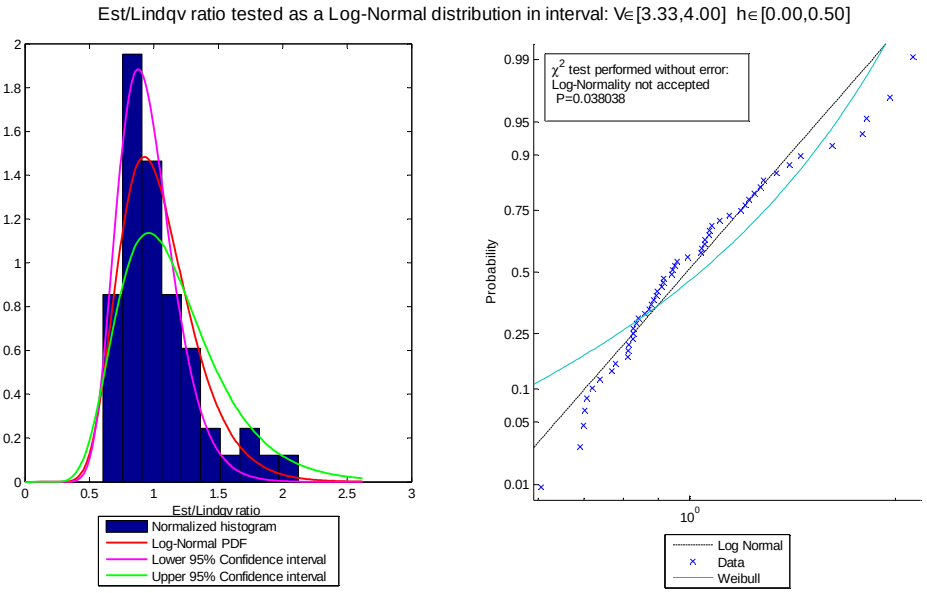

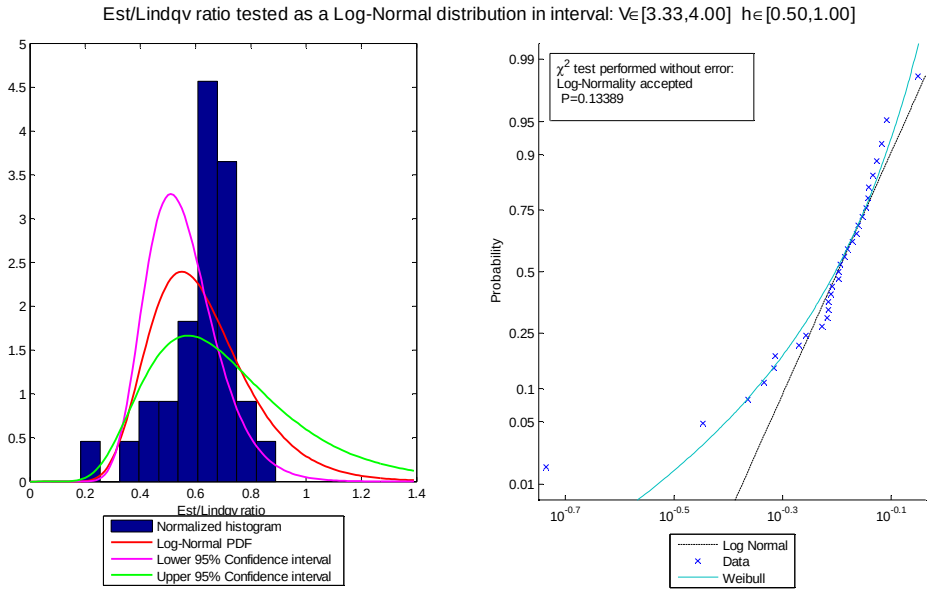
Est/Lindqv ratio tested as a Log-Normal distribution in interval: V∈[3.33,4.00] h∈[0.50,1.00]
Est/Lindqv ratio
Normalized histogram
Log-Normal PDF
Lower 95% Confidence interval
Upper 95% Confidence interval
χ2 test performed without error:
Log-Normality accepted
P=0.13389
Probability
Log Normal
Data
Weibull

F Lognormal probability plots for Riska formulation

F.1 Speed ∈[0,0.67]

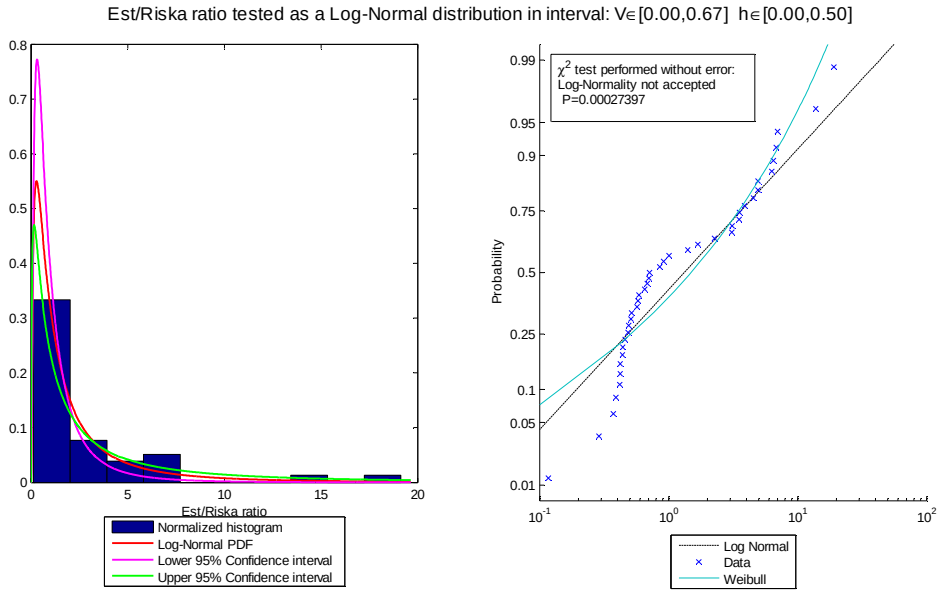

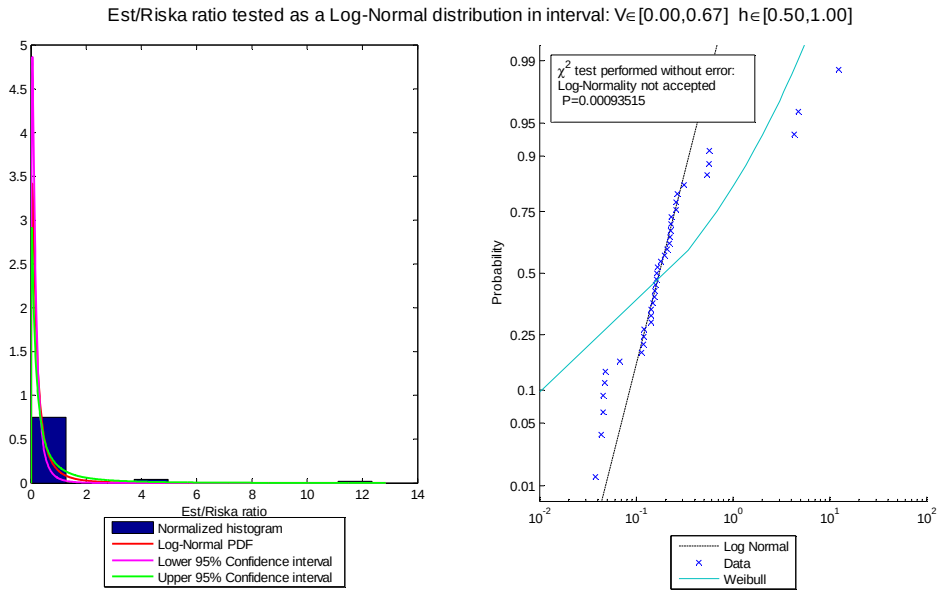

F.2 Speed ∈[0.67,0.67]

Est/Riska ratio tested as a Log-Normal distribution in interval: V∈[0.67,1.33] h∈[0.00,0.50]

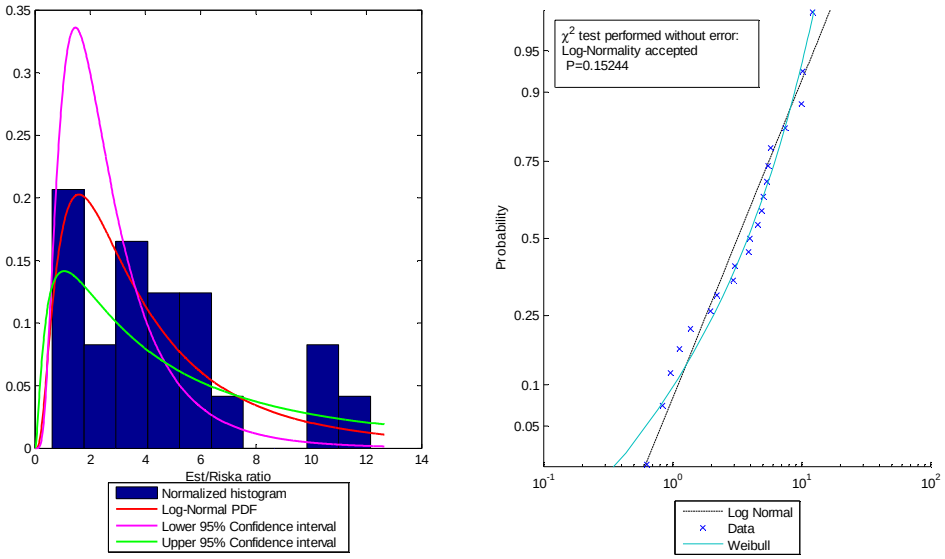

Est/Riska ratio tested as a Log-Normal distribution in interval: V∈[0.67,1.33] h∈[0.50,1.00]

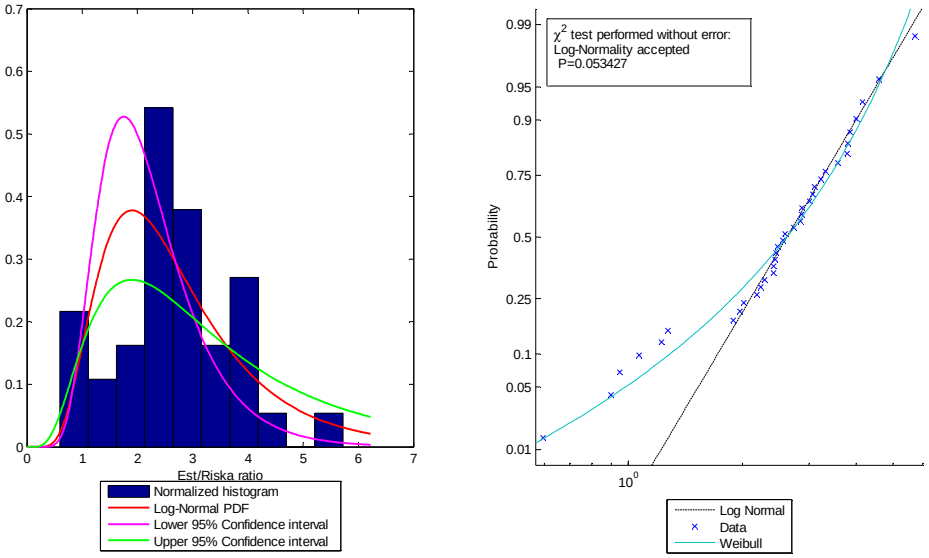

Est/Riska ratio tested as a Log-Normal distribution in interval: V∈[0.67,1.33] h∈[1.00,1.50]

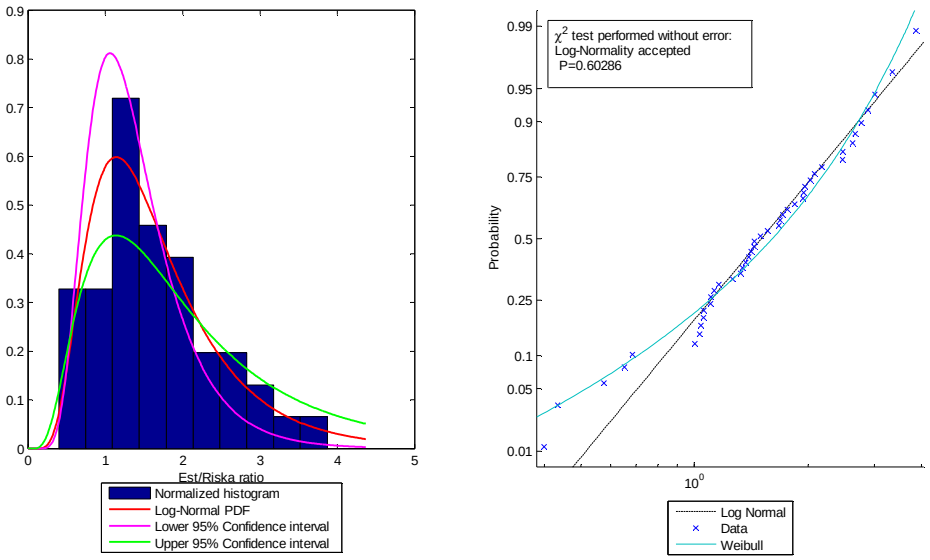

Est/Riska ratio tested as a Log-Normal distribution in interval: V∈[0.67,1.33] h∈[1.50,2.00]

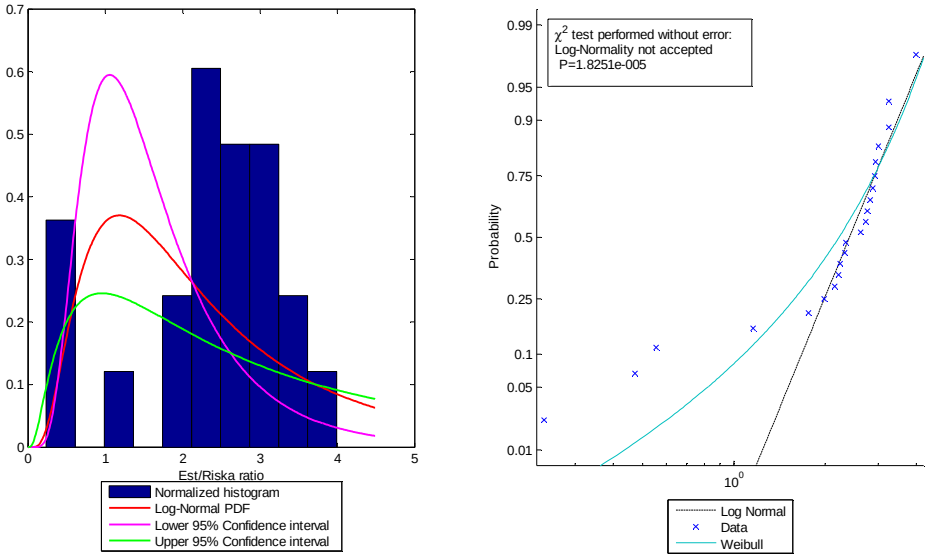

F.3 Speed ∈[1.33,2.0]

Est/Riska ratio tested as a Log-Normal distribution in interval: V∈[1.33,2.00] h∈[0.00,0.50]

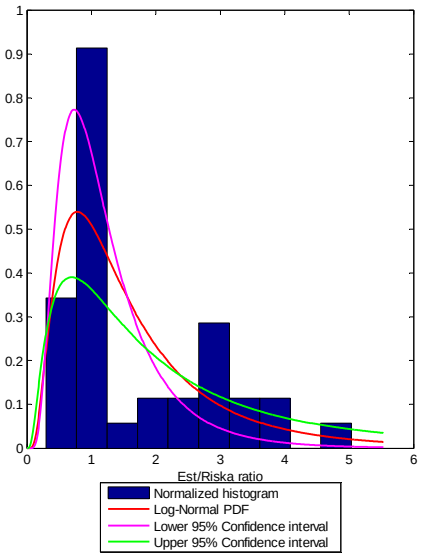

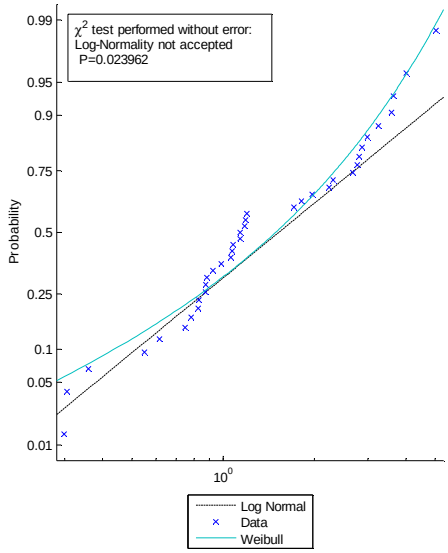

Est/Riska ratio tested as a Log-Normal distribution in interval: V∈[1.33,2.00] h∈[0.50,1.00]

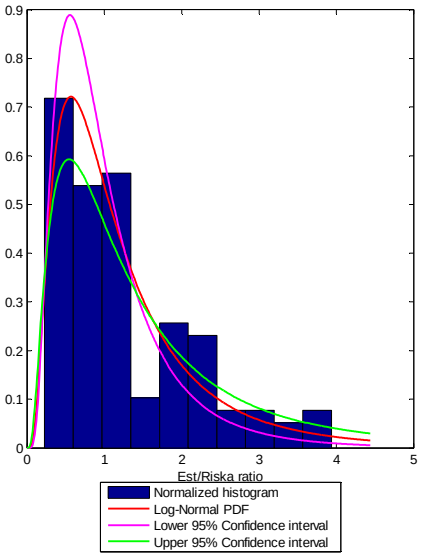

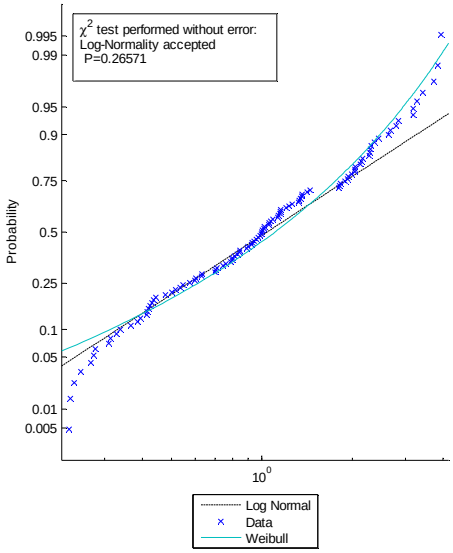

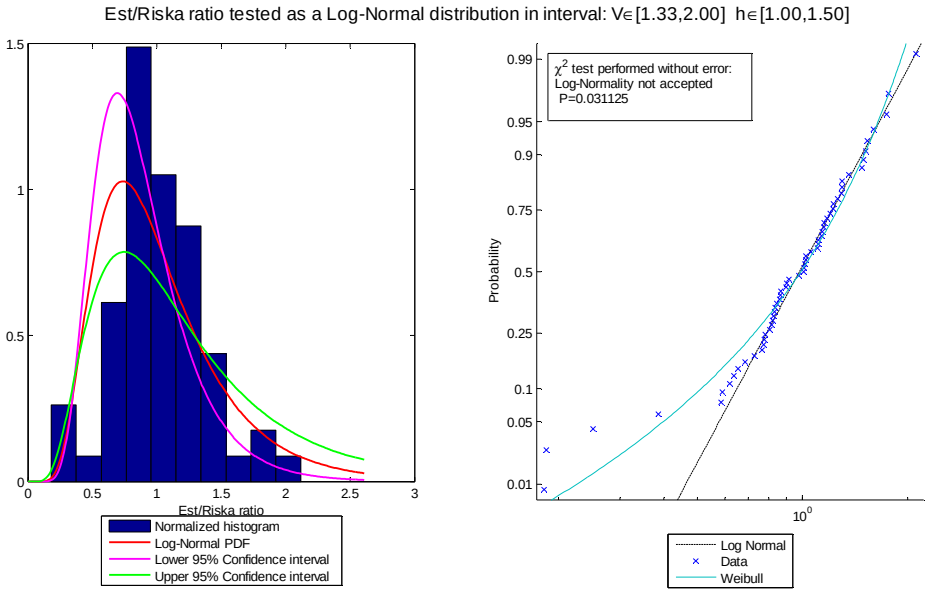

F.4 Speed ∈[2.0,2.67]

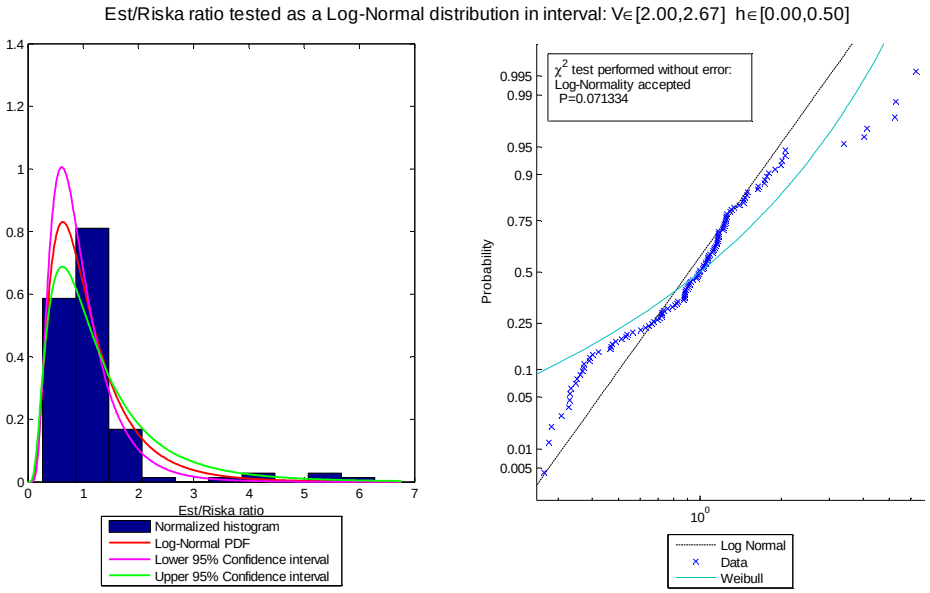

Est/Riska ratio tested as a Log-Normal distribution in interval: V∈[2.00,2.67] h∈[0.50,1.00]

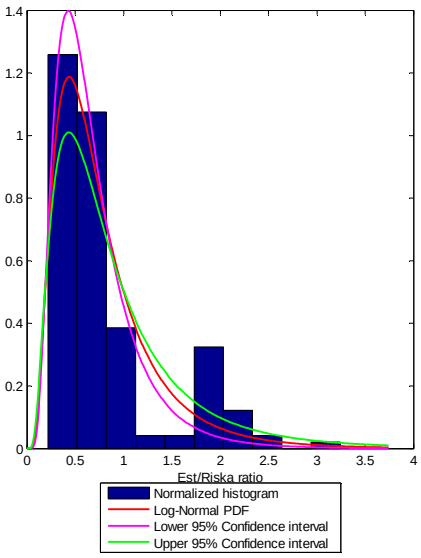

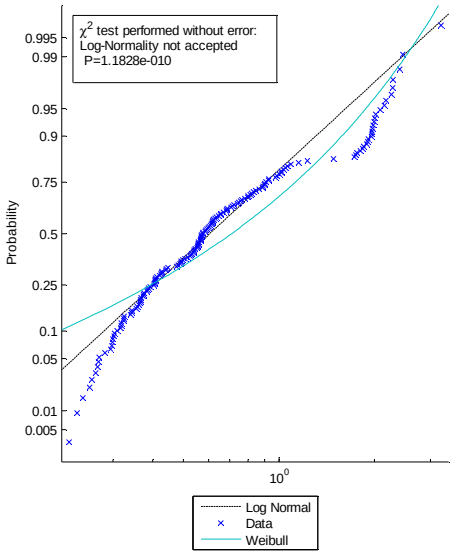

Est/Riska ratio tested as a Log-Normal distribution in interval: V∈[2.00,2.67] h∈[1.00,1.50]

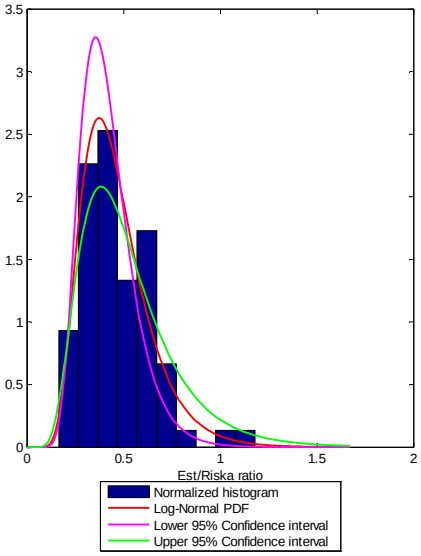

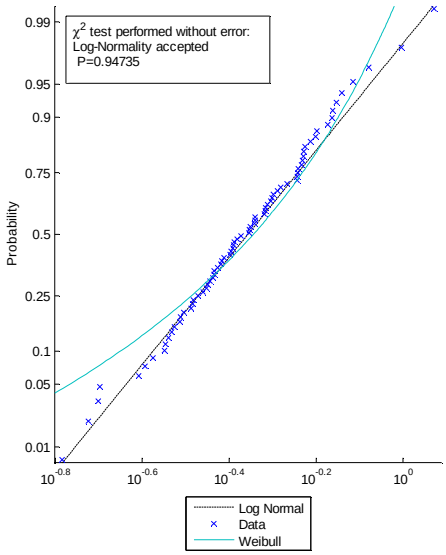

F.5 Speed ∈[2.67,3.33]

Est/Riska ratio tested as a Log-Normal distribution in interval: V∈[2.67,3.33] h∈[0.00,0.50]

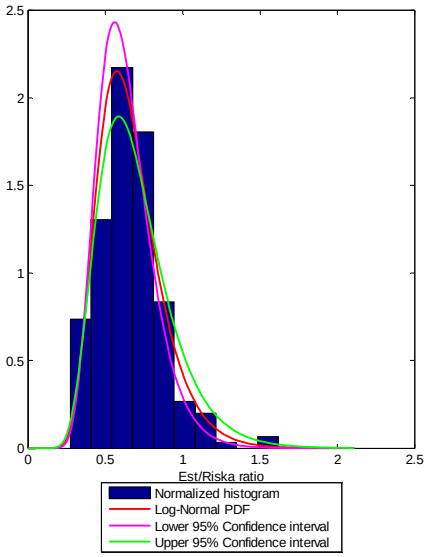

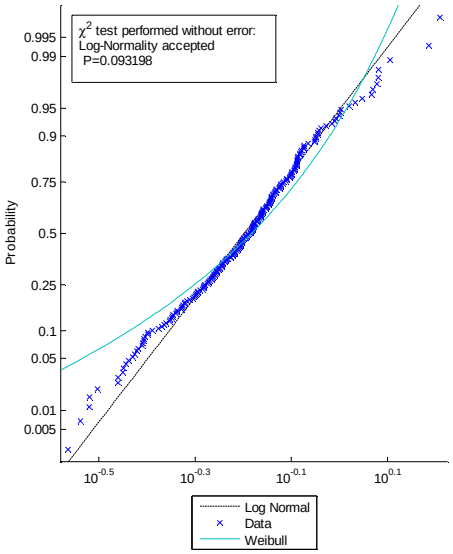

Est/Riska ratio tested as a Log-Normal distribution in interval: V∈[2.67,3.33] h∈[0.50,1.00]

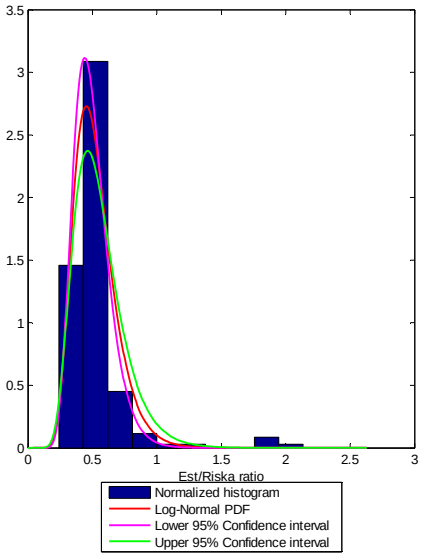

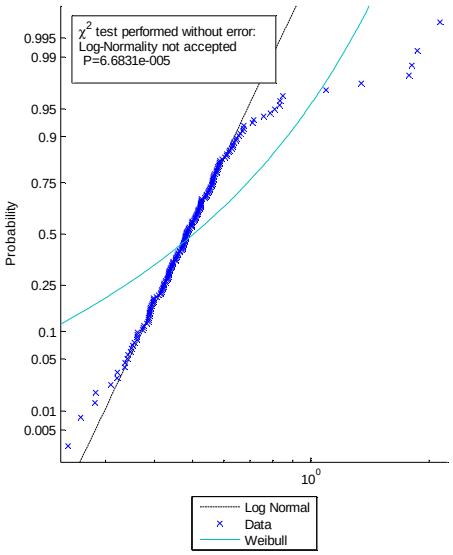

Est/Riska ratio tested as a Log-Normal distribution in interval: V∈[2.67,3.33] h∈[1.00,1.50]

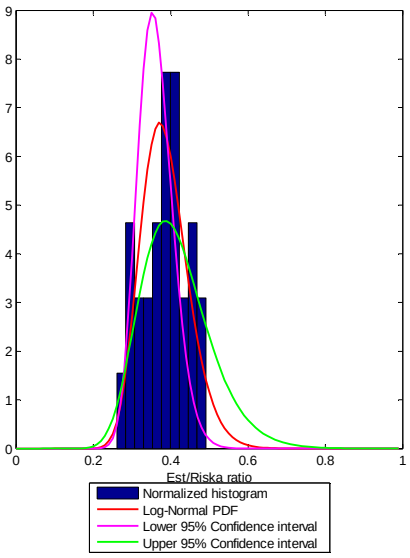

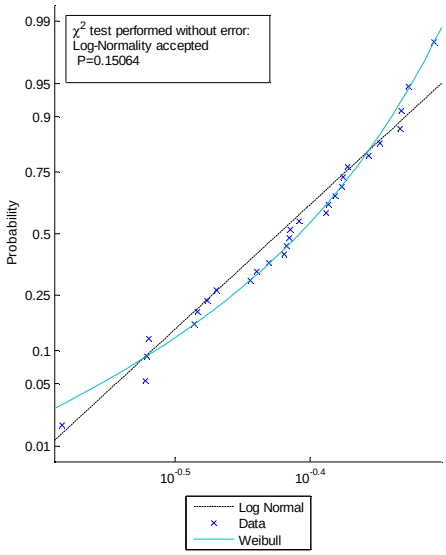

F.6 Speed ∈[3.33,4.00]

Est/Riska ratio tested as a Log-Normal distribution in interval: V∈[3.33,4.00] h∈[0.00,0.50]

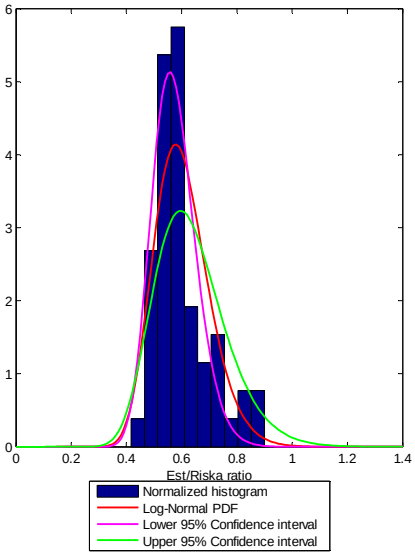

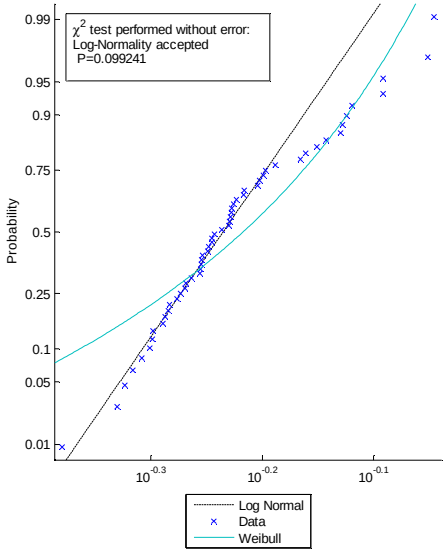

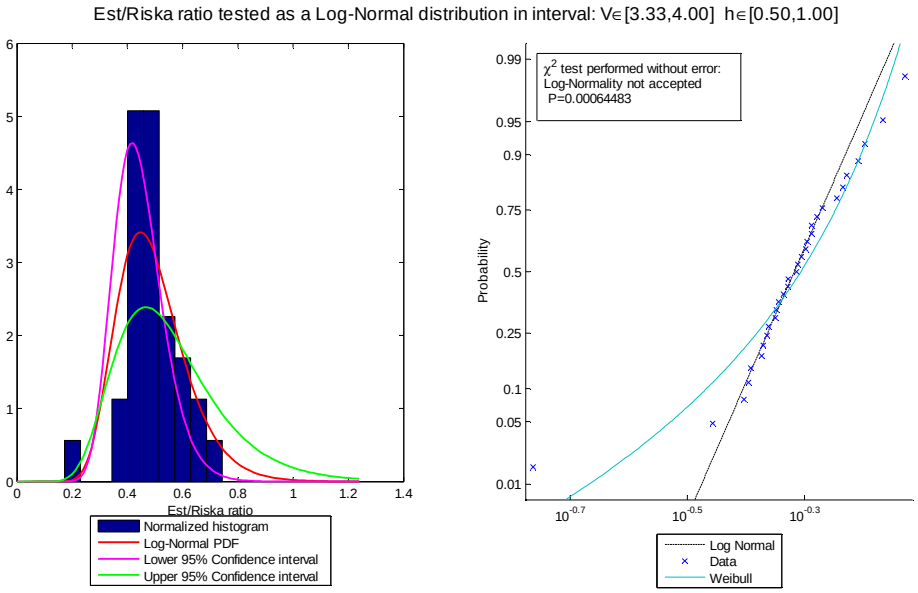
Est/Riska ratio tested as a Log-Normal distribution in interval: V∈[3.33,4.00] h∈[0.50,1.00]
Est/Riska ratio
Normalized histogram
Log-Normal PDF
Lower 95% Confidence interval
Upper 95% Confidence interval
χ2 test performed without error:
Log-Normality not accepted
P=0.00064483
Probability
Log Normal
Data
Weibull